STRUCTURAL STUDIES ON NOVEL EARLY TRANSITION METAL COMPLEXES WITH ACTIVE ORGANIC SUBSTRATES

NOBUKO KANEHISA

OSAKA UNIVERSITY

1992

STRUCTURAL STUDIES ON NOVEL EARLY TRANSITION METAL COMPLEXES WITH ACTIVE ORGANIC SUBSTRATES

活性有機基質の前周期遷移金属錯体に関する
構造化学的研究

NOBUKO KANEHISA

OSAKA UNIVERSITY

1992

Contents

Introduction

During past decade the chemistry of early transition metal organometallic compounds have attained rapid progress and it trebles the publication of the papers concerning the chemistry of group 3-5 organometallics. Such a pronounced advance is greatly indebted to the success in the isolation of an unprecedented series of highly reactive metal complexes utilizing sensible auxiliary ligands such as Cp [Cp=cyclopentadienyl], OR [R=alkyl, aryl], bulky neopentyl or silyl groups. The most striking feature emerged in the chemistry of early transition metal complexes lies in its high reactivity towards both electrophiles and unsaturated hydrocarbons. In some favorable cases, they can proceed highly regio- and stereo-selective catalytic or stoichiometric hydrocarbon conversion. Crystallographic analysis of this class of complexes is the fundamental requirement to penetrate into the origin of their unique chemical behavior, reaction pathways and to reveal their own structural characteristics.

This thesis focuses the structural characteristics of a series of early transition metal organometallic complexes involving dienes, and inserted products of diene complexes by heterocumulenes, ketones, and alkynes, together with the bulky phenoxide complexes studied by X-ray diffraction method.

Chapter 1 describes the unique coordination geometry of 1,3-dienes in early transition metal complexes.

Chapter 2 concerns with the diverse reaction courses in the controlled carbometallation of heterocumulenes, ketones, and alkynes with zirconium-diene complexes.

Chapter 3 describes the versatile bonding character of bulky phenoxy ligands in early transition metal complexes.

Chapter 1. Unique Coordination Geometry of 1,3-Dienes in Early Transition Metal Complexes

In recent years the chemistry of metal-diene complex has entered a new phase with the advent of highly reactive group 4 metal-diene complexes as $Cp_2M(diene)$(M=Ti, Zr, Hf) which furnish the synthetically useful selective carbon-carbon bond-forming reactions, reflecting their polar M-C bondings. They react not only with alkenes, dienes, and alkynes but also with carbonyl compounds such as aldehydes, ketones and esters with extremely high regioselectivity. Their structural pattern is also unique and the s-*trans* coordination of a diene to a mononuclear metal complex has been suggested by ^1H NMR spectroscopy for Zr and Hf complexes.[1-7]

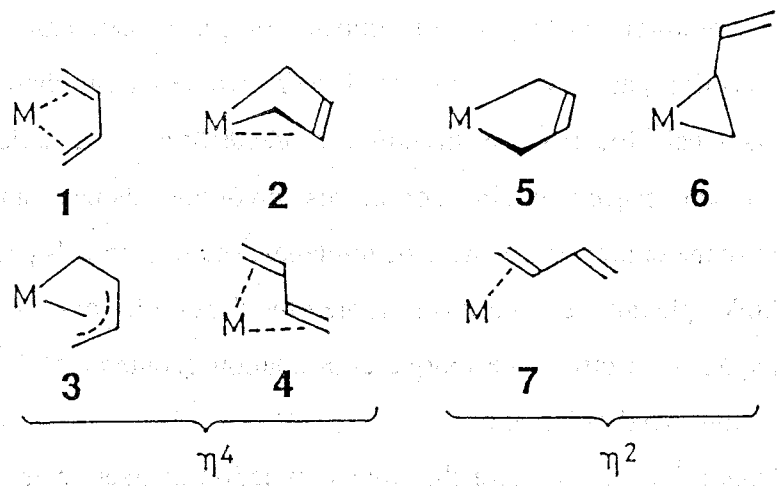

For the conjugated diene complexes, exemplified by 1,3-butadiene complexes, structures **1** - **7** seem possible. Conventional diene complexes containing middle or late transition metals are already well known to assume either the π-bonded η^4-s-*cis*-1,3-diene structure (**1**) or the η^2-1,3-diene structure (**7**). This situation changed recently by the advent of a variety of early transition metal-diene complexes. The diene complexes containing group 4 (Ti, Zr, Hf) and group 5 (Nb, Ta) elements always prefer the unique bent metallacyclo-3-

pentene structure **2** or novel s-*trans*-diene coordination structure **4**. Although the complexation of the type **5**, **6**, and **7** has been proposed as intermediates in various reactions, their exact molecular structures are still obscure. In order to obtain more detailed structural information, the X-ray crystal structure determinations of a series of early-transition metal-diene complexes have been carried out.

1-1. X-Ray Evidence for a Mononuclear s-*trans*-η^4-1,3-Diene Complex

1-1-1. Molecular structure of $Zr(\eta^5\text{-}C_5H_5)_2$(s-trans-PhCH=CH-CH=CHPh)

Novel s-*trans*-η^4-coordination of butadiene to a single metal atom was confirmed by the X-ray crystal structure analysis of thermally stable $Zr(\eta^5\text{-}C_5H_5)_2$(PhCH=CH-CH=CHPh); this agrees with the solution structure determined by ^{1}H NMR spectroscopy.

A series of 1,3-diene complexes of Zr of the $ZrCp_2$(1,3-diene) (Cp=cyclopentadienyl) was recently prepared by (a) reaction of $ZrCl_2Cp_2$ with enediylmagnesium[7] and (b) photolysis of $ZrCp_2(aryl)_2$ in the presence of 1,3-dienes.[1] In the case of butadiene, the first method gave the conventional s-*cis*-1,3-diene complex exclusively while the second method provided the thermally less stable s-*trans*-1,3-diene complex (the s-*cis*/s-*trans* ratio at 25°C being 55/45). The recent X-ray work on $ZrCp_2$(s-*trans*-buta-1,3-diene) remains equivocal about the conformation of the diene group because of the positional ambiguity of its two central carbon atoms.[1] In order to obtain exact coordination geometry of 1,4-butadiene to Zr atom we have proceeded the X-ray structure analysis of $ZrCp_2$(1,4-diphenylbuta-1,3-diene) complex. In solution, this complex, prepared by method (a), is assigned the s-*trans*-η^4-1,3-diene conformation from the ^{1}H NMR spectrum.

The X-ray diffraction data were collected on a Rigaku automated four-

circle diffractometer with graphite-monochromatized MoKα radiation. As the compound is very air-sensitive, crystals were sealed in thin-walled glass capillary tubes under argon atmosphere. Integrated intensities were measured by the θ-2θ scan technique with background countings at each end of the scan range for 5 s. The total number of reflections measured up to 2 θ of 50° were 3972 among which non-zero reflections were 3419. Three monitor reflections were measured for each block of 61 reflections to check for radiation damage and for any change in orientations of the crystal. During the measurement the average intensity of the monitor reflections decreased gradually down to 0.887 in $|F|$'s. The correction of radiation damage was applied by assuming the linear decay of intensities. The measured intensities were corrected for Lorentz and polarization effects but not for absorption.

The crystal structure was solved by the conventional heavy atom method and refined by the block-diagonal least-squares procedure (HBLS-V).[8] The atomic scattering factors were taken from the International Tables for X-Ray Crystallography.[9] Hydrogen atoms were searched for on the difference Fourier maps calculated after the anisotropic refinements of non-hydrogen atoms. The weighting scheme applied was $w=[\sigma^2(F_o)+a(F_o)+b(F_o)^2]^{-1}$ for non-zero and $w=c$ for zero reflections.[8] The final R index defined by $R=\Sigma(|F_o|-|F_c|)/\Sigma|F_o|$ was 0.058. The weighted R index defined by $R_w=[\Sigma w(|F_o|-|F_c|)^2/\Sigma w|F_o|^2]^{1/2}$ was 0.084. The crystal data and parameters for structure determination are summarized in Table 1-1. The final atomic coordinates are listed in Table 1-2.

The crystal structure obtained includes two crystallographically independent molecules (I) and (II), which make an enantiomorphic pair related by a pseudo-local center of symmetry shown in Fig. 1-1. Two independent molecules have essentially the same molecular structures as compared in Fig. 1-2. The bond distances and angles are listed in Table 1-3. The most important features of the molecular structure are as follows. (i) The molecule has approximate C_2 symmetry. (ii) The Zr atom is coordinated pseudotetrahedrally

Table 1-1. Crystal Data and Experimental Parameters for X-Ray Structure Determination of $(\eta^5\text{-}C_5H_5)_2Zr(C_6H_5CH{=}CH\text{-}CH{=}CHC_6H_5)$

Formula	$C_{26}H_{24}Zr$
Formula weight	427.7
Crystal system	orthorhombic
Space group	$P2_12_12_1$
Temp., °C	22
a,[a] Å	8.481(1)
b, Å	21.803(3)
c, Å	21.667(5)
V, Å^3	4006.4(11)
Z	8
D_{calcd}, g cm^{-3}	1.418
F(000), e	1760
μ(MoKα), cm^{-1}	5.5
Crystal size, mm	0.45x0.40x0.40
2θ range,[b] deg	4<2θ<50
Scan width, deg in 2θ	2.50+0.70tanθ
Scan speed, deg min^{-1}	4
Background count, s	5
Reflections measured	3972
Reflections observed[c]	3419
Radiation damage	yes(corrected)
No. of variables	600
GOF[d]	1.132
R[e]	0.058
R_w[f]	0.084

[a)]Least-squares refinement of the θ values for 25 reflections with 2θ>25°. [b)]Intensity data were collected on a Rigaku four-circle diffractometer using graphite-monochromatized MoKα radiation by the θ-2θ scan method. [c)]non-zero reflections. [d)]$[\Sigma w(|F_o|-|F_c|)^2/(n-m)]^{1/2}$, where n and m are the No. of reflections used and variables refined, respectively. [e)]$R=\Sigma(|F_o|-|F_c|)/\Sigma|F_o|$. [f)]$R_w=[\Sigma w(|F_o|-|F_c|)^2/\Sigma w|F_o|^2]^{1/2}$, $w=[\sigma^2(F_o)+a(F_o)+b(F_o)^2]^{-1}$ for non-zero and $w=c$ for zero reflections, where a=0.0460, b=0.00221 and c=0.0124.

Table 1-2. Final Atomic Coordinates and Equivalent Isotropic Temperature Factors for Nonhydrogen Atoms in $(\eta^5\text{-}C_5H_5)_2Zr(C_6H_5CH{=}CH\text{-}CH{=}CHC_6H_5)$ with Estimated Standard Deviations in Parentheses[a]

Atom	x	y	z	B_{eq}
Zr(1)	0.47568(10)	0.02146(4)	0.34695(4)	3.57
Zr(2)	-0.00516(10)	0.22088(4)	0.13971(4)	3.40
C(11)	0.6642(12)	0.1082(5)	0.3278(5)	3.3
C(12)	0.5196(14)	0.1151(4)	0.2933(5)	3.7
C(13)	0.4716(14)	0.0715(5)	0.2484(5)	3.6
C(14)	0.3234(14)	0.0436(5)	0.2504(5)	3.5
C(111)	0.7186(11)	0.1517(4)	0.3746(5)	2.9
C(112)	0.8457(14)	0.1363(5)	0.4120(6)	4.1
C(113)	0.9011(14)	0.1760(6)	0.4579(6)	5.1
C(114)	0.8355(17)	0.2328(7)	0.4660(6)	5.7
C(115)	0.7045(17)	0.2491(6)	0.4293(7)	5.6
C(116)	0.6498(13)	0.2097(6)	0.3844(6)	4.5
C(121)	0.2687(12)	-0.0029(5)	0.2048(5)	3.3
C(122)	0.3456(14)	-0.0145(6)	0.1498(5)	4.6
C(123)	0.2882(17)	-0.0569(7)	0.1080(7)	6.2
C(124)	0.1557(16)	-0.0905(6)	0.1203(6)	5.1
C(125)	0.0752(14)	-0.0774(6)	0.1750(6)	4.9
C(126)	0.1328(14)	-0.0360(5)	0.2159(5)	4.2
C(21)	-0.1884(12)	0.1338(4)	0.1578(5)	3.1
C(22)	-0.0505(14)	0.1266(4)	0.1905(5)	3.8
C(23)	0.0019(15)	0.1697(4)	0.2368(4)	3.4
C(24)	0.1484(14)	0.1976(5)	0.2358(5)	3.6
C(211)	-0.2480(12)	0.0903(5)	0.1100(5)	3.5
C(212)	-0.3727(14)	0.1060(5)	0.0725(6)	4.4
C(213)	-0.4354(16)	0.0657(7)	0.0295(6)	5.5
C(214)	-0.3731(16)	0.0084(6)	0.0224(6)	5.6
C(215)	-0.2491(17)	-0.0097(6)	0.0601(7)	5.6
C(216)	-0.1909(13)	0.0310(6)	0.1049(6)	4.3
C(221)	0.2064(12)	0.2423(5)	0.2824(5)	3.2
C(222)	0.1275(12)	0.2532(5)	0.3385(6)	4.0
C(223)	0.1812(14)	0.2936(6)	0.3799(5)	4.6
C(224)	0.3178(17)	0.3262(6)	0.3704(6)	5.7
C(225)	0.3970(15)	0.3152(6)	0.3145(6)	5.2
C(226)	0.3430(14)	0.2752(6)	0.2728(5)	4.4
C(131)	0.2068(13)	0.0328(9)	0.3954(6)	6.9
C(132)	0.2892(18)	-0.0095(8)	0.4312(7)	7.5

[a]Positional parameters are in fraction of cell edges and B_{eq} is the equivalent isotropic temperature factors calculated from the corresponding anisotropic thermal parameters.

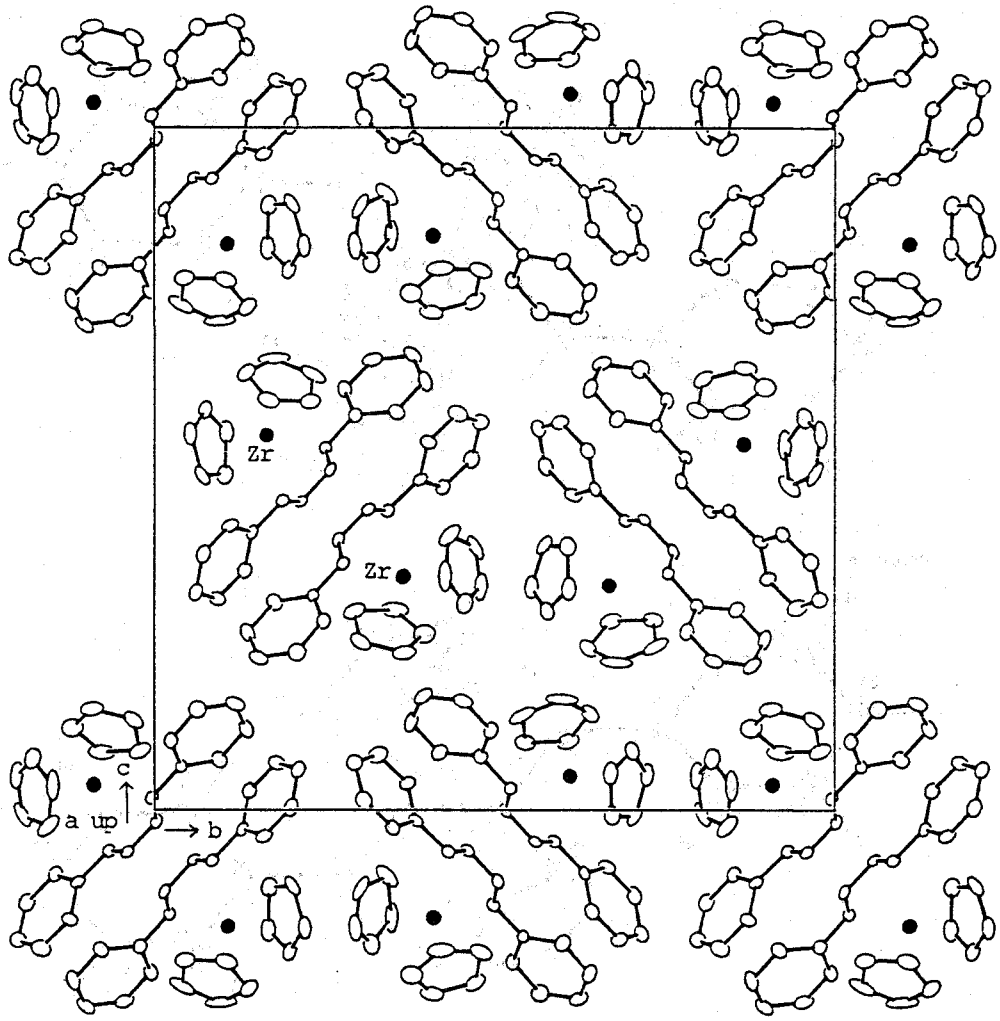

Fig. 1-1. Crystal structure of $(C_5H_5)_2Zr$(s-*trans*-PhCH=CH-CH=CHPh); two crystallographically independent molecules are related by the pseudo center of symmetry.

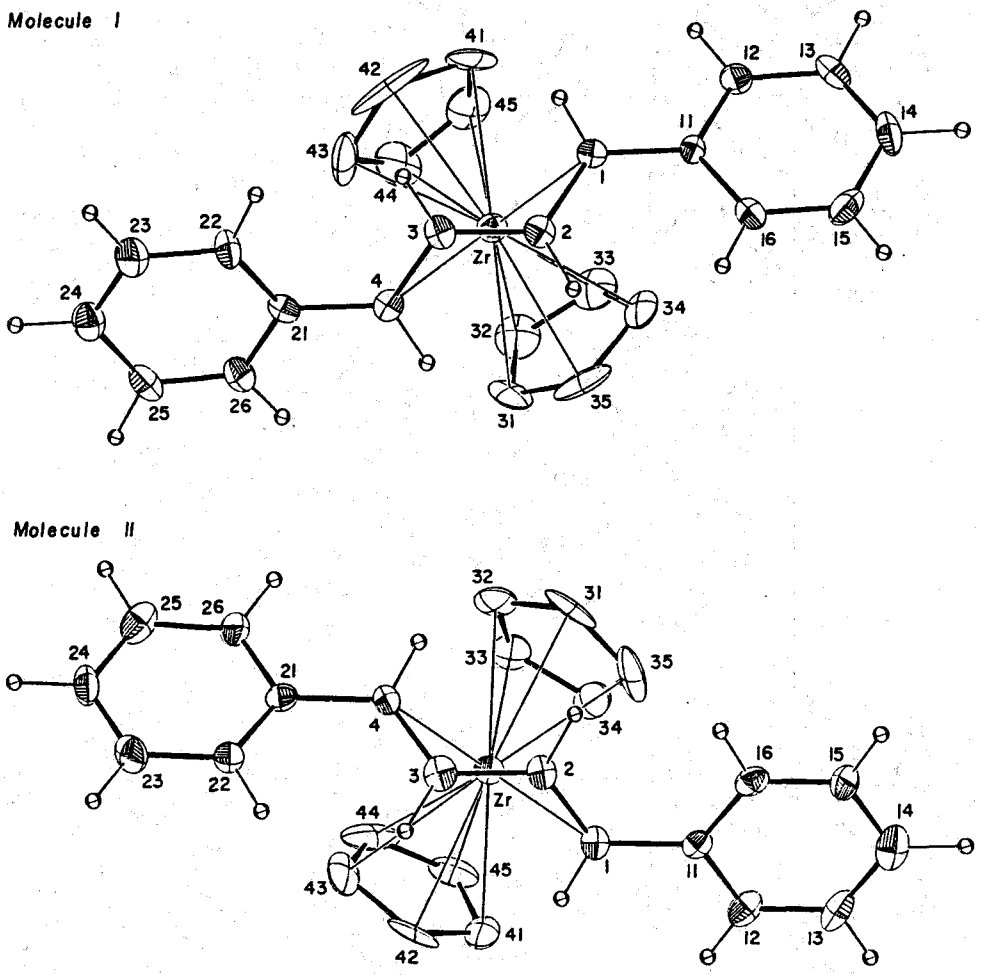

Fig. 1-2. Molecular structure of $(C_5H_5)_2Zr$(s-*trans*-PhCH=CH-CH=CHPh); two crystallographically independent molecules are shown as Molecule I and II.

Table 1-3. Interatomic Bond Distances (Å) and Angles (°) in $(\eta^5\text{-}C_5H_5)_2Zr(C_6H_5CH{=}CH\text{-}CH{=}CHC_6H_5)$ with Estimated Standard Deviations in Parentheses[a]

Bond distance

Zr(1)	- C(11)	2.511(10)	Zr(1)	- C(12)	2.378(11)
Zr(1)	- C(13)	2.398(12)	Zr(1)	- C(14)	2.506(11)
Zr(1)	- A(12)	2.337	Zr(1)	- A(34)	2.351
Zr(1)	- CPA(1)	2.221	Zr(1)	- CPA(2)	2.207
Zr(2)	- C(21)	2.485(10)	Zr(2)	- C(22)	2.363(11)
Zr(2)	- C(23)	2.382(12)	Zr(2)	- C(24)	2.508(11)
Zr(2)	- B(12)	2.325	Zr(2)	- B(34)	2.346
Zr(2)	- CPB(1)	2.238	Zr(2)	- CPB(2)	2.232
C(11)	- C(12)	1.444(15)	C(11)	- C(111)	1.463(14)
C(12)	- C(13)	1.419(16)	C(13)	- C(14)	1.397(16)
C(14)	- C(121)	1.488(15)	C(21)	- C(22)	1.376(15)
C(21)	- C(211)	1.491(14)	C(22)	- C(23)	1.446(17)
C(23)	- C(24)	1.383(16)	C(24)	- C(221)	1.487(15)

Bond angle

C(11)	-Zr(1) -C(12)	34.2(4)	C(12)	-Zr(1) -C(13)	34.6(4)
C(13)	-Zr(1) -C(14)	33.0(4)	A(12)	-Zr(1) -A(34)	62.2(0)
A(12)	-Zr(1) -CPA(1)	109.7(0)	A(12)	-Zr(1) -CPA(2)	118.0(0)
A(34)	-Zr(1) -CPA(1)	116.2(0)	A(34)	-Zr(1) -CPA(2)	109.9(0)
CPA(1)	-Zr(1) -CPA(2)	124.7(0)	C(21)	-Zr(2) -C(22)	32.9(4)
C(22)	-Zr(2) -C(23)	35.5(4)	C(23)	-Zr(2) -C(24)	32.7(4)
B(12)	-Zr(2) -B(34)	62.7(0)	B(12)	-Zr(2) -CPB(1)	107.6(0)
B(12)	-Zr(2) -CPB(2)	115.4(0)	B(34)	-Zr(2) -CPB(1)	115.1(0)
B(34)	-Zr(2) -CPB(2)	108.6(0)	CPB(1)	-Zr(2) -CPB(2)	128.9(0)
C(12)	-C(11) -C(111)	124.0(9)	C(11)	-C(12) -C(13)	121.9(10)
C(12)	-C(13) -C(14)	121.9(11)	C(13)	-C(14) -C(121)	123.8(10)
C(22)	-C(21) -C(211)	125.0(9)	C(21)	-C(22) -C(23)	123.0(10)
C(22)	-C(23) -C(24)	123.5(11)	C(23)	-C(24) -C(221)	125.2(10)

[a]The first figure of atomic numbering, 1 or 2, means that for molecule I or molecule II; CPA(1), CPA(2), CPB(1), and CPB(2) are the centroids of Cp ligands of C(131)-C(135), C(141)-C(145), C(231)-C(235), and C(241)-C(245), respectively; A(12), A(34), B(12), and B(34) are the midpoints of C(11)-C(12), C(13)-C(14), C(21)-C(22), and C(23)-C(24) bonds, respectively.

to two η^5-C_5H_5 ligands [Cp-Zr-Cp; 124.7° in (I) and 128.9° in (II)] and the diene double bonds. (iii) The torsional angles around the C(2)-C(3) bond are 126.0° in (I) and 125.3° in (II). (iv) The bond distances of Zr-C(1) [2.511Å in (I) and 2.485Å in (II)] and Zr-C(4) (2.506Å and 2.508Å) are longer than Zr-C(2)(2.378Å and 2.363Å) and Zr-C(3) (2.398Å and 2.382Å). (v) The bond distances in the two diene ligands show different characters. In molecule II, C(1)-C(2) [1.376Å] and C(3)-C(4) [1.383Å] lengths are shorter than C(2)-C(3) [1.446Å] length showing the η^4-diene coordination. In molecule I, however, C(1)-C(2) [1.444Å], C(2)-C(3) [1.419Å] and C(3)-C(4) [1.397Å] are not significantly different from each other by the consideration of estimated standard deviation around 0.015Å. These observations show the conformation of 1,4-diphenyl-buta-1,3-diene to be s-*trans*, however, the torsional angles around C(2)-C(3) bonds show large deviation from the exact *trans* conformation probably for releasing the steric repulsion between the cyclopentadienyl ligands and expected exact *trans*-1,4-diphenylbutadiene. This is the first clear evidence for s-*trans* diene coordination to a single metal atom obtained by X-ray work; some binuclear and trinuclear s-*trans*-1,3-dienes have been reported previously. The important structural parameters of the present complex are compared with those of the polynuclear s-*trans*-diene complexes in Table 1-4. The torsional angle around the central C-C bond shows little deviation from exact *trans* geometry in polynuclear diene-complexes.

1-1-2. Molecular structure of $Mg(THF)_3$(s-cis-PhCH=CH-CH=CHPh)

The structure of magnesium-diene complexes prepared from 1,3-diene and activated magnesium is of considerable importance in organomagnesium chemistry. Five-membered metalacyclic or cyclic oligomeric structure has been proposed for these compounds.[10,11] These classes of compounds are valuable as a reagent for organic[12,13] as well as organometallic synthesis.[2,14,15] This

Table 1-4. Coordination Geometry of *s-trans*-Butadiene Ligands in mono- and poly-nuclear Metal Complexes

Mononuclear Complex

	φ (°)	M-C distance (Å)
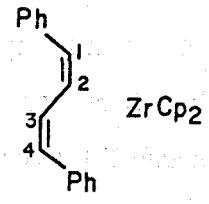 $ZrCp_2$	126·0 125·3	av. Zr-C1=2·503 Zr-C2=2·380

Polynuclear Complexes

	φ (°)	M-C distance (Å)
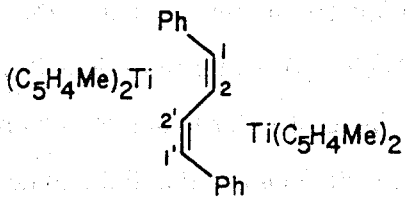	180·0	Ti-C1 = 2·084 Ti-C2= 2·325 Ti-C2'= 2·153
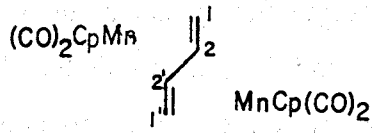	180·0	Mn-C1 = 2·200 Mn-C2=2·284
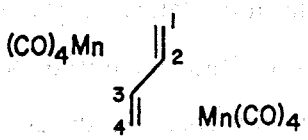	162·4	av. Mn-C1=2·236 Mn-C2=2·285
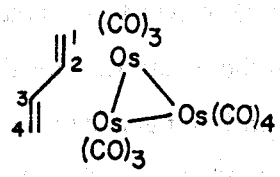	174·9	av. Os-C1 = 2·228 Os-C2= 2·311

type of regent has recently been used in the preparation of $ZrCp_2$(RCH=CH-CH=CHR) (Cp=cyclopentadienyl, R=H or Ph) which reveals the first example of s-*trans*-diene coordination to mononuclear metal species.[1,4] The chemical nature of the Mg-C bond is interesting since the diene ligand behaves as η^4-coordinated diene when oxidized by air or I_2 releasing the coordinated diene while it behaves as 2-butene-diylmagnesium toward alkylene dihalide, dienes and protic agents.[10,11] This is the first X-ray structure analysis of a magnesium-diene complex, 1,4-diphenyl-2-butene-1,4-diylmagnesium crystallized from the THF solution.

The X-ray experiments and crystal structure analysis were proceeded similarly as for the $ZrCp_2$(1,4-diphenylbutadiene). The crystal data and parameters for the structure determination are summarized in Table 1-5. The final atomic coordinates are listed in Table 1-6, while the selected interatomic distances and angles are in Table 1-7. The molecular structure is shown in Fig. 1-3. One of the important features of this molecule is that the magnesium atom is penta-coordinated by three oxygen atoms of THF ligands and C(1) and C(4) atoms of the butadiene ligand. The coordination geometry of magnesium is distorted trigonal bipyramid. The C(1) and C(4) atoms of butadiene ligand occupy the axial and equatorial positions, respectively. The only previous X-ray example of penta-coordinated organomagnesium complex is $MgBr(CH_3)(THF)_3$,[16] in which magnesium takes trigonal bipyramidal coordination with Br and methyl ligands on the equatorial positions. The butadiene ligand takes s-*cis* conformation with four carbon atoms of C(1) to C(4) on a plane, from which magnesium atom deviates 1.71Å away. The Mg-C(1) bond (2.32Å) is slightly longer than Mg-C(4) bond (2.62Å), the former locating on the axial and the latter on the equatorial position, respectively. The observed Mg-C distances are significantly longer than those in $MgPh_2$.TMEDA (Mg-C=2.167(3)Å)[17] and $MgMe_2$.TMEDA (Mg-C=2.166(6)Å).[18] The C(2)-C(1)-Mg and C(3)-C(4)-Mg bond angles are 82.7 and 82.1°, respectively. These

Table 1-5. Crystal Data and Experimental Parameters for X-Ray Structure Determination of $Mg(THF)_3$(*s-cis*-PhCH=CH-CH=CHPh)

Formula	$C_{28}H_{38}O_3Mg$
Formula weight	446.9
Crystal system	monoclinic
Space group	$P2_1/c$
Temp., °C	20
a,[a] Å	14.529(2)
b, Å	15.929(2)
c, Å	11.440(2)
β, deg	102.03(1)
V, Å^3	2589.4(6)
Z	4
D_{calcd}, g cm^{-3}	1.146
F(000), e	968
μ(MoKα), cm^{-1}	1.73
2θ range,[b] deg	4<2θ<45
Scan width, deg in 2θ	2.5+0.70tanθ
Scan speed, deg min^{-1}	4
Background count, s	5
Reflections measured	1850
Reflections observed[c]	1362
Radiation damage	no
No. of variables	290
R[d]	0.139

[a]Least-squares refinement of the θ values for 25 reflections with 2θ>19°. [b]Intensity data were collected on a Rigaku four-circle diffractometer using graphite-monochromatized MoKα radiation by the θ-2θ scan method. [c]$|F_o|>3\sigma(F_o)$. [d]$R=\Sigma(|F_o|-|F_c|)/\Sigma|F_o|$.

Table 1-6. Final Atomic Coordinates and Equivalent Isotropic Temperature Factors for Nonhydrogen Atoms in $Mg(THF)_3$(s-*cis*-PhCH=CH-CH=CHPh) with Estimated Standard Deviations in Parentheses[a]

Atom	x	y	z	B_{eq}/Å^2
Mg	0.2625(5)	0.4003(4)	0.2063(6)	5.0
C(1)	0.1591(12)	0.2911(10)	0.2155(17)	6.0
C(2)	0.2123(14)	0.2508(11)	0.1404(19)	7.2
C(3)	0.3123(14)	0.2521(11)	0.1734(17)	6.6
C(4)	0.3610(12)	0.2955(10)	0.2829(16)	5.7
C(41)	0.0562(14)	0.2971(11)	0.1705(17)	7.0
C(42)	-0.0053(14)	0.3159(13)	0.2503(20)	7.6
C(43)	-0.1096(16)	0.3187(15)	0.2023(23)	10.1
C(44)	-0.1454(17)	0.3098(15)	0.0838(20)	9.5
C(45)	-0.0868(14)	0.2935(12)	0.0051(18)	7.6
C(46)	0.0109(13)	0.2868(10)	0.0462(17)	6.5
C(51)	0.4635(12)	0.3026(10)	0.2919(15)	5.1
C(52)	0.5062(13)	0.3072(13)	0.1951(17)	7.0
C(53)	0.6071(14)	0.3151(13)	0.2161(19)	7.8
C(54)	0.6611(14)	0.3195(15)	0.3276(21)	9.6
C(55)	0.6190(16)	0.3167(15)	0.4291(20)	9.4
C(56)	0.5203(12)	0.3088(12)	0.4104(17)	6.6
O(1)	0.3659(9)	0.5005(8)	0.2157(11)	7.4
C(11)	0.3846(20)	0.5629(19)	0.1304(24)	13.7
C(12)	0.4882(19)	0.5765(16)	0.1627(24)	12.6
C(13)	0.5163(18)	0.5502(18)	0.2854(25)	12.5
C(14)	0.4325(16)	0.5138(16)	0.3268(19)	9.4
O(2)	0.2201(9)	0.4345(8)	0.0298(10)	6.2
C(21)	0.1294(13)	0.4668(14)	-0.0246(19)	8.1
C(22)	0.1192(19)	0.4504(16)	-0.1573(20)	11.2
C(23)	0.2172(21)	0.4427(16)	-0.1719(19)	11.4
C(24)	0.2668(18)	0.3998(15)	-0.0603(18)	9.6
O(3)	0.2089(9)	0.4817(8)	0.3224(11)	7.3
C(31)	0.2106(20)	0.4595(18)	0.4427(19)	11.8
C(32)	0.1417(22)	0.5092(18)	0.4804(24)	13.2
C(33)	0.1110(18)	0.5701(16)	0.3970(20)	11.1
C(34)	0.1541(19)	0.5575(14)	0.2892(23)	12.1

[a]Positional parameters are in fraction of cell edges and B_{eq} is the equivalent isotropic temperature factors calculated from the corresponding anisotropic thermal parameters.

Table 1-7. Selected Bond Distances (Å) and Angles (°) in $Mg(THF)_3$(s-*cis*-PhCH=CH-CH=CHPh) with Estimated Standard Deviations in Parentheses

Bond distances			
Mg(1)-O(1)	2.179(14)	Mg(1)-O(2)	2.058(13)
Mg(1)-O(3)	2.116(14)	Mg(1)-C(1)	2.315(20)
Mg(1)-C(2)	2.559(22)	Mg(1)-C(3)	2.521(20)
Mg(1)-C(4)	2.255(19)	C(1) -C(2)	1.424(28)
C(1) -C(41)	1.479(28)	C(2) -C(3)	1.423(28)
C(3) -C(4)	1.476(26)	C(4) -C(51)	1.476(25)
Bond angles around the Mg atom			
C(1)-Mg-O(1)	174.4(7)	C(1)-Mg-C(4)	77.9(7)
C(1)-Mg-O(2)	100.3(6)	C(1)-Mg-O(3)	96.0(6)
O(1)-Mg-C(4)	98.5(6)	O(1)-Mg-O(2)	85.3(5)
O(1)-Mg-O(3)	82.0(5)	C(4)-Mg-O(2)	127.8(6)
C(4)-Mg-O(3)	119.7(6)	O(2)-Mg-O(3)	112.3(6)

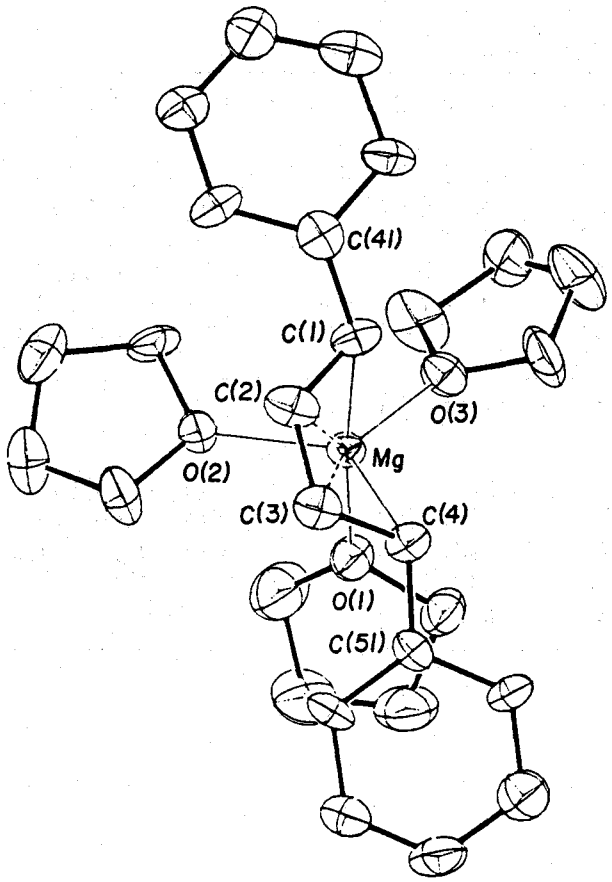

Fig. 1-3. Molecular structure of $Mg(THF)_3$(s-*cis*-PhCH=CH-CH=CHPh).

angles are very close to the corresponding angle of η^4-coordinated diene complex of $ZrCp_2$(2,3-dimethylbutadiene) (84.4°)[1] and are larger than those of Fe(CO)(1,4-diphenylbutadiene) (66.3, 67.1°).[19]

The geometry of butadiene ligand is also interesting. The C(1)-C(2) (1.42Å) and C(2)-C(3) (1.42Å) bond distances are identical with each other but slightly shorter than that of C(3)-C(4) (1.48Å). The C(2)-C(1)-C(41) bond angle (117.1°) is close to that of the sp^2 carbon in contrast to the C(3)-C(4)-C(51) bond angle (113.2°) being close to that of the sp^3 carbon. The relatively large deformation of butadiene ligand from the geometry of conventional η^4-diene or 2-butene-1,4-diyl coordination may result from the trigonal bipyramidal coordination of magnesium atom. Though rather low accuracy of the molecular parameters observed in the present compound, the structure determination of this complex is valuable to understand the correlation between the structure and the unique behavior observed generally for magnesium-diene complexes.

1-2. Unique Bonding and Geometry in η^5-Cyclopentadienyltantalum-Diene Complexes

The X-ray and NMR analyses of the s-*cis* isomers of zirconium-1,3-diene complexes revealed that they have the novel bent metallacyclopent-3-ene structure (**2**) in which the dihedral angle between the planes defined by C(1),M, C(4) and C(1), C(2), C(3), C(4) atoms are greater than 90° and the C(2)-C(3) bond is significantly shorter than C(1)-C(2) and C(3)-C(4) bonds.[20-22] The vast majority of the diene complexes reported so far have the s-*cis*-η^4-1,3-diene structure (**1**) having bond lengths of C(2)-C(3)≥C(1)-C(2) [C(3)-C(4)] and M-C(1)≥M-C(2), the dihedral angles of which are generally acute, <90°.

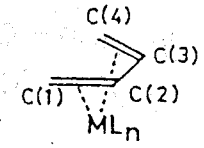

1

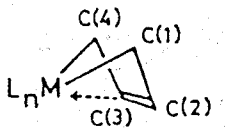

2

The marked contrast in structure and reactivity observed between the group 4 metal-diene and the group 8-10 metal-diene complexes prompted me to proceed the structure determination of the corresponding tantalum-diene complexes to clarify the structural chemistry distinctive to the group 5 metal-diene complexes.

1-2-1. Mode of diene coordination in tantalum-mono(diene)complexes

With the advent of reactive new bifunctional organomagnesium reagents, a series of new tantalum-diene complexes, $CpTaCl_2$(diene) and Cp^*TaCl_2(diene) [Cp^*=pentamethylcyclopentadienyl], has first been prepared according to the reaction shown below.

$$(\eta\text{-}C_5R^1{}_5)TaCl_4 + \frac{1}{n}MgCH_2CR^2{=}CR^3CH_2 \longrightarrow$$

R^1, H; CH_3

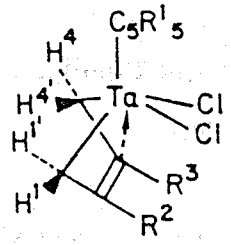

8, $R^{1\text{-}3}$=H **11**, R^1=CH_3; $R^{2,3}$=H
9, $R^{1\text{-}2}$=H; R^3=CH_3 **12**, R^1=R^3=CH_3; R^2=H
10, R^1=H; $R^{2,3}$=CH_3 **13**, $R^{1\text{-}3}$=CH_3

From the NMR studies, the structure of **8** may be expressed as the bent metallacyclopent-3-ene structure **14** or **15** rather than the conventional metal-η^4-1,3-diene structure **16**(*supine*) or **17**(*prone*).

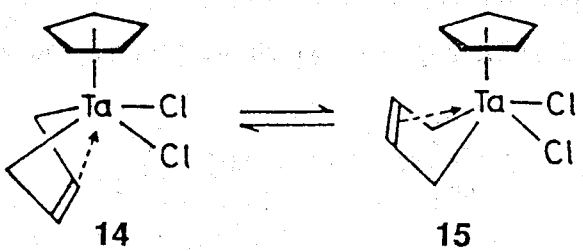

14 **15**

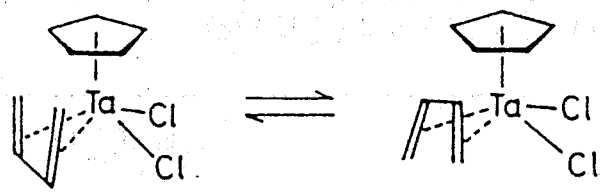

16 (supine) **17** (prone)

The molecular structure of **8** was established by single-crystal X-ray diffraction technique. The measurement of X-ray diffraction data and the analysis and refinement of the crystal structure were proceeded analogously as the complex $Zr(\eta^5\text{-}C_5H_5)_2$(s-*trans*-PhCH=CH-CH=CHPh). The crystal data and parameters for structure determination for complex **8** are summarized in Table 1-8. The final atomic coordinates are listed in Table 1-9. The interatomic bond distances and angles are summarized in Table 1-10. Different view of the molecule, along with the numbering scheme adopted, are displayed in Fig. 1-4. The structure of **8** is best described as having the geometry **14**, where butadiene is bound to the metal in 1,4-fashion and the Cp ring is symmetrically pentahapto-bound with the Ta-C distances in a narrow range. The coordination sphere of the Ta atom resembles that found in a saturated metallacycle, $Cp^*TaCl_2(C_4H_8)$ (**18**).[23]

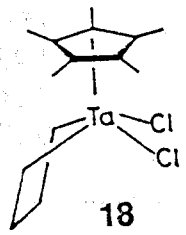

18

However, the bond distances and angles for **8** significantly differ from those for **18** in the following aspects. (1) The C(2)-C(3) distance (1.375Å) is shorter than the C(2)-C(3) bond distance of **18** reflecting the 2-butene-1,4-diyl structure. The distance is among the shortest C(2)-C(3) bond distances reported for metal-diene complexes and close to or even slightly shorter than those in Cp_2Zr(diene) complexes (1.391-1.398Å)[20-22] and $Fe(CO)_4(C_4F_6)$ (1.38Å).[24] (2) The C(1)-C(2) (1.458Å) and C(3)-C(4) (1.453Å) bond distances for **8** are

Table 1-8. Crystal Data and Experimental Parameters for X-Ray Structure Determination of $(\eta^5\text{-}C_5H_5)TaCl_2(C_4H_6)$ (**8**)

Formula	$C_9H_{11}Cl_2Ta$
Formula weight	371.0
Crystal system	monoclinic
Space group	$P2_1/n$
Temp., °C	20
a,[a] Å	6.615(1)
b, Å	10.962(1)
c, Å	14.348(2)
β, deg	97.02(1)
V, Å^3	1032.6(2)
Z	4
D_{calcd}, g cm^{-3}	2.386
$F(000)$, e	688
μ(MoKα), cm^{-1}	109.9
Crystal size, mm	0.45x0.20x0.10
2θ range,[b] deg	4<2θ<75
Scan width, deg in 2θ	2.0+0.70tanθ
Scan speed, deg min^{-1}	4.0
Background count, s	5
Reflections measured	5425
Reflections observed[c]	3876
Radiation damage	no
No. of variables	153
GOF[d]	1.438
R[e]	0.048
R_w[f]	0.073

[a]Least-squares refinement of the θ values for 30 reflections with 2θ>25°. [b]Intensity data were collected on a Rigaku four-circle diffractometer using graphite-monochromatized MoKα radiation by the θ-2θ scan method. [c]$|F_o|>3\sigma(F_o)$. [d]$[\Sigma w(|F_o|-|F_c|)^2/(n-m)]^{1/2}$, where n and m are the No. of reflections used and variables refined, respectively. [e]$R=\Sigma(|F_o|-|F_c|)/\Sigma|F_o|$. [f]$R_w=[\Sigma w(|F_o|-|F_c|)^2/\Sigma w|F_o|^2]^{1/2}$, $w=[\sigma^2(F_o)+g(F_o)^2]^{-1}$, and g=0.003.

Table 1-9. Final Atomic Coordinates and Equivalent Isotropic Temperature Factors for Nonhydrogen Atoms in $(\eta^5\text{-}C_5H_5)TaCl_2(C_4H_6)$ (**8**) with Estimated Standard Deviations in Parentheses[a]

atom	x	y	z	B_{eq}
Ta	0.373958(6)	0.259463(3)	0.1083120(14)	2.42
Cl(1)	0.65982(5)	0.33367(3)	0.033953(14)	4.5
Cl(2)	0.58747(6)	0.101284(19)	0.183084(14)	4.4
C(1)	0.1248(3)	0.11806(9)	0.08437(6)	4.4
C(2)	0.2484(3)	0.08931(9)	0.00987(6)	4.3
C(3)	0.2859(3)	0.18344(10)	-0.04899(5)	4.3
C(4)	0.1961(3)	0.30120(10)	-0.03245(5)	3.8
C(21)	0.1345(3)	0.33259(11)	0.20752(6)	5.2
C(22)	0.3140(3)	0.30724(9)	0.26740(5)	4.7
C(23)	0.4687(3)	0.38709(10)	0.24355(6)	4.9
C(24)	0.3769(4)	0.46404(8)	0.17045(7)	5.8
C(25)	0.1719(3)	0.42998(9)	0.14775(6)	5.1

[a]Positional parameters are in fraction of cell edges and B_{eq} is the equivalent isotropic temperature factors calculated from the corresponding anisotropic thermal parameters.

Table 1-10. Interatomic Bond Distances (Å) and Angles (°) in (η^5-C_5H_5)$TaCl_2(C_4H_6)$ (**8**) with Estimated Standard Deviations in Parentheses

Atoms	Distance	Atoms	Distance
Ta-Cl(1)	2.423(3)	C(1) -C(2)	1.458(16)
Ta-Cl(2)	2.405(3)	C(2) -C(3)	1.375(16)
Ta-C(1)	2.258(12)	C(3) -C(4)	1.453(16)
Ta-C(2)	2.424(11)	C(21)-C(22)	1.405(17)
Ta-C(3)	2.410(12)	C(21)-C(25)	1.410(17)
Ta-C(4)	2.257(11)	C(22)-C(23)	1.420(17)
Ta-C(21)	2.393(13)	C(23)-C(24)	1.423(19)
Ta-C(22)	2.421(12)	C(24)-C(25)	1.406(19)
Ta-C(23)	2.412(12)	Mean[d] C-H	1.03(13) (0.89-1.10)
Ta-C(24)	2.413(15)		
Ta-C(25)	2.405(12)		
Ta-CCP[a]	2.088		
Ta-M1[b]	1.811		
Ta-M2[c]	1.714		

Atoms	Angle	Atoms	Angle
Cl(1)-Ta-Cl(2)	89.5(1)	C(1) -C(2) -C(3)	116.6(10)
C(1) -Ta-C(4)	73.3(4)	C(2) -C(3) -C(4)	117.3(10)
C(2)-C(1)-Ta	78.2(7)	C(22)-C(21)-C(25)	108.9(11)
C(3)-C(4)-Ta	77.7(7)	C(21)-C(22)-C(23)	108.1(10)
CCP -Ta-M1	113.4	C(22)-C(23)-C(24)	106.7(11)
CCP -Ta-M2	120.1	C(23)-C(24)-C(25)	109.0(12)
M1 -Ta-M2	126.5	C(24)-C(25)-C(21)	107.2(11)
		Mean[d] C-C-H(diene)	121(7) (115-125)
		C-C-H(Cp)	126(7) (121-131)
		H-C-H	119(11) (114-124)

[a]CCP: centroid of cyclopentadienyl ligand (Cp). [b]M1: midpoint of C(1) and C(4). [c]M2: midpoint of Cl(1) and Cl(2). [d]Only mean values of bond distances and angles involving hydrogen atoms are listed. The individual e.s.d's are in the first set of parentheses after the value and the ranges are in the second set.

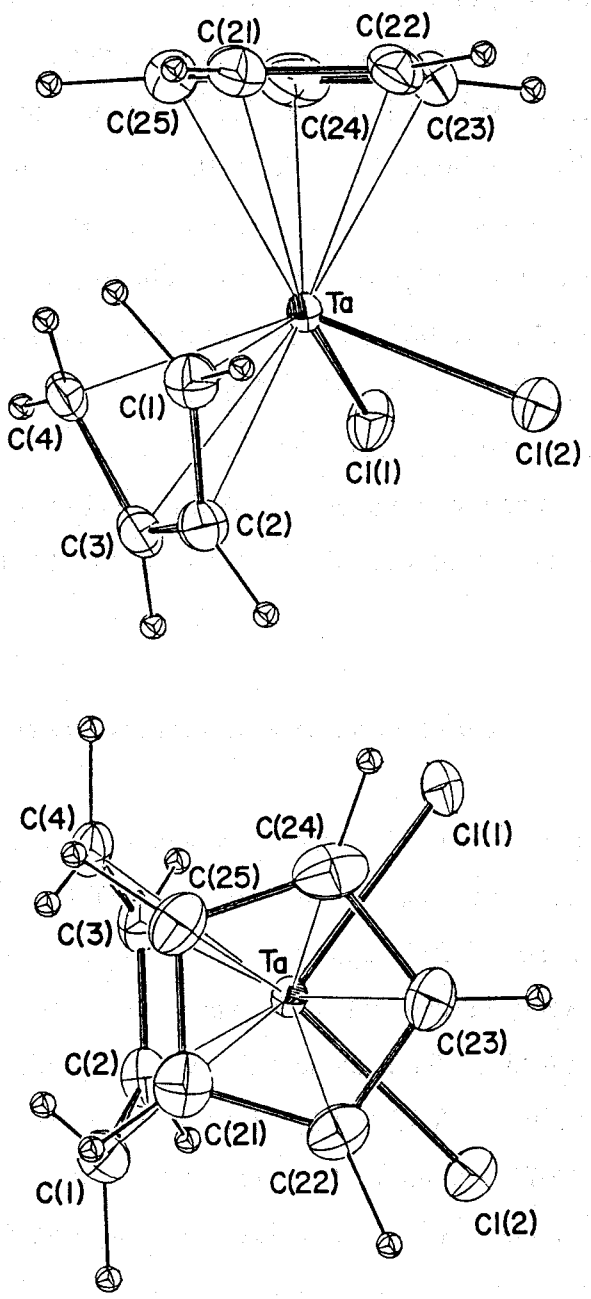

Fig. 1-4. Molecular structure of $(\eta^5\text{-}C_5H_5)TaCl_2(C_4H_6)$ (**8**).

shorter than that of the C(1)-C(2) single bond in **18** (1.552Å) but nearly equal to those (1.451-1.474Å) observed for Cp_2Zr(diene).[20-22] (3) Ta-C(2) (2.424Å) and Ta-C(3) (2.410Å) bond distances are much shorter than those (2.869Å) in **18**, while Ta-C(1) (2.258Å) and Ta-C(4) (2.257Å) bonds are slightly longer than the Ta-C(1) and Ta-C(4) bonds (2.217Å) in **18**. (4) The bent angle between the C(1)-C(2)-C(3)-C(4) and C(1)-Ta-C(4) planes (94.9°) is remarkably small compared with that (116.3°) for **18**. The value is intermediate between the angle for Cp_2Zr(diene) (112.0-123.4°) and that for the diene complexes of group 8-10 transition metals (<90°). (5) The C(1)-C(2)-C(3) (116.6°) and C(2)-C(3)-C(4) (117.3°) angles are larger than that in **18** (110.1°) but smaller than those (121.2-129.7°) for Cp_2Zr(diene) complexes. These differences support the idea that a strong π-interaction exists between the metal and the unsaturated C(2)-C(3) bond in **8**.

1-2-2. Mode of diene coordination in tantalum-bis(diene)complexes

$CpTa(diene)_2$ and $Cp^*Ta(diene)_2$ containing two diene ligands in a molecule were prepared in good yield by treating $CpTaCl_4$ or Cp^*TaCl_4 with 2 equiv of (2-butene-1,4-diyl)magnesium or its higher homologous in tetrahydrofuran. Recrystallization from hexane at -20°C followed by sublimation gave complexes **19-23** as diamagnetic pale yellow crystals. Under argon the tantalum-diene complexes, **8-13** and **19-23**, are thermally stable indefinitely, but in air complexes **19-20** decomposed in a few minutes and complexes **8-13** and **21-23** in several hours. All the complexes are immediately decomposed in protic solvents.

In general, the following three structures are to be considered for metal-bis(diene)complexes. Most of the bis(diene)metal complexes of the type $LM(diene)_2$ including $FeL(butadiene)_2$(L = CO,PR_3),[25,26] $Ru(CO)(diene)_2$,[27] $RhCl(butadiene)_2$,[28,29] $IrCl(butadiene)_2$,[30] and $MnL(butadiene)_2$(L=PR_3,

$(\eta\text{-}C_5R^1{}_5)TaCl_4 + \text{-}[\text{-}MgCH_2CR^2{=}CR^3CH_2\text{-}]_n\text{-} \longrightarrow$

R^1, H; CH_3

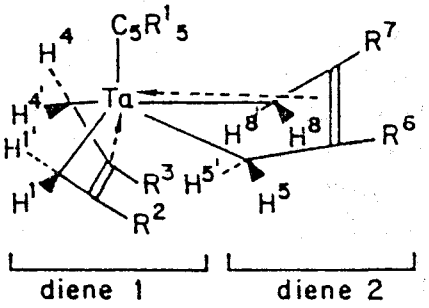

19, $R^{1\text{-}3}$=$R^{6,7}$=H　　**21**, R^1=CH_3; $R^{2,3}$=$R^{6,7}$=H

20, R^1=H; $R^{2,3}$=$R^{6,7}$=CH_3　　**22**, R^1=R^3=R^7=CH_3; R^2=R^6=H

23, $R^{1\text{-}3}$=$R^{6,7}$=CH_3

CO)[31,32] assume the structure **24** with nearly C_{2v} symmetry where two diene ligands lie *supine* if the Cp ring looks upward. The complexes with structure **25** or **26** where two dienes lie in *prone-prone* or *supine-prone* have not been reported so far (see ref 33 for nomenclature). The NMR studies on the complexes **19-23** indicate that these complexes assume structure **26**, the first example of this type of complexation where two diene entities are magnetically nonequivalent. The validity of this assignment was eventually justified by X-ray analysis of **20** and **23** and also by MO calculations.[34]

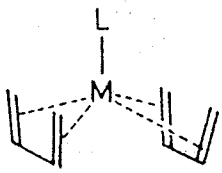

24
(supine-supine)

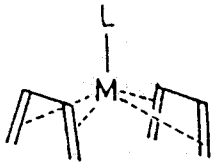

25
(prone-prone)

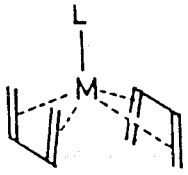

26
(supine-prone)

The crystal data and parameters for structure determination are summarized in Table 1-11. Final atomic coordinates are listed in Table 1-12. The molecular structure of **20** deduced from X-ray analysis is shown in Fig. 1-5. The molecule locates on a crystallographic mirror symmetry which passes through Ta, C(23) atoms and midpoints of C(2)-C(2'), C(21)-C(21'), and C(12)-

Table 1-11. Crystal Data and Experimental Parameters for X-Ray Structure Determination of $(\eta^5\text{-}C_5H_5)Ta(C_6H_{10})_2$ (**20**) and $(\eta^5\text{-}C_5Me_5)Ta(C_6H_{10})_2$ (**23**)

Complex	**20**	**23**
Formula	$C_{17}H_{25}Ta$	$C_{20}H_{31}Ta$
Formula weight	410.3	480.5
Crystal system	orthorhombic	monoclinic
Space group	*Pnma*	$P2_1$
Temp., °C	20	20
a,[a] Å	8.947(1)	10.468(2)
b, Å	12.291(2)	12.442(2)
c, Å	13.512(2)	8.020(1)
β, deg		106.68(2)
V, Å^3	1486.0(4)	1000.6(3)
Z	4	2
D_{calcd}, g cm^{-3}	1.834	1.594
F(000), e	800	480
μ(MoKα), cm^{-1}	72.9	54.2
Crystal size, mm	0.45x0.35x0.30	0.45x0.30x0.25
2θ range,[b] deg	4<2θ<75	4<2θ<70
Scan width, deg in 2θ	2.0+0.70tanθ	2.0+0.70tanθ
Scan speed,deg min^{-1}	8.0	8.0
Background count, s	4	4
Reflections measured	4029	3971
Reflections observed[c]	3206	3462
Radiation damage	no	no
No. of variables	207	207
GOF[d]	0.555	0.843
R[e]	0.061	0.049
R_w[f]	0.079	0.062

[a)]Least-squares refinement of the θ values for 25 (**20**) or 34 (**23**) reflections with 2θ>25°. [b)]Intensity data were collected on a Rigaku four-circle diffractometer using graphite-monochromatized MoKα radiation by the θ-2θ scan method. [c)] $|F_o|>3\sigma(F_o)$. [d)] $[\Sigma w(|F_o|-|F_c|)^2/(n-m)]^{1/2}$, where n and m are the No. of reflections used and variables refined, respectively. [e)] $R=\Sigma(|F_o|-|F_c|)/\Sigma|F_o|$. [f)] $R_w=[\Sigma w(|F_o|-|F_c|)^2/\Sigma w|F_o|^2]^{1/2}$, $w=[\sigma^2(F_o)+g(F_o)^2]^{-1}$, and $g=0.003$.

Table 1-12. Final Atomic Coordinates and Equivalent Isotropic Temperature Factors for Nonhydrogen Atoms in $(\eta^5\text{-}C_5H_5)Ta(C_6H_{10})_2$ (**20**) with Estimated Standard Deviations in Parentheses[a]

atom	x	y	z	B_{eq}
Ta	0.131600(4)	0.25000	0.4865800(15)	1.91
C(1)	0.21185(9)	0.13821(6)	0.36476(5)	3.2
C(2)	0.35361(8)	0.19502(5)	0.38304(4)	2.8
C(5)	0.49255(9)	0.12732(7)	0.40505(5)	4.2
C(11)	0.26645(9)	0.36569(5)	0.58517(4)	3.1
C(12)	0.18016(9)	0.30464(6)	0.65977(4)	2.9
C(15)	0.08197(13)	0.37370(7)	0.72968(6)	4.8
C(21)	-0.09994(10)	0.19280(8)	0.39978(6)	4.4
C(22)	-0.10405(11)	0.15632(9)	0.50130(6)	4.1
C(23)	-0.11357(11)	0.25000	0.56201(9)	4.3

[a]Positional parameters are in fraction of cell edges and B_{eq} is the equivalent isotropic temperature factors calculated from the corresponding anisotropic thermal parameters.

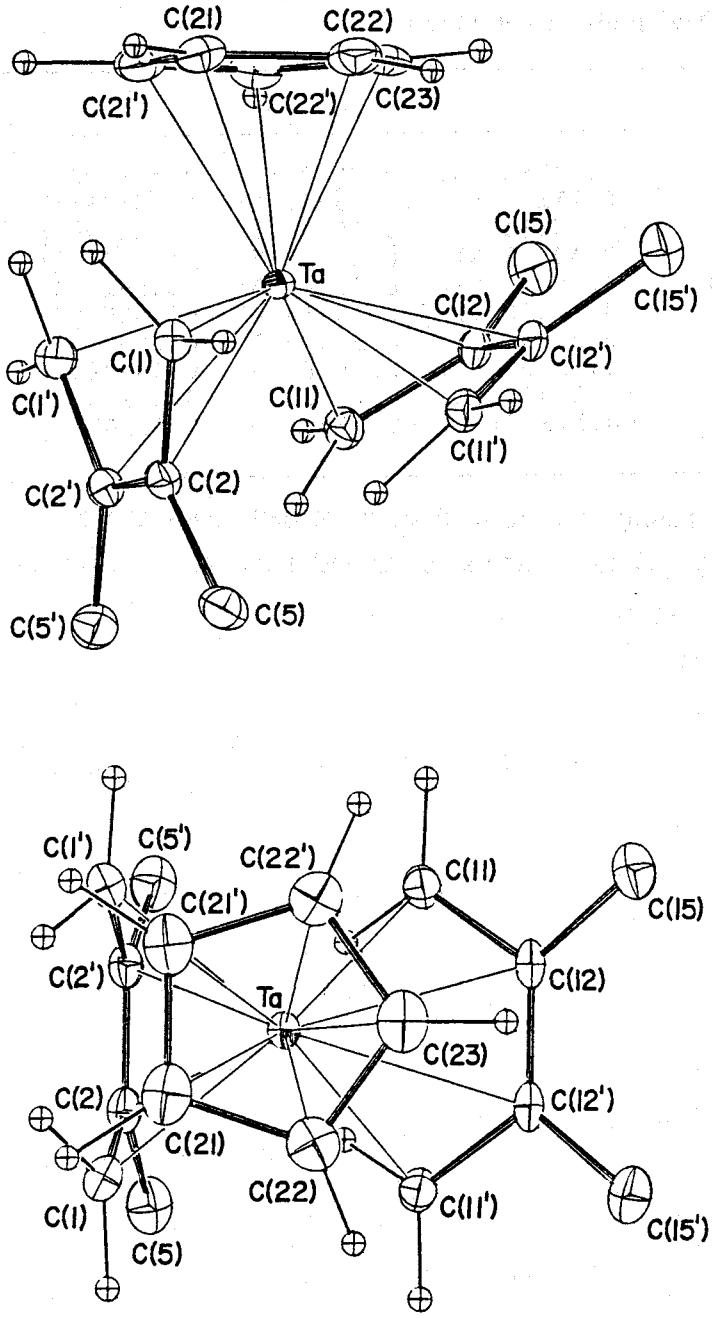

Fig. 1-5. Molecular structure of $(\eta^5\text{-}C_5H_5)Ta(C_6H_{10})_2$ (**20**).

Table 1-13. Interatomic Bond Distances (Å) and Angles (°) in (η^5-C_5H_5)Ta(C_6H_{10})$_2$ (**20**) with Estimated Standard Deviations in Parentheses

Atoms	Distance	Atoms	Distance
Ta-C(1)	2.261(8)	C(1) -C(2)	1.469(11)
Ta-C(2)	2.522(7)	C(2) -C(2')	1.352(14)
Ta-C(11)	2.292(7)	C(2) -C(5)	1.525(12)
Ta-C(12)	2.473(8)	C(11)-C(12)	1.475(11)
Ta-C(21)	2.482(11)	C(12)-C(12')	1.343(15)
Ta-C(22)	2.411(13)	C(12)-C(15)	1.544(13)
Ta-C(23)	2.419(16)	C(21)-C(22)	1.444(16)
Ta-CCP[a]	2.119	C(21)-C(21')	1.406(21)
Ta-M1[b]	1.796	C(22)-C(23)	1.416(20)
Ta-M2[c]	1.797	Mean[d] C-H	1.07(12) (0.99-1.17)

Atoms	Angle	Atoms	Angle
C(1) -Ta-C(1')	74.8(3)	C(1) -C(2)-C(2')	118.4(7)
C(11)-Ta-C(11')	76.7(3)	C(1) -C(2)-C(5)	118.5(7)
C(2)-C(1)-Ta	82.1(4)	C(5) -C(2)-C(2')	123.1(7)
C(12)-C(11)-Ta	78.8(4)	C(11)-C(12)-C(12')	120.6(7)
CCP -Ta-M1	108.5	C(11)-C(12)-C(15)	115.9(7)
CCP -Ta-M2	137.2	C(15)-C(12)-C(12')	123.3(7)
M1 -Ta-M2	114.3	C(22)-C(21)-C(21')	108.1(10)
		C(21)-C(22)-C(23)	107.4(11)
		C(22)-C(23)-C(22')	108.8(13)
		Mean[d] C-C-H(diene)	119(6) (114-123)
		C-C-H(Cp)	126(7) (121-131)
		H-C-H	120(9) (118-122)

[a,d]CCP and Mean are the same as those in Table 10. [b]M1: midpoint of C(1) and C(1'). [c]M2: midpoint of C(11) and C(11').

C(12') bonds. Selected bond distances and angles are summarized in Table 1-13. The tantalum atom may be described as having a pseudo-square-pyramidal geometry if the Cp group is considered to occupy only one coordination site and each of the 2,3-dimethylbutadiene ligands is assumed to bind via the two terminal carbon atoms. The most noteworthy feature is the unique orientation of the two diene ligands that comprises the *supine-prone* structure. Such type of coordination has not yet been reported. The plane of the diene-1 ligand composed of C(1), C(2), C(2'), and C(1') is nearly perpendicular to the Cp ring, the dihedral angle being 81.5°, slightly larger than that in **8** (71.9°) but smaller than that in **18** (92.5°). On the other hand, the plane of diene-2 defined by C(11), C(12), C(12'), and C(11') makes an acute angle (35.0°) with the Cp ring. The dihedral angle between the two diene planes is 63.6°. An examination of the bond lengths support as the view obtained from the NMR studies that the diene is bound in the bent 2-butene-1,4-diyl fashion rather than conventional η^4-1,3-diene coordination; i.e., both the C(2)-C(2') (1.352Å) and the C(12)-C(12') (1.343Å) bonds are shorter than the C(1)-C(2), C(1')-C(2'), C(11)-C(12), or C(11')-C(12') bonds by ca. 0.11-0.13 Å. The dihedral angles for the tantalacyclopent-3-ene moieties containing diene-1 and diene-2 are 102.5° and 100.4°, respectively, 5.5, 7.6° larger than that in **8**. The Ta-C(1) and Ta-C(11) distances (2.261 and 2.292Å) are similar to those in $CpTaCl_2(C_4H_6)$(**8**), while the Ta-C(2) (2.522Å) and Ta-C(12) (2.473Å) bonds are longer than those in **8**. Thus, the whole geometry of **20** is not superimposable to any of the geometry reported for $L_nM(diene)_2$(M: Fe, Rh, Ir, Mn) of *supine-supine* orientation. The geometry is also different from the uniquely distorted octahedral structure reported for Hf(butadiene)$_2$(1,2-bis(dimethylphosphino)ethane) where two diene ligands are in a skewed position to each other.[34)]

In order to get more detailed structural information of the coordination property of diene ligands to Ta atom, the crystal structure of Cp^*_2Ta(2,3-dimethylbutadiene) (**23**) has been carried out. The crystal data and parameters

for structure determination are summarized in Table 1-11. The final atomic coordinates are listed in Table 1-14.

The molecular structure of **23** is shown in Fig. 1-6. The important bond distances and angles are listed in Table 1-15. The molecule has no crystallographic symmetry, however, it has an approximate mirror symmetry like complex **20**. The geometrical situation of the two diene ligands surrounding the Ta atom is essentially the same as that in complex **20** except for the following. The plane of diene-2 composed of the C(11)-C(14) atoms is nearly parallel to the Cp plane, the dihedral angle being 18.5°. The significantly small dihedral angle compared with that of **20** may be attributed to the nonbonded interatomic repulsions between the methyl groups attached to the Cp and the diene-2. The interatomic distance for C(15)-C(28) and C(16)-C(28) are 3.38 and 3.43Å, respectively. So far such a planar metal-diene skeleton has only been reported for the metallacyclic structure of $Fe(CO)_4(CF_2CF{=}CFCF_2)$ where the π-interaction between Fe and the C(2)-C(3) double bond is absent.[28,29] The dihedral angle between the Cp and diene-1 planes (83.5°) is comparable to that for **20**. As a consequence, the dihedral angle between the two diene planes becomes larger (78.6°) by 15° than that observed for **20**.

The structural parameters are of limited accuracy due to the rather big thermal vibrations at 20°C. Therefore, The X-ray diffraction data of **23** were also collected at -60°C to estimate the effect of thermal motion of the molecule in the crystal lattice. The accuracy of the molecular structure of **23** at 20°C has not been improved significantly by redetermination of the structure at -60°C (R=0.059, R_w=0.070).[36] However, the comparison of the X-ray data obtained at both temperatures revealed that the thermal motion of diene-2 fragment is more temperature dependent than that of the diene-1. This result agrees with the NMR prediction that the diene-2 ligand is far more fluxional than the diene-1 at room temperature.

Extended-Huckel MO calculations revealed that the observed orientation

Table 1-14. Final Atomic Coordinates and Equivalent Isotropic Temperature Factors for Nonhydrogen Atoms in $(\eta^5\text{-}C_5Me_5)Ta(C_6H_{10})_2$ (**23**) with Estimated Standard Deviations in Parentheses[a]

atom	x	y	z	B_{eq}
Ta	0.180970(3)	0.25000	0.235398(5)	2.84
C(1)	-0.00671(10)	0.34166(9)	0.2442(3)	4.2
C(2)	-0.06907(10)	0.2610(3)	0.1015(3)	4.6
C(3)	-0.01986(9)	0.26171(14)	-0.03480(18)	3.7
C(4)	0.09381(11)	0.33371(8)	-0.02816(18)	3.8
C(5)	-0.18471(11)	0.19913(13)	0.1180(3)	6.0
C(6)	-0.07154(13)	0.18652(10)	-0.1860(3)	5.0
C(11)	0.20047(12)	0.10995(8)	0.0769(3)	4.1
C(12)	0.2771(3)	0.05670(14)	0.2350(5)	5.2
C(13)	0.2307(3)	0.05971(13)	0.3727(4)	5.2
C(14)	0.09234(14)	0.12724(10)	0.3627(3)	5.3
C(15)	0.40849(16)	0.01397(11)	0.2377(4)	6.6
C(16)	0.29479(19)	0.01909(15)	0.5695(4)	8.2
C(21)	0.25642(15)	0.42406(10)	0.3948(3)	3.5
C(22)	0.31258(12)	0.34653(10)	0.49571(19)	4.3
C(23)	0.40887(11)	0.29135(8)	0.4188(3)	4.5
C(24)	0.39792(10)	0.33685(8)	0.26340(19)	3.6
C(25)	0.30570(16)	0.42751(11)	0.2495(3)	3.3
C(26)	0.1818(3)	0.51680(15)	0.4430(6)	10.9
C(27)	0.2960(3)	0.3356(3)	0.6760(3)	12.1
C(28)	0.51762(18)	0.21970(12)	0.5272(5)	8.9
C(29)	0.48170(14)	0.30941(14)	0.1380(4)	7.0
C(30)	0.2972(3)	0.50750(15)	0.1016(4)	8.7

[a]Positional parameters are in fraction of cell edges and B_{eq} is the equivalent isotropic temperature factors calculated from the corresponding anisotropic thermal parameters.

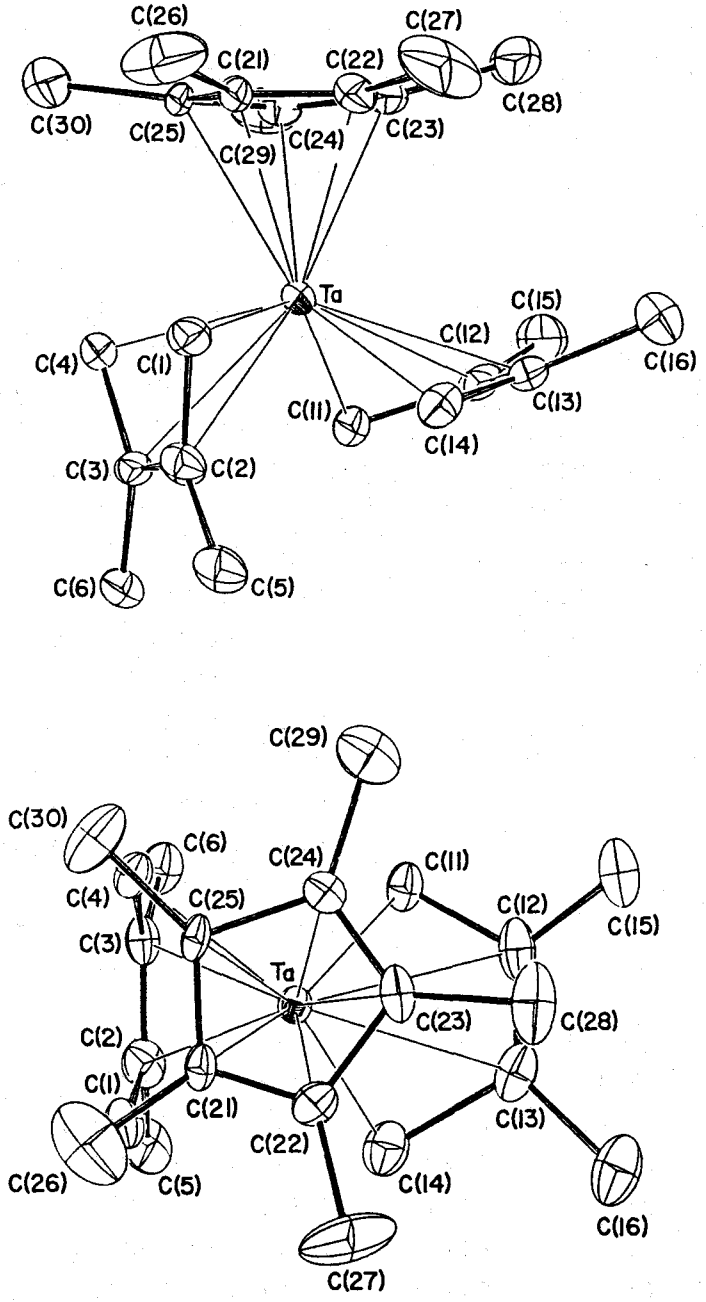

Fig. 1-6. Molecular structure of $(\eta^5\text{-}C_5Me_5)Ta(C_6H_{10})_2$ (23).

Table 1-15. Interatomic Bond Distances (Å) and Angles (°) in (η^5-C_5Me_5)Ta(C_6H_{10})$_2$ (**23**) with Estimated Standard Deviations in Parentheses

Atoms	Distance	Atoms	Distances
Ta-C(1)	2.29(2)	C(1) -C(2)	1.52(4)
Ta-C(2)	2.53(4)	C(2) -C(3)	1.34(4)
Ta-C(3)	2.55(2)	C(3) -C(4)	1.48(2)
Ta-C(4)	2.30(1)	C(2) -C(5)	1.47(4)
Ta-C(11)	2.20(1)	C(3) -C(6)	1.50(3)
Ta-C(12)	2.61(3)	C(11)-C(12)	1.45(3)
Ta-C(13)	2.60(2)	C(12)-C(13)	1.33(4)
Ta-C(14)	2.19(2)	C(13)-C(14)	1.66(3)
Ta-C(21)	2.52(2)	C(12)-C(15)	1.47(4)
Ta-C(22)	2.46(1)	C(13)-C(16)	1.61(3)
Ta-C(23)	2.47(2)	C(21)-C(22)	1.29(2)
Ta-C(24)	2.47(1)	C(21)-C(25)	1.40(2)
Ta-C(25)	2.55(2)	C(22)-C(23)	1.49(2)
Ta-CCP[a]	2.19	C(23)-C(24)	1.34(2)
Ta-M1[b]	1.86	C(24)-C(25)	1.47(2)
Ta-M2[c]	1.67	C(21)-C(26)	1.51(4)
		C(22)-C(27)	1.51(4)
		C(23)-C(28)	1.51(3)
		C(24)-C(29)	1.55(2)
		C(25)-C(30)	1.53(3)

Atoms	Angle	Atoms	Angle
C(1) -Ta -C(4)	71.7(5)	C(12)-C(13)-C(14)	120(2)
C(11)-Ta -C(14)	80.1(5)	C(12)-C(13)-C(16)	131(2)
C(2) -C(1) -Ta	80(2)	C(14)-C(13)-C(16)	109(2)
C(3) -C(4) -Ta	82(1)	C(22)-C(21)-C(25)	110(2)
C(12)-C(11)-Ta	89(1)	C(22)-C(21)-C(26)	126(2)
C(13)-C(14)-Ta	84(1)	C(25)-C(21)-C(26)	122(2)
CCP -Ta -M1	103.3	C(21)-C(22)-C(23)	109(1)
CCP -Ta -M2	140.7	C(21)-C(22)-C(27)	121(2)
M1 -Ta -M2	115.9	C(23)-C(22)-C(27)	129(2)

Table 15 (cont.)

Atoms	Angle	Atoms	Angle
C(1) -C(2) -C(3)	115(3)	C(22)-C(23)-C(24)	108(1)
C(1) -C(2) -C(5)	118(3)	C(22)-C(23)-C(28)	121(2)
C(3) -C(2) -C(5)	127(3)	C(24)-C(23)-C(28)	129(2)
C(2) -C(3) -C(4)	118(2)	C(23)-C(24)-C(25)	106(1)
C(2) -C(3) -C(6)	122(2)	C(23)-C(24)-C(29)	127(1)
C(4) -C(3) -C(6)	120(2)	C(25)-C(24)-C(29)	127(1)
C(11)-C(12)-C(13)	118(2)	C(21)-C(25)-C(24)	108(1)
C(11)-C(12)-C(15)	117(2)	C(21)-C(25)-C(30)	135(2)
C(13)-C(12)-C(15)	124(2)	C(24)-C(25)-C(30)	117(2)

[a,b]CCP and M1 are the same as those in Table 1-10. [c]M2: midpoint of C(11) and C(14).

of the butadiene ligand in $CpTaCl_2(C_4H_6)$ (lying *supine*) is 15.7 kcal more stable than the geometrical isomer where the butadiene lying *prone* is coordinated to metal. Among the three structures considered for $CpTa(butadiene)_2$, the observed structure is computed to the most stable, 28.4 kcal more stable than the *supine-supine* geometry where the two dienes are oriented toward the Cp ring and 23.3 kcal more stable than another isomer (*prone-prone*) where the CH_2 groups at the diene termini are pointed away form the Cp ring.

The molecular structures of tantalum-diene complexes thus far obtained include interesting characteristics compared with the conventional metal-diene complexes. To extract the unique structural features the correlation plots between some structural parameters in these complexes are considered. The correlation between the bent angle (θ) subtended by the C(1)-M-C(4) and C(1)-C(4) planes and the difference in M-C bond distances (Δd) defined by Δd=[d(M-C(1)+d(M-C(4))]/2-[d(M-C(2))+d(M-C(3))]/2 are plotted in Fig. 1-7a. The bent angles for group 7 and 8-10 metal-diene complexes are in the narrow range 80-85° and the Δd ranges from 0 to 0.1 Å; i.e., the M-C(1) and M-C(4) bonds are nearly equal or slightly longer than the M-C(2) or M-C(3) bond. On the other hand, the bent angles in the group 4 and 5 metal complexes are larger than 90° and vary over a wide range, 95-120°, with a corresponding change in Δd of -0.4 to 0.0 Å. Thus the bent angles increase with decreasing Δd. The observed structural parameters for the group 4 and 5 metal complexes resemble those found for a magnesium-diene adduct, $Mg(PhCHCH=CHCHPh)(THF)_3$,[37] rather than those for the group 7 and 8-10 metal complexes.

As a rough estimate, a linear correlation is also observed between the bent angle and the difference in bond lengths defined by Δl=[l(C(1)-C(2))+l(C(3)-C(4))]/2-l(C(2)-C(3)) as shown in Fig. 1-7b. The bent angle (θ) increases with an increase of Δl. Thus the Δl for group 7 and 8-10 metal-diene complexes varies from -0.1 to 0.0Å while the Δl for Mg-, Zr-, Hf-, and Ta-diene complexes ranges from 0.0 to 0.2Å. The points for tantalum complexes (Ta-2,

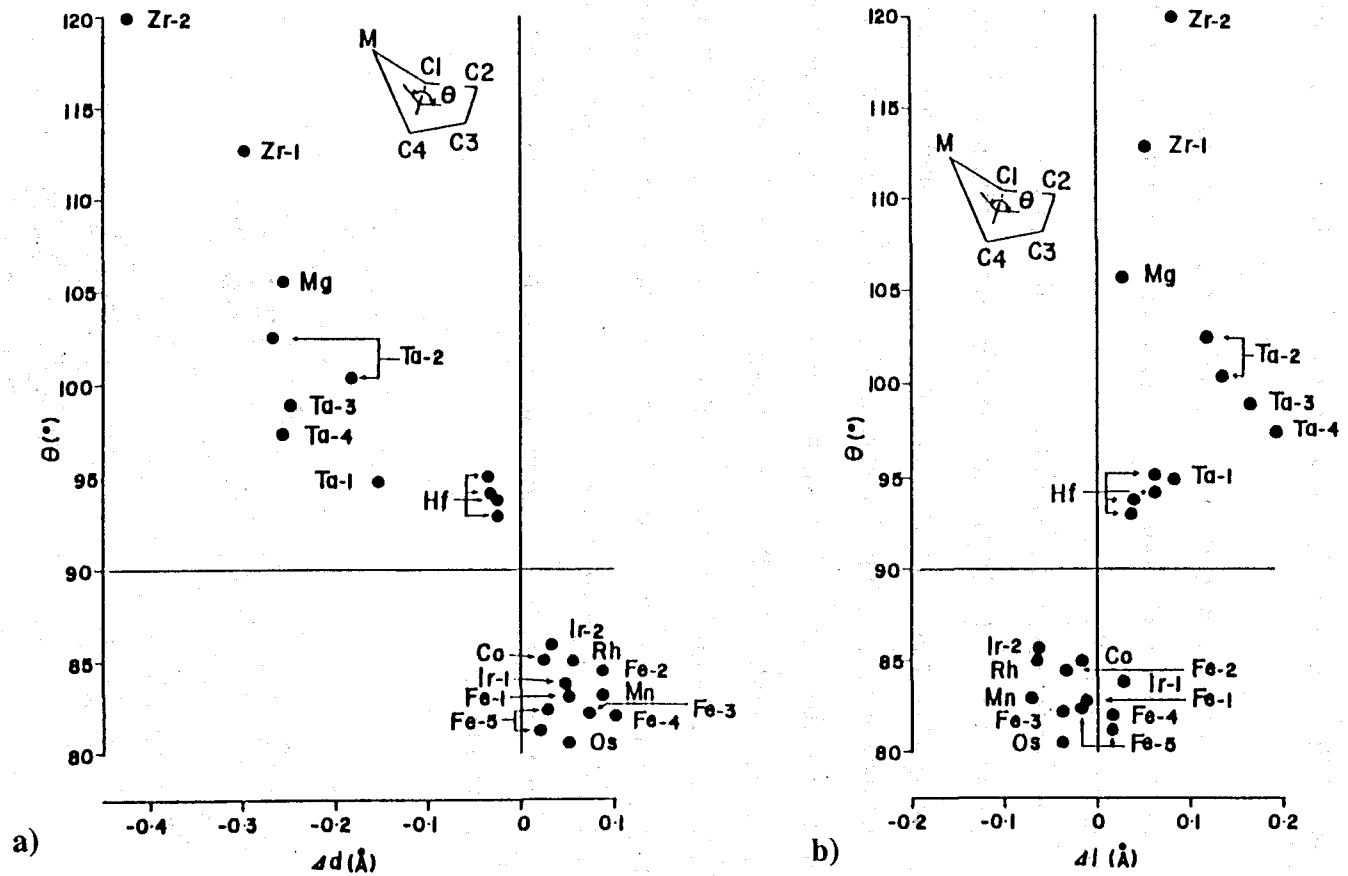

Fig. 1-7. Correlation plots between the bent angle (θ) and the metal-carbon distance (*d*) or the carbon-carbon bond length (*l*) in the metal-diene complexes.

Ta-3) deviate slightly from the straight line even when the positional ambiguity is considered.

1-2-3. Mode of diene coordination in tantalum-mixed bis(diene) complex

From the structural studies on the tantalum-bis(diene) complexes, the interesting *supine-prone* (**26**) coordination geometry was found instead of *supine-supine* structure (**24**).

It is expected that the difference of steric and electrostatic characteristics between butadiene and 2,3-dimethylbutadiene may reveal additional parameters to modify the coordination geometry of the bis(diene) complexes. Mixed bis(diene) complexes of tantalum have been thus synthesized in a stepwise manner either by reaction of $TaCl_2L$(butadiene) of *supine*(*exo*) geometry (L=C_5Me_5, C_5H_5) with (2,3-dimethyl-2-butene-1,4-diyl)magnesium or by reaction of $TaCl_2L$(2,3-dimethylbutadiene) of *supine* geometry with (2-butene-1,4-diyl)magnesium. NMR spectroscopy suggested that the initial geometry of the coordinated diene changes from *supine* to *prone*(*endo*) in the former reaction while, in the latter reaction, the *supine* geometry of the 2,3-dimethylbutadiene ligand was maintained.

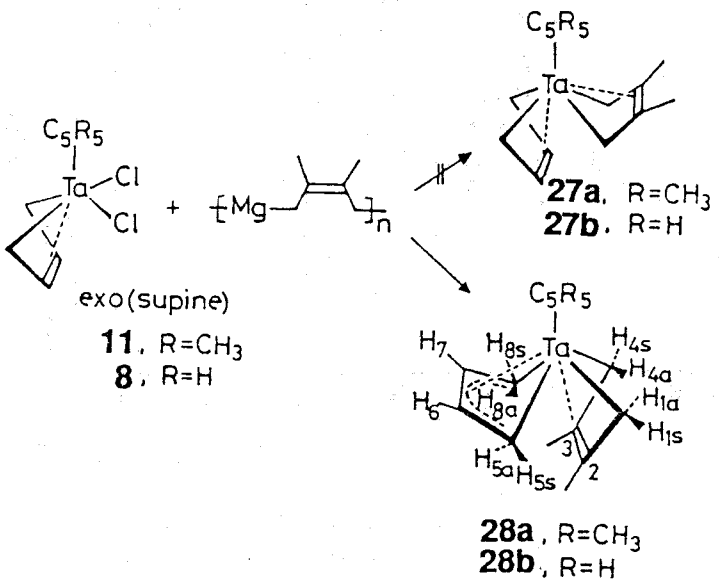

The X-ray diffraction study of $Ta(C_5Me_5)$(butadiene)(2,3-dimethylbutadiene) clearly confirms the structure **28a** where the s-*cis* butadiene lies *prone*. The crystal data and important parameters for structure determination are summarized in Table 1-16. Final atomic coordinates are listed in Table 1-17, and relevant interatomic bond distances and angles are in Table 1-18. The ORTEP drawings of **28a** are given as two different projections in Fig. 1-8 with atomic numbering scheme. Table 1-19 summarizes the geometrical parameters to define the coordination sphere of the Ta atom in **28a** in comparison with those in $Ta(C_5H_5)$(2,3-dimethylbutadiene)$_2$ (**20**) and $Ta(C_5Me_5)$(2,3-dimethylbutadiene)$_2$ (**23**). Marked difference is observed in he dihedral angle θ_2 among **28a**, **20**, and **23**. The magnitude of θ_2 for **23** is remarkably larger than the magnitude in **28a** and **20**, of θ_2 and consequently α_2, the dihedral angle between C_5R_5 and *prone* diene ligands, for **23**(18.5°) becomes smaller than α_2, in **28a** (38.6°) and **20** (35.0°). The severe steric congestion between the methyl groups in C_5Me_5 and 2,3-dimethylbutadiene in **23** may imply the above difference. The α_1 angles are, however, comparable through all these complexes.

The C(2)-C(3) bond (1.373Å) in the 2,3-dimethylbutadiene moiety in **28a** is shorter by 0.07 and 0.10Å than its C(1)-C(2) and C(3)-C(4) bonds, respectively. The metal-terminal carbon bonds Ta-C(1) (2.250Å) and Ta-C(4) (2.251Å) are significantly shorter (average 0.30Å) than the Ta-C(2) and Ta-C(3) bonds. The bent angle defined by the C(1)-C(2)-C(3)-C(4) and C(1)-Ta-C(4) planes is 103.9°. Thus, the Ta-(2,3-dimethylbutadiene) unit in **28a** is best described as bent metallacyclo-3-pentene structure as commonly found for group 4A transition metal-diene complexes.[38-40] In the contrast to the above, the *prone* butadiene unit shows a short-long-short bond alternation; i. e., the external C-C bonds C(11)-C(12) and C(13)-C(14) are slightly (average 0.04Å) shorter than the internal C(12)-C(13) bonds. The bond lengths between Ta and butadiene terminal carbons [Ta-C(11) and Ta-C(14)] are only slightly longer

Table 1-16. Crystal Data and Experimental Parameters for X-Ray Structure Determination of $(\eta^5\text{-}C_5Me_5)Ta(C_4H_6)(C_6H_{10})$ (**28a**)

Formula	$C_{20}H_{31}Ta$
Formula weight	452.4
Crystal system	orthorhombic
Space group	*Pbca*
Temp., °C	20
a,[a] Å	14.173(3)
b, Å	16.524(3)
c, Å	15.244(3)
V, Å^3	3593.4(11)
Z	8
D_{calcd}, g cm^{-3}	1.672
$F(000)$, e	1792
μ(MoKα), cm^{-1}	91.7
Crystal size, mm	0.25x0.25x0.40
2θ range,[b] deg	4<2θ<65
Scan width, deg in 2θ	2.0+0.70tanθ
Scan speed, deg min^{-1}	4.0
Background count, s	5
Reflections measured	6495
Reflections observed[c]	3763
Radiation damage	no
No. of variables	315
GOF[d]	0.571
R[e]	0.061
R_w[f]	0.083

[a]Least-squares refinement of the θ values for 25 reflections with 2θ>25°. [b]Intensity data were collected on a Rigaku four-circle diffractometer using graphite-monochromatized MoKα radiation by the θ-2θ scan method. [c]$|F_o|>3\sigma(F_o)$. [d]$[\Sigma w(|F_o|-|F_c|)^2/(n-m)]^{1/2}$, where n and m are the No. of reflections used and variables refined, respectively. [e]$R=\Sigma(|F_o|-|F_c|)/\Sigma|F_o|$. [f]$R_w=[\Sigma w(|F_o|-|F_c|)^2/\Sigma w|F_o|^2]^{1/2}$, $w=[\sigma^2(F_o)+g(F_o)^2]^{-1}$, and g=0.003.

Table 1-17. Final Atomic Coordinates and Equivalent Isotropic Temperature Factors for Nonhydrogen Atoms in (η^5-C_5Me_5)Ta(C_4H_6)(C_6H_{10}) (**28a**) with Estimated Standard Deviations in Parentheses[a]

Atom	x	y	z	B_{eq}
Ta	0.24270(3)	0.45912(3)	0.10369(3)	2.58
C(1)	0.1429(9)	0.4852(8)	-0.0068(8)	4.1
C(2)	0.1189(7)	0.5554(6)	0.0446(8)	2.8
C(3)	0.0951(8)	0.5447(8)	0.1305(8)	3.5
C(4)	0.0975(8)	0.4607(8)	0.1631(9)	4.3
C(5)	0.1245(10)	0.6395(8)	0.0035(10)	4.9
C(6)	0.0704(9)	0.6155(8)	0.1904(9)	4.6
C(11)	0.2787(11)	0.5424(11)	0.2229(11)	6.3
C(12)	0.3669(10)	0.5194(9)	0.1890(12)	5.6
C(13)	0.3896(9)	0.5287(9)	0.0979(13)	6.1
C(14)	0.3260(10)	0.5636(9)	0.0384(11)	5.4
C(21)	0.2242(8)	0.3233(7)	0.0343(9)	3.1
C(22)	0.3203(7)	0.3496(6)	0.0260(7)	2.7
C(23)	0.3588(8)	0.3493(7)	0.1111(8)	3.2
C(24)	0.2851(11)	0.3329(8)	0.1715(8)	4.1
C(25)	0.2038(9)	0.3110(7)	0.1205(8)	3.5
C(26)	0.1607(10)	0.2997(8)	-0.0414(11)	4.8
C(27)	0.3714(11)	0.3601(10)	-0.0573(10)	5.5
C(28)	0.4642(9)	0.3509(8)	0.1306(11)	4.8
C(29)	0.2985(14)	0.3215(11)	0.2681(10)	6.6
C(30)	0.1149(11)	0.2754(9)	0.1581(13)	6.0

[a]Positional parameters are in fraction of cell edges and B_{eq} is the equivalent isotropic temperature factors calculated from the corresponding anisotropic thermal parameters.

Table 1-18. Interatomic Bond Distances (Å) and Angles (°) in (η^5-C_5H_5)Ta(C_4H_6)(C_6H_{10}) (**28a**) with Estimated Standard Deviations in Parentheses

(a) Bond distance

atoms		distance	atoms		distance
Ta	- C(1)	2.250(12)	Ta	- C(2)	2.537(11)
Ta	- C(3)	2.558(12)	Ta	- C(4)	2.251(14)
Ta	- C(11)	2.346(17)	Ta	- C(12)	2.409(18)
Ta	- C(13)	2.379(20)	Ta	- C(14)	2.320(16)
Ta	- C(21)	2.497(12)	Ta	- C(22)	2.430(10)
Ta	- C(23)	2.453(11)	Ta	- C(24)	2.408(15)
Ta	- C(25)	2.522(12)	C(1)	- C(2)	1.445(17)
C(2)	- C(3)	1.373(16)	C(2)	- C(5)	1.527(18)
C(3)	- C(4)	1.474(18)	C(3)	- C(6)	1.527(18)
C(11)	- C(12)	1.407(25)	C(12)	- C(13)	1.442(27)
C(13)	- C(14)	1.407(26)	C(21)	- C(22)	1.436(16)
C(21)	- C(25)	1.369(17)	C(21)	- C(26)	1.520(20)
C(22)	- C(23)	1.415(15)	C(22)	- C(27)	1.479(18)
C(23)	- C(24)	1.423(18)	C(23)	- C(28)	1.524(20)
C(24)	- C(25)	1.440(19)	C(24)	- C(29)	1.506(24)
C(25)	- C(30)	1.506(23)			

(b) Bond angle

atoms			angle	atoms			angle
C(1)	-Ta	-C(4)	74.2(5)	C(11)	-Ta	-C(14)	77.9(6)
Ta	-C(1)	-C(2)	83.7(7)	C(1)	-C(2)	-C(3)	118.6(10)
C(1)	-C(2)	-C(5)	119.5(10)	C(3)	-C(2)	-C(5)	121.8(10)
C(2)	-C(3)	-C(4)	116.2(11)	C(2)	-C(3)	-C(6)	122.3(11)
C(4)	-C(3)	-C(6)	121.5(11)	Ta	-C(4)	-C(3)	84.0(8)
C(11)	-C(12)	-C(13)	121.8(16)	C(12)	-C(13)	-C(14)	122.1(17)
Ta	-C(14)	-C(13)	74.9(11)	Ta	-C(21)	-C(22)	70.5(6)
C(22)	-C(21)	-C(25)	109.3(11)	C(22)	-C(21)	-C(26)	124.8(11)
C(25)	-C(21)	-C(26)	125.1(12)	C(21)	-C(22)	-C(23)	106.5(9)
C(21)	-C(22)	-C(27)	125.2(10)	C(23)	-C(22)	-C(27)	127.5(10)
C(22)	-C(23)	-C(24)	108.6(10)	C(22)	-C(23)	-C(28)	124.0(11)
C(24)	-C(23)	-C(28)	126.5(11)	C(23)	-C(24)	-C(25)	106.3(11)
C(23)	-C(24)	-C(29)	124.9(13)	C(25)	-C(24)	-C(29)	127.2(13)
C(21)	-C(25)	-C(24)	108.6(11)	C(21)	-C(25)	-C(30)	127.2(13)
C(24)	-C(25)	-C(30)	124.1(13)				

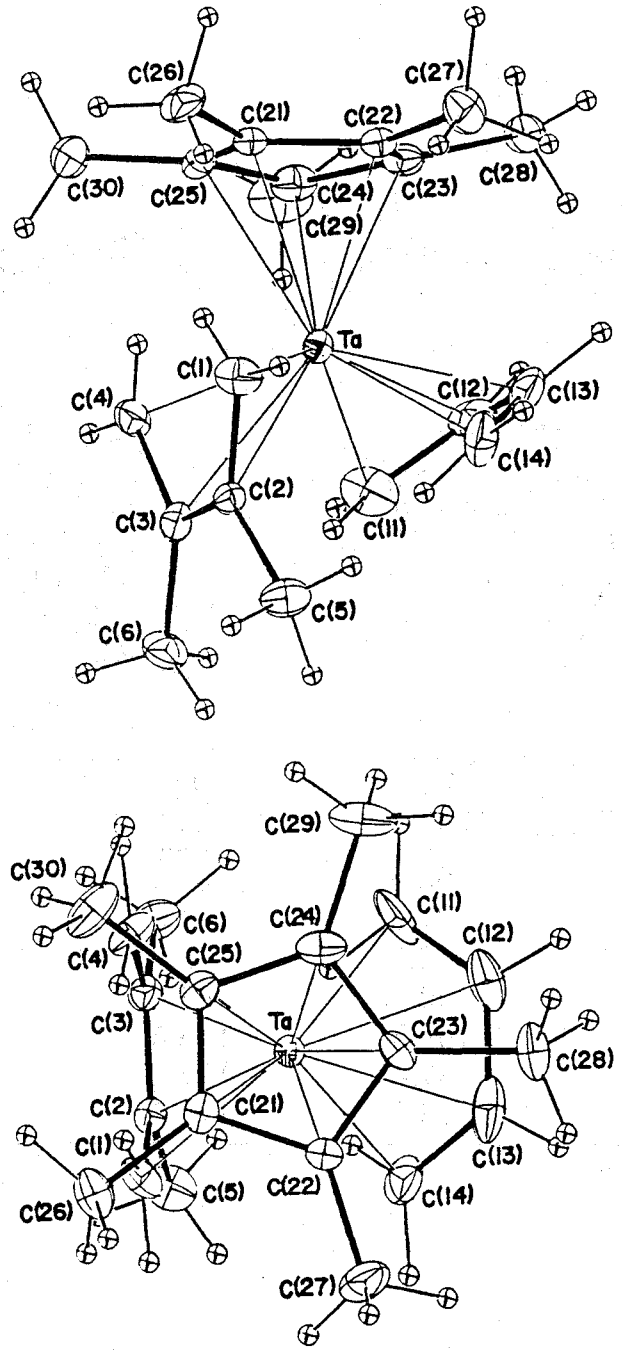

Fig. 1-8. Molecular structure of $(\eta^5\text{-}C_5Me_5)Ta(C_4H_6)(C_6H_{10})$ (**28a**).

Table 1-19. Structural Parameters in Diene Coordination for **28a** and Related Complexes

(a) Coordination geometry (°)

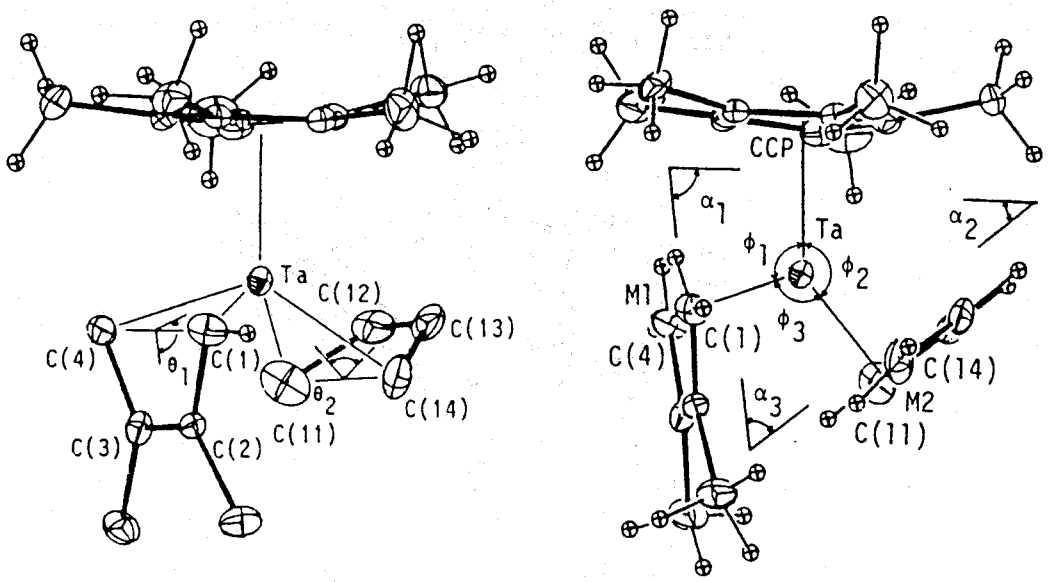

	28a	**20**	**23**
θ_1	103.9	102.5	98.9
θ_2	96.6	100.4	112.0
α_1	81.8	81.5	83.5
α_2	38.6	35.0	18.5
α_3	59.6	63.6	78.6
ϕ_1	109.5	108.5	103.1
ϕ_2	137.4	137.2	142.1
ϕ_3	113.1	114.3	114.6

Table 1-19 (cont.)

(b) Selected bond distances (Å)

	28a	**20**	**8**
Ta–C(1)	2.251 (av)	2.261	2.258 (av)
Ta–C(4)			
Ta–C(2)	2.548 (av)	2.522	2.417 (av)
Ta–C(3)			
C(1)–C(2)	1.460 (av)	1.469	1.456 (av)
C(3)–C(4)			
C(2)–C(3)	1.373	1.352	1.375
Ta–C(11)	2.333 (av)	2.292	
Ta–C(14)			
Ta–C(12)	2.394 (av)	2.473	
Ta–C(13)			
C(11)–C(12)	1.407 (av)	1.475	
C(13)–C(14)			
C(12)–C(13)	1.442	1.343	
Ta–CCP[a]	2.148	2.119	2.088
Ta–M1[b]	1.795	1.796	1.811
Ta–M2[c]	1.815	1.797	

[a]Centroid of cyclopentadienyl ligand. [b]M1: midpoint of C(1) and C(4). [c]M2: midpoint of C(11) and C(14).

than those for the Ta-butadiene internal carbons [Ta-C(12) and Ta-C(13)]. Judging from these C-C and Ta-C bond lengths, a substantial participation of the π-bonded η^4-diene character is expected for the *prone* Ta-butadiene unit in **28a**.

Although the gross structural features of **28a** are similar to those of TaCp(2,3-dimethylbutadiene)$_2$(**20**) and $TaCl_2$Cp(butadiene)(**8**), close comparison of these structures reveals several perturbations as shown in Table 1-19. The Ta-C and C-C bond lengths for the *supine* 2,3-dimethylbutadiene in **28a** is very close to those for the *supine* dienes in **20** and **8**. However, the Ta-C(11) and Ta-C(14) bonds for the *prone* butadiene unit in **28a** is significantly longer than the corresponding bonds for the *prone* diene in **20** along with the *supine* dienes in **28a**, **20**, and **8**. On the other hand, the averaged bond distance of tantalum-butadiene inner carbons, Ta-C(12) and Ta-C(13), in **28a** is remarkably shorter than the corresponding bonds in **20** along with the Ta-C(2) and Ta-C(3) bonds in **28a**, **20**, and **8**. The relatively large π-bonding property of the *prone* butadiene in **28a** may invoke such a marked difference.

The Ta-C(terminal) bond distances in the present complexes are nearly equal to the Ta-C bond distances in Ta-ethylene (2.257Å)[41] and those in tantalacyclopentenes (2.217Å),[23b] while the Ta-acetylene complexes have shortened M-C bond distances (ca. 2.07Å) because of their metal-carbene character.[42]

1-3. Molecular Structure of Novel Mono- and Bis(diene) Complexes of Niobium

The chemistry of diene complexes of early transition metals is attracting increasing interests, since these complexes display a distinctive chemistry reflecting their unique M-C bonding property and their ability to perform the highly selective reactions. As a series of structural studies of early-transition

metal-diene complexes crystal structure of novel mono- and bis(diene) complexes of niobium have been determined. A series of novel mono(diene)-niobium complexes of the type $NbCl_2(C_5H_5)$(s-*cis*-diene) (R=CH_3, H; diene=2,3-dimetylbutadiene, isoprene, butadiene) of *supine*(exo) conformation was synthesized by the 1:1 reaction of $NbCl_4(C_5R_5)$ with (2-butene-1,4-diyl)magnesium or its higher homologue. Using a similar procedure, binuclear niobium-diene complexes, $[Nb(\mu\text{-}Cl)(C_5H_5)(butadiene)]_2$ and $[Nb(\mu\text{-}Cl)(C_5H_5)(isoprene)]_2$, could also be isolated as crystals and the X-ray analysis was proceeded for the former complex. The 1:2 reaction of $NbCl_4(C_5R_5)$ with (2-butene-1,4-diyl)magnesium or its derivatives leads to $Nb(C_5R_5)$(s-*cis*-diene)$_2$ of *supine-prone*(exo-endo) conformation in good yields. The isolated binuclear Nb-diene complexes and bis(diene)niobium complexes exhibit a fairly good catalytic activity for the polymerization a butadiene, linear dimerization of isoprene, and cyclic trimerization of 1-alkynes. In order to elucidate exact structure of these complexes the X-ray crystal structure analysis of **34** has been carried out.

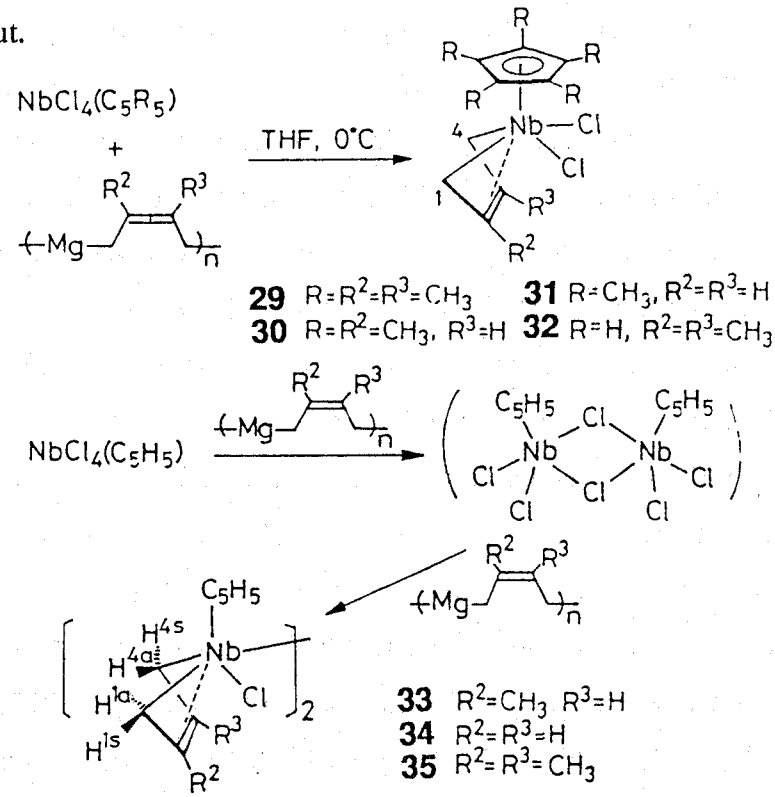

1-3-1. Coordination geometry of diene in binuclear niobium-mono(diene) complex

Crystal data and parameters for structure determination of **34** are summarized in Table 1-20 and final atomic coordinates in Table 1-21. Selected interatomic distances and angles are summarized in Table 1-22. The molecular structure of **34** shown in Fig. 1-9 clearly confirms its dimeric characteristics. The molecules contains a non-crystallographic mirror symmetry passing through the centroids of C_5H_5 rings, niobium atoms, and midpoints of butadiene inner C-C bonds. The expected additional mirror symmetry passing through two chlorine atoms and normal to the Nb(1)---Nb(2) vector is broken by the unique relative portion of two Cp ligands, i.e., one is eclipsed and another is staggered to the butadiene ligand in the molecular projection shown in Fig. 1-9.

Of particular interest is the location of the two Cp ligands (or two C_4H_4 ligands) in the *cis* position (on the same side of the Nb_2-Cl_2 core). The molecular structure however does not provide any persuasive reason for the preference of the *cis* geometry (even the *trans* geometry seems probable from the view of interspatial interaction among the ligands). The observed geometry may therefore be considered as a result of the heterogeneous reaction on the surface of the magnesium compound as mentioned before. The dihedral angle between two Cp rings (58.5°) is smaller than the dihedral angle between the two butadiene planes (83.5°). The distances of four Nb-Cl are comparable (av. 2.459Å) and are slightly longer than those reported for $[Nb(C_5H_4Me)(CO)_2Cl(\mu\text{-}Cl)]_2$ (2.459Å) and $[Nb(C_5H_4Me)(ArC{\equiv}CAr)(\mu\text{-}Cl)]_2$ (2.235Å).[43] The Nb_2Cl_2 core adopts a little folded rhombus. Its puckered angle is 10.3°. Strictly planar Nb_2Cl_2 core is reported for $[Nb(C_5H_4Me)(CO)_2Cl(\mu\text{-}Cl)]_2$ while the extensively folded Nb_2Cl_2 core is known for $[Nb(C_5H_4Me)(CO)_2(\mu\text{-}Cl)]_2$ containing semibridged two chlorine atoms.[43] The Nb-Nb distance of 3.364Å for **34** is marginally larger when compared with those of $[Nb(_5H_4Me)(CO)_2(\mu\text{-}Cl)]_2$ (3.056Å) and $[Nb(C_5H_4Me)(ArC{\equiv}CAr)(\mu\text{-}Cl)]_2$ (3.072Å), which contain planar

Table 1-20. Crystal Data and Experimental Parameters for X-Ray Structure Determination of $[(\eta^5\text{-}C_5H_5)Nb(\mu\text{-}Cl)(C_4H_6)]_2$ (**34**).

Formula	$C_{18}H_{22}Cl_2Nb_2$
Formula weight	495.1
Crystal system	monoclinic
Space group	$P2_1/c$
Temp., °C	20
a,[a] Å	12.257(2)
b, Å	8.088(1)
c, Å	19.049(4)
β, deg	108.39(1)
V, Å^3	1791.9(51)
Z	4
D_{calcd}, g cm^{-3}	1.835
$F(000)$, e	984
μ(MoKα), cm^{-1}	15.3
Crystal size, mm	0.20x0.25x0.35
2θ range,[b] deg	4<2θ<65
Scan width, deg in 2θ	2.0+0.70tanθ
Scan speed, deg min^{-1}	4.0
Background count, s	5
Reflections measured	6460
Reflections observed[c]	4674
Radiation damage	no
No. of variables	288
GOF[d]	1.360
R[e]	0.039
R_w[f]	0.064

[a)]Least-squares refinement of the θ values for 25 reflections with 2θ>25°. [b)]Intensity data were collected on a Rigaku four-circle diffractometer using graphite-monochromatized MoKα radiation by the θ-2θ scan method. [c)] $|F_o|>3\sigma(F_o)$. [d)] $[\Sigma w(|F_o|-|F_c|)^2/(n-m)]^{1/2}$, where n and m are the No. of reflections used and variables refined, respectively. [e)] $R=\Sigma(|F_o|-|F_c|)/\Sigma|F_o|$. [f)] $R_w=[\Sigma w(|F_o|-|F_c|)^2/\Sigma w|F_o|^2]^{1/2}$, $w=[\sigma^2(F_o)+g(F_o)^2]^{-1}$, and $g=0.003$.

Table 1-21. Final Atomic Coordinates and Equivalent Isotropic Temperature Factors for Nonhydrogen Atoms in $[(\eta^5\text{-}C_5H_5)Nb(\mu\text{-}Cl)(C_4H_6)]_2$ (**34**) with Estimated Standard Deviations in Parentheses[a]

Atom	x	y	z	B_{eq}
Nb(1)	0.23396(3)	-0.01166(5)	0.172732(19)	2.62
Nb(2)	0.26321(3)	0.09631(5)	0.348270(18)	2.66
Cl(1)	0.09076(8)	0.09541(13)	0.23251(6)	2.33
Cl(2)	0.41054(9)	0.02473(14)	0.28465(6)	2.61
C(11)	0.1194(5)	0.1396(7)	0.0741(3)	4.2
C(12)	0.1926(6)	0.2585(7)	0.1199(3)	4.5
C(13)	0.3115(6)	0.2378(7)	0.1392(3)	5.1
C(14)	0.3527(5)	0.0996(8)	0.1118(4)	5.3
C(21)	0.1749(5)	0.3344(6)	0.3705(3)	3.3
C(22)	0.2363(5)	0.3860(6)	0.3213(3)	3.3
C(23)	0.3549(5)	0.3566(6)	0.3425(3)	3.3
C(24)	0.4073(4)	0.2784(6)	0.4124(3)	3.2
C(31)	0.1495(5)	-0.2790(6)	0.1838(3)	3.3
C(32)	0.1128(5)	-0.2320(7)	0.1084(3)	3.3
C(33)	0.2131(6)	-0.2278(7)	0.0848(4)	4.1
C(34)	0.3073(5)	-0.2688(7)	0.1464(4)	4.4
C(35)	0.2680(5)	-0.3015(6)	0.2071(3)	3.7
C(41)	0.1465(6)	-0.0825(9)	0.3950(4)	7.3
C(42)	0.2252(7)	-0.1829(7)	0.3745(4)	5.8
C(43)	0.3323(7)	-0.1415(10)	0.4224(5)	9.0
C(44)	0.3196(7)	-0.0210(9)	0.4700(4)	6.7
C(45)	0.2098(8)	0.0161(8)	0.4539(4)	6.3

[a]Positional parameters are in fraction of cell edges and B_{eq} is the equivalent isotropic temperature factors calculated from the corresponding anisotropic thermal parameters.

Table 1-22. Interatomic Bond Distances (Å) and Angles (°) in $[(\eta^5\text{-}C_5H_5)Nb(\mu\text{-}Cl)(C_4H_6)]_2$ (**34**)

(a) Bond Distances			
Nb(1)–Nb(2)	3.364 (1)		
Nb(1)–Cl(1)	2.528 (1)	Nb(2)–Cl(1)	2.528 (1)
Nb(1)–Cl(2)	2.531 (1)	Nb(2)–Cl(2)	2.539 (1)
Nb(1)–C(11)	2.309 (6)	Nb(2)–C(21)	2.313 (6)
Nb(1)–C(12)	2.392 (7)	Nb(2)–C(22)	2.399 (6)
Nb(1)–C(13)	2.401 (7)	Nb(2)–C(23)	2.405 (6)
Nb(1)–C(14)	2.311 (7)	Nb(2)–C(24)	2.328 (5)
Nb(1)–C(31)	2.435 (6)	Nb(2)–C(41)	2.394 (8)
Nb(1)–C(32)	2.395 (6)	Nb(2)–C(42)	2.390 (9)
Nb(1)–C(33)	2.378 (7)	Nb(2)–C(43)	2.378 (8)
Nb(1)–C(34)	2.380 (8)	Nb(2)–C(44)	2.396 (9)
Nb(1)–C(35)	2.434 (6)	Nb(2)–C(45)	2.394 (10)
C(11)–C(12)	1.412 (9)	C(21)–C(22)	1.437 (8)
C(12)–C(13)	1.396 (9)	C(22)–C(23)	1.400 (8)
C(13)–C(14)	1.395 (9)	C(23)–C(24)	1.430 (8)
C(31)–C(32)	1.415 (8)	C(41)–C(42)	1.407 (12)
C(32)–C(33)	1.436 (9)	C(42)–C(43)	1.383 (12)
C(33)–C(34)	1.401 (10)	C(43)–C(44)	1.373 (12)
C(34)–C(35)	1.410 (10)	C(44)–C(45)	1.317 (14)
C(31)–C(35)	1.390 (8)	C(41)–C(45)	1.396 (12)
(b) Bond Angles			
Cl(1)–Nb(1)–Cl(2)	96.4 (1)	Cl(1)–Nb(2)–Cl(2)	96.2 (1)
Nb(1)–Cl(1)–Nb(2)	83.4 (1)	Nb(1)–Cl(2)–Nb(2)	83.1 (1)
C(11)–Nb(1)–C(14)	72.7 (2)	C(21)–Nb(2)–C(24)	72.5 (2)
C(11)–C(12)–C(13)	119.2 (6)	C(21)–C(22)–C(23)	118.1 (5)
C(12)–C(13)–C(14)	117.9 (6)	C(22)–C(23)–C(24)	117.7 (5)
C(32)–C(31)–C(35)	108.9 (5)	C(42)–C(41)–C(45)	107.3 (7)
C(31)–C(32)–C(33)	107.1 (5)	C(41)–C(42)–C(43)	105.6 (7)
C(32)–C(33)–C(34)	107.0 (6)	C(42)–C(43)–C(44)	109.0 (8)
C(33)–C(34)–C(35)	109.1 (6)	C(43)–C(44)–C(45)	109.2 (8)
C(31)–C(35)–C(34)	107.9 (6)	C(41)–C(45)–C(44)	108.9 (8)

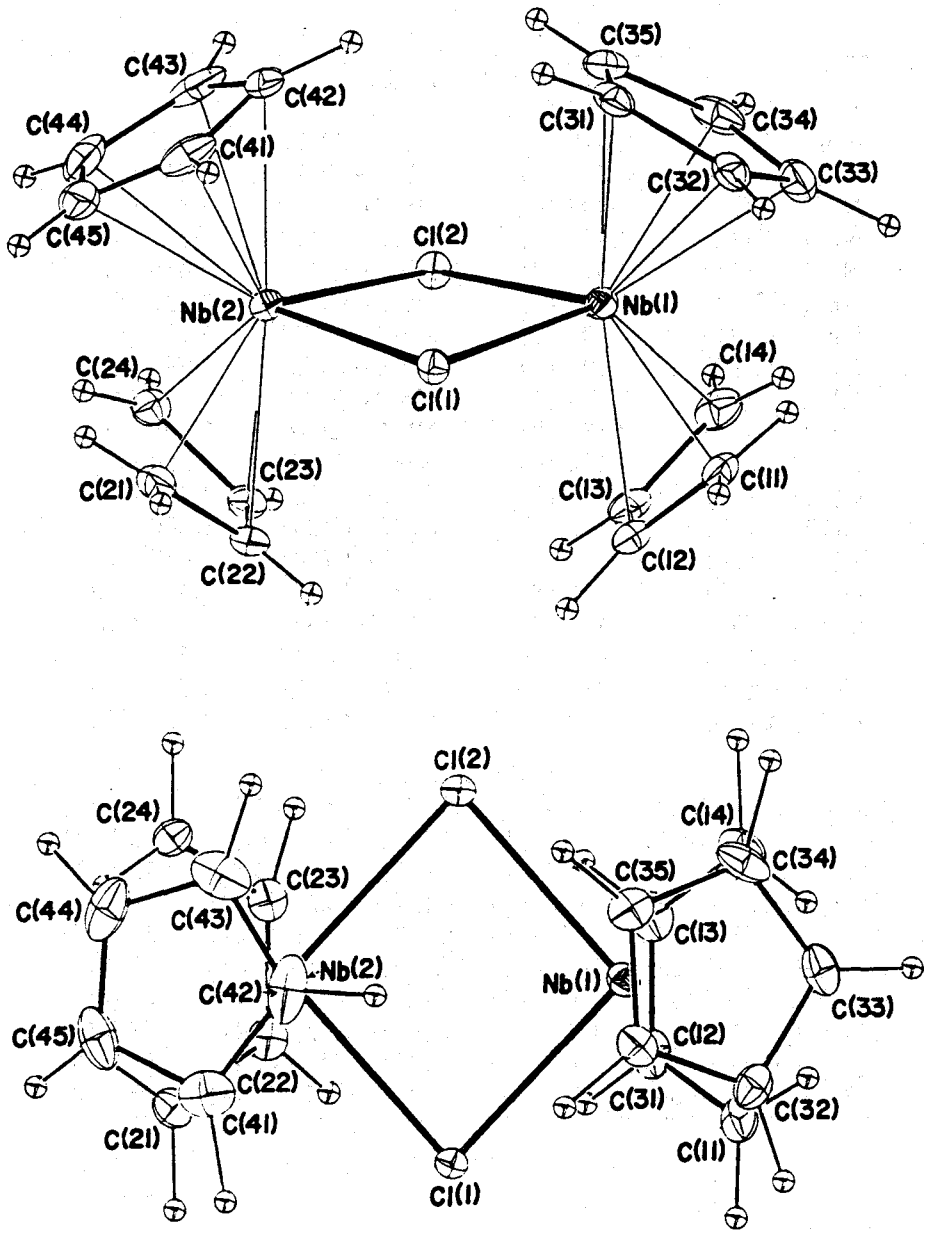

Fig. 1-9. Molecular structure of $[(\eta^5\text{-}C_5H_5)Nb(\mu\text{-}Cl)(C_4H_6)]_2$ (34).

Nb_2Cl_2 cores and two C_5H_4Me ligands on the opposite side (*trans* position) of the Nb_2C_2 square array. The N-bridged $Nb_2N_2L_2$-type binuclear niobium (2.83-2.92Å, e.g., $[NbCp_2NCAr)]_2$)[44], S-bridged niobium compounds (3.13-3.16Å, e.g., $[NbCp_2S]_2$)[45] and O-bridged niobium compound (2.781Å for $[NbCl_2(OMe)_2.MeOH]_2$)[46] generally exhibit much shorter Nb-Nb bonds. In spite of the anormalously long Nb-Nb bond distance, the compound **34** maintains the diamagnetic nature as confirmed by the NMR spectroscopy. This is indicative of the presence of direct Nb-Nb spin coupling. Each of the butadiene-Nb units is composed of the bent σ^2, π-metallacyclo-3-pentene structure familiar to tantalum-diene and zirconium-diene complexes, although the bonding property of the limiting π^2-η^4-diene-metal species contributes significantly to the present metallacycle as estimated from the respective C-C bond lengths.

1-3-2. Coordination geometry of diene in mononuclear niobium-bis(diene) complex

As a typical example of niobium-bis(diene), NbCp(2,3-dimethylbutadiene)$_2$ **36** was subjected to the X-ray crystallographic analysis. Comparison of the molecular structure of **36** with that of isomorphous TaCp(2,3-dimethylbutadiene)$_2$, a well-defined bis(diene)tantalum complex[34] will surely provide a nice opportunity to find the absolute effect of metal on the coordination geometry along with the M-C bonding property emerged by replacement of Ta with Nb. The crystal data and parameters for structure determination are summarized in Table 1-23. Final atomic coordinates are listed in Table 1-24 and selected bond distances and angles are in Table 1-25, together with those in $(\eta^5\text{-}C_5H_5)Ta(C_6H_{10})_2$. The molecular structure is shown in Fig. 1-10. The gross structure of **36** resembles very well that of TaCp(2,3-dimethylbutadiene)$_2$ and again assumes the *supine-prone* geometry in fair

Table 1-23. Crystal Data and Experimental Parameters for X-Ray Structure Determination of $(\eta^5\text{-}C_5H_5)Nb(C_6H_{10})_2$ (**36**).

Formula	$C_{17}H_{25}Nb$
Formula weight	322.3
Crystal system	orthorhombic
Space group	*Pnma*
Temp., °C	20
a,[a] Å	8.961(1)
b, Å	12.305(2)
c, Å	13.530(2)
V, Å^3	1491.9(4)
Z	4
D_{calcd}, g cm^{-3}	1.434
$F(000)$, e	672
μ(MoKα), cm^{-1}	7.7
Crystal size, mm	0.10x0.25x0.25
2θ range,[b] deg	4<2θ<65
Scan width, deg in 2θ	2.0+0.70tanθ
Scan speed, deg min^{-1}	4.0
Background count, s	5
Reflections measured	3389
Reflections observed[c]	1626
Radiation damage	no
No. of variables	136
GOF[d]	1.256
R[e]	0.056
R_w[f]	0.077

[a]Least-squares refinement of the θ values for 25 reflections with 2θ>25°. [b]Intensity data were collected on a Rigaku four-circle diffractometer using graphite-monochromatized MoKα radiation by the θ-2θ scan method. [c]$|F_o|>3\sigma(F_o)$. [d]$[\Sigma w(|F_o|-|F_c|)^2/(n-m)]^{1/2}$, where n and m are the No. of reflections used and variables refined, respectively. [e]$R=\Sigma(|F_o|-|F_c|)/\Sigma|F_o|$. [f]$R_w=[\Sigma w(|F_o|-|F_c|)^2/\Sigma w|F_o|^2]^{1/2}$, $w=[\sigma^2(F_o)+g(F_o)^2]^{-1}$, and g=0.003.

Table 1-24. Frinal Atomic Coordinates and Equivalent Isotropic Temperature Factors for Nonhydrogen Atoms in $(\eta^5\text{-}C_5H_5)Nb(C_6H_{10})_2$ (**36**) with Estimated Standard Deviations in Parentheses[a]

atom	x	y	z	B_{eq}
Nb	0.12949 (8)	0.2500	0.48721 (5)	2.3
C(1)	0.2093 (8)	0.1376 (7)	0.3635 (5)	3.1
C(2)	0.3500 (7)	0.1943 (6)	0.3834 (5)	2.9
C(5)	0.4881 (10)	0.1287 (10)	0.4061 (7)	4.4
C(11)	0.2686 (9)	0.1344 (7)	0.5870 (5)	3.1
C(12)	0.1827 (8)	0.1929 (6)	0.6584 (5)	3.0
C(15)	0.0822 (13)	0.1260 (10)	0.7282 (8)	4.8
C(21)	−0.1022 (8)	0.1921 (8)	0.4009 (7)	4.3
C(22)	−0.1055 (9)	0.1560 (9)	0.4990 (6)	4.4
C(23)	−0.1174 (12)	0.2500	0.5603 (9)	4.2

[a]Positional parameters are in fraction of cell edges and B_{eq} is the equivalent isotropic temperature factors calculated from the corresponding anisotropic thermal parameters.

Table 1-25. Interatomic Bond Distances (Å) and Angles (°) in (η^5-C_5H_5)Nb(C_6H_{10})$_2$ (**36**), together with those in (η^5-C_5H_5)Ta(C_6H_{10})$_2$

	36	TaCp(C_6H_{10})$_2$[d]
	(a) Bond Distances	
Nb/Ta–C(1)	2.286 (8)	2.261 (8)
Nb/Ta–C(2)	2.519 (7)	2.522 (7)
Nb/Ta–C(11)	2.324 (8)	2.292 (6)
Nb/Ta–C(12)	2.467 (7)	2.473 (6)
Nb/Ta–C(21)	2.486 (9)	2.482 (11)
Nb/Ta–C(22)	2.408 (10)	2.411 (13)
Nb/Ta–C(23)	2.424 (11)	2.419 (16)
C(1)–C(2)	1.466 (10)	1.469 (11)
C(2)–C(2′)	1.371 (13)	1.352 (11)
C(11)–C(12)	1.429 (10)	1.475 (10)
C(12)–C(12′)	1.405 (14)	1.343 (11)
C(2)–C(5)	1.509 (14)	1.525 (12)
C(12)–C(15)	1.543 (13)	1.544 (13)
C(21)–C(22)	1.400 (14)	
C(22)–C(23)	1.427 (15)	
C(21)–C(21′)	1.424 (19)	
Nb/Ta–CCP[a]	2.253	2.119
Nb/Ta–M1[b]	1.820	1.796
Nb/Ta–M2[c]	1.838	1.797
	(b) Bond Angles	
C(1)–Nb/Ta–C(1′)	74.4 (3)	74.8 (3)
C(11)–Nb/Ta–C(11′)	75.5 (3)	76.7 (3)
C(1)–C(2)–C(2′)	118.4 (6)	118.4 (7)
C(11)–C(12)–C(12′)	120.2 (7)	120.6 (7)
C(1)–C(2)–C(5)	119.3 (7)	118.5 (7)
C(11)–C(12)–C(15)	117.3 (7)	115.9 (7)
C(2′)–C(2)–C(5)	122.3 (7)	123.1 (7)
C(12′)–C(12)–C(15)	122.2 (7)	123.3 (7)
C(22)–C(21)–C(21′)	108.5 (8)	108.1 (10)
C(22)–C(23)–C(22′)	108.2 (9)	108.8 (13)

[a]CCP: centroid of cyclopentadienyl ligand. [b]M1: midpoint of C(1) and C(1'). [c]M2: midpoint of C(11) and C(11'). [d]See *1-2-2*.

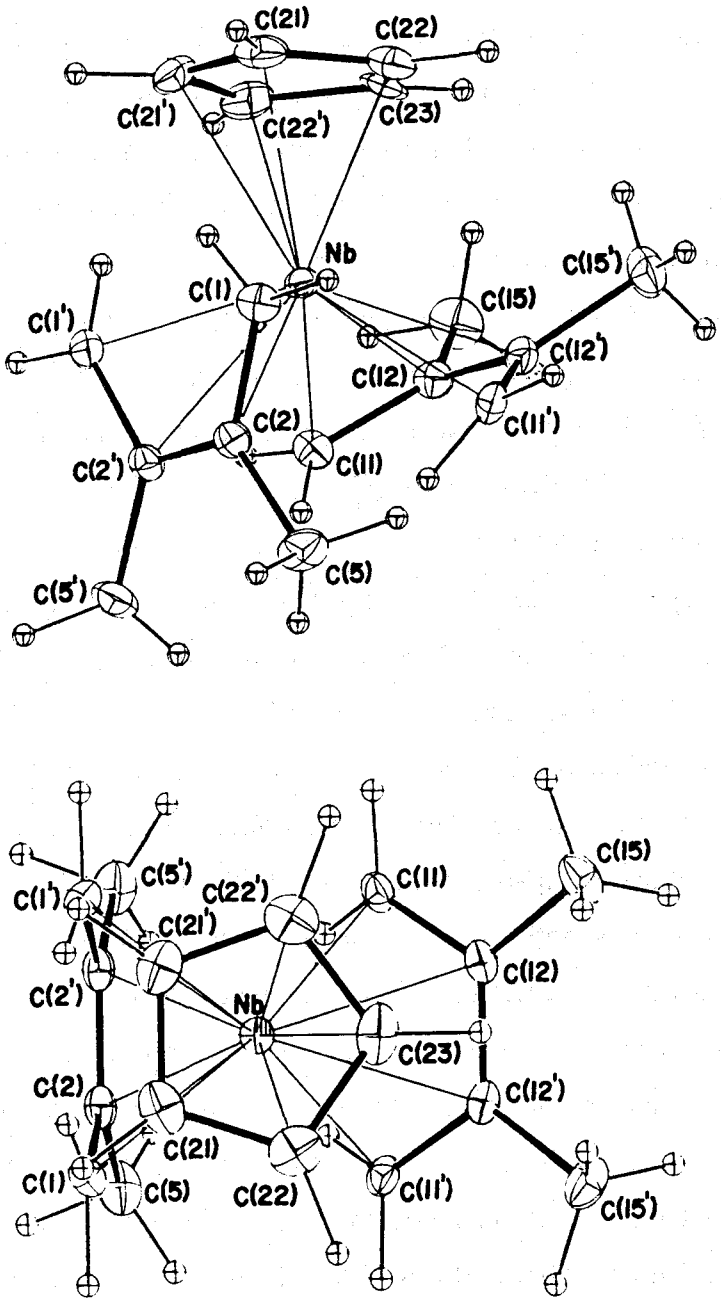

Fig. 1-10. Molecular structure of $(\eta^5\text{-}C_5H_5)Nb(C_6H_{10})_2$ (36).

agreement with the solution structure. The M-C(terminal) and M-C(central) bond distances of **36** are almost in parallel with the corresponding M-C bond distances found in the tantalum analogue within 0.03Å (Table 1-26). Also comparable are the coordination geometry around the metal (see ϕ_1, ϕ_2, and ϕ_3 defined in the Table and dihedral angles between the planes of Cp and *supine*-diene (α_1) and that between the planes of Cp and *prone*-diene (α_2) together with that between planes of two diene units (α_3)).

In spite of the above noted close resemblance, complex **36** shows an appreciable structural perturbation from the tantalum derivative. Perhaps the most important potentially is the relatively small difference in the C-C bond distances by Δl=l[C-C(external)]-l[C-C(internal)]. Although TaCp(2,3-dimethylbutadiene)$_2$ exhibits a relatively large Δl of 0.132Å for the *prone*-diene unit, the corresponding value for complex **36** diminishes significantly to 0.024Å. The binuclear niobium complex **34** also shows very small Δl of av 0.021Å. This indicates that the displacement of Ta with Nb commonly causes a slight shift from the σ,π-metallacyclic limit to the (π^2-diene)metal limit for the *prone*-diene. Another feature is seen in the relatively small difference between the M-C bond lengths, Δd, defined by d[M-C(terminal)]-d[M-C(central)]. The value $|\Delta d|$ for **36** (av 0.188Å) is slightly smaller than that (av 0.221Å) observed for the corresponding tantalum analogue. When the metal-diene complex approaches the σ^2,π-metallacyclo-3-pentene limit as found for ZrCp$_2$(2,3-dimethylbutadiene) and HfCp*(2,3-dimethylbutadiene), the value Δd reaches -0.297 and -0.243Å, respectively. The metal in diene complexes of middle and late transition metals is usually situated in positions directly above the η^4-coordinated diene and hence Δd falls in the region of 0.0 to 0.1 Å. Thus the magnitude of Δd for bis(diene) complex **36** is intermediate between the values reported for the two limits but that for mono(diene) complex **34** is consistent with the value for η^4-diene-metal complexes. As a consequence the bent angle (θ_1 and θ_2) between the C(terminal)-M-C(terminal) and the diene planes for **36** (98.8°, 101.1°) governs

Table 1-26 Structural Parameters in Diene Coordination for **36** and Related Complexes (°)

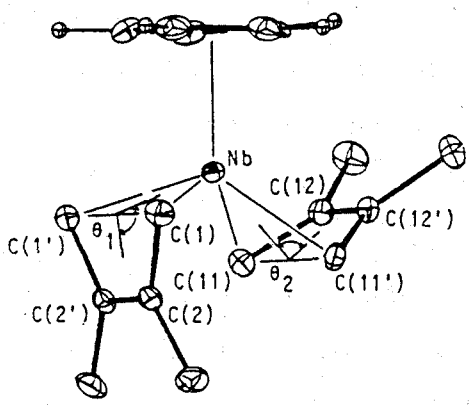

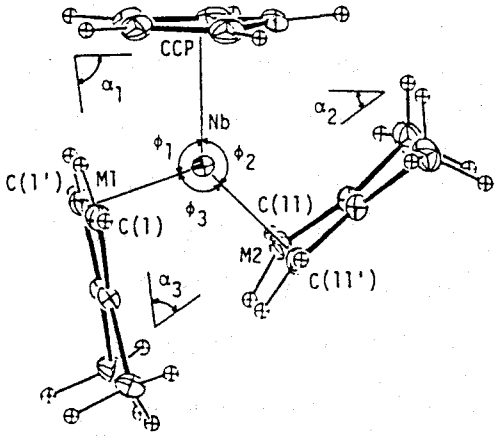

	36	$TaCp(C_6H_{10})_2$
θ_1	101.1	102.5
θ_2	98.8	100.4
α_1	80.5	81.5
α_2	36.0	35.0
α_3	63.5	63.6
ϕ_1	107.6	108.5
ϕ_2	138.2	137.2
ϕ_3	114.2	114.3

also the intermediates value between the angles reported for group 4A metal-diene complexes (110-120°) and the group 8 metal-diene complexes (75-92°), whereas the bent angle for **34** (86.6° for Nb(1) and 87.9° for Nb(2)) is almost comparable with those for group 8 metal-diene complexes. The Nb-C(terminal) bond distances for **36** and **34** are in accord with the Nb-alkyl single bond distance found for $NbCp_2Et(C_2H_4)$ (2.290Å)[47] and $NbCp_2(CH_2SiMe_2CH_2)$ (2.275Å) and $NbCp_2(CH_2SiMe_2CH_2)$ (2.275Å),[48] but larger than the Nb-acetylene bonds (2.038-2.125Å)[49] which possesses partially the Nb=C double bond character. On the basis of these structural parameters, it will be safe to say that σ^2,π-metallacyclic property is more pronounced in the mono(diene)niobium complexes while a substantial participation of π^2-η^4-diene-metal type bonding is recognized in the bis(diene)niobium complexes.

$NbCl_2(C_5H_5)$(s-*cis*-diene) were found to assume always the *supine* conformation and bis(diene)complexes, $Nb(C_5R_5)$(s-*cis*-diene)$_2$, the unique *supine-prone* conformation. The large propensity to Nb(V) to be reduced to Nb(IV) species allows the formation of novel binuclear niobium-diene complexes in some favorable cases, while such type of complexation has not yet been received for the Ta series. The versatile catalysis of niobium-diene complexes observed in the polymerization or oligomerization of dienes and alkynes will promise further utility of this class of complexes as a potential new type of catalysis for the conversion of various hydrocarbons. The present structural studies provide a good experimental basis for penetrating into the reaction mechanisms for these catalytic reactions.

References

1) G. Erker, J. Wicher, K. Engel, F. Rosenfeldt, W. Dietrich, and C. Krüger, *J. Am. Chem. Soc.*, **102**, 6346 (1980).

2) H. Yasuda, Y. Kajihara, K. Mashima, K. Nagasuna, K. Lee, and A. Nakamura, *Organometallics*, **1**, 388 (1982).

3) H. Yasuda, Y. Kajihara, K. Mashima, K. Nagasuna, K. Lee, and A. Nakamura, *Organometallics*, **2**, 478 (1983).

4) Y. Kai, N. Kanehisa, K. Miki, N. Kasai, K. Mashima, K. Nagasuna, H. Yasuda, and A. Nakamura, *J. Chem. Soc., Chem. Commun.*, **1982**, 191.

5) H. Yasuda, K. Nagasuna, M. Akita, K. Lee, and A. Nakamura, *Organometallics*, **3**, 1470 ,(1984).

6) R. Benn and G. Schroth, *J. Organomet. Chem.*, **228**, 71 (1982).

7) H. Yasuda, Y. Kajihara, K. Mashima, K. Lee, and A. Nakamura, *Chem.Lett.*, **1981**, 519.

8) Refinement of the crystal structure was proceeded by using HBLS-V[a)] or XRAY-76[b)] program system. Weighting scheme used for the refinement of each complex is shown in the Table for crystal and experimental parameters. (a)T. Ashida, The Universal Crystallographic Computing System -Osaka, The computer Center, Osaka University, 1979, pp.53-59. (b)J. M. Stewart, Report TR-446, University of Maryland, MD, 1976.

9) "International Tables for X-Ray Crystallography," Kynoch Press, Birmingham (1974), Vol. IV, p.71.

10) K. Fujita, Y. Ohnuma, H. Yasuda, and H. Tani, *J. Organomet. Chem.*, **113**, 201 (1976).

11) Y. Nakao, K. Natsukawa, H. Yasuda, and H. Tani, *Macromolecules*, **11**, 586 (1978).

12) M. Yang, K. Yamamoto, N. Otake, M. Ando, and K. Takase, *Tetrahedron Lett.*, **1970**, 3843.

13) H. Yasuda, Y. Kajihara, T. Ishikawa, and A. Nakamura, *Bull. Chem. Soc. Jpn.*, **53**, 3035 (1980).

14) S. S. Wreford and J. F. Whitney, *Inorg. Chem.*, **20**, 3918 (1981).

15) G. Wilke, *Fundam. Res. Homogeneous Catal.*, **3**, 1 (1979).

16) M. Vallino, *J. Organomet. Chem.*, **20**, 1 (1969).

17) D. Thoennes and E. Weiss, *Chem. Ber.*, **111**, 3381 (1978).

18) T. Greiser, J. Kopf, D. Thoennes, and E. Weiss, *J. Organomet. Chem.*, **191**,

1 (1980).
19) A. De Cian, P. M. L'Huillier, and R. Weiss, *Bull. Soc. Chim. Fr.*, **1973**, 451.
20) G. Erker, J. Wicher, K. Engel, C. Krüger, *Chem. Ber.*, **115**, 3300 (1982).
21) G. Erker, K. Engel, C. Kruger, A. -P. Chiang, *ibid.*, **115**, 3311 (1982).
22) G. Erker and K. Engel, *Organometallics*, **3**, 128 (1984).
23) (a) M. R. Churchill and W. J. Youngs, *J. Am. Chem. Soc.*, **101**, 6462 (1979).
(b) M. R. Churchill and W. J. Youngs, *Inorg. Chem.*, **19**, 3106 (1980).
24) P. B. Hitchcock and R. Mason, *J. Chem. Soc., Chem. Commun.*, **1967**, 242.
25) D. A. Whiting, *Cryst. Struct. Commun.*, **1**, 379 (1972).
26) I. Fischler and E. A. Koerner von Gustorf, *Z. Naturforsch., B*, **30b**, 291 (1975).
27) I. Noda, H. Yasuda, and A. Nakamura, *Organometallics*, **2**, 1207 (1983).
28) L. Porri, A. Lionetti, G. Allegra, and A. Immirzi, *J. Chem. Soc., Chem. Commun.*, **1965**, 336.
29) A. Immirzi and G. Allegra, *Acta Crystallogr., Sect. B*, **B25**, 120 (1969).
30) T. C. van Soet, A. van der Ent, and E. C. Royers, *Cryst. Struct. Commun.*, **3**, 527 (1973).
31) G. Huttner, D. Neugebauer, and A. Razavi, *Angew. Chem.*, **87**, 353 (1975).
32) R. L. Harlow, P. J. Krusic, R. J. McKinney, and S. S. Wreford, *Organometallics*, **1**, 1506 (1982).
33) The terms *prone* and *supine* were used in the paper (ref 27) to describe the orientation of the coordinated dienes. The conventional naming, *exo* and *endo*, does not seem suitable for the present unique stereochemistry.
34) H. Yasuda, K. Tatsumi, T. Okamoto, K. Mashima, K. Lee, A. Nakamura, Y. Kai, N. Kanehisa, and N. Kasai, *J. Am. Chem. Soc.*, **107**, 2410 (1985).
35) S. S. Wreford and J. F. Whitney, *Inorg. Chem.*, **20**, 3918 (1981).
36) Crystallographic data of $(\eta^5\text{-}C_5Me_5)Ta(C_4H_6)(C_6H_{10})$: *F.W.*=452.4, orthorhombic, $Pca2_1$, 20°C, a=15.352(2), b=8.259(1), c=14.168(3)Å, D_c=1.672 g cm^{-3}, F(000)=896, μ(Mo$K\alpha$)=91.7 cm^{-1}.
37) Y. Kai, N. Kanehisa, K. Miki, N. Kasai, K. Mashima, H. Yasuda, and A. Nakamura, *Chem. Lett.*, **1982**, 1277.
38) H. Yasuda and A. Nakamura, *Angew. Chem.*, **99**, 745 (1987); *Angew. Chem., Int. Ed. Engl.*, **26**, 723 (1987).
39) H. Yasuda, K. Tatsumi, and A. Nakamura, *Acc. Chem. Res.*, **18**, 120 (1985).
40) G. Erker, C. Kruger, and G. Muller, *Adv. Organomet. Chem.*, **24**, 1 (1985).
41) A. J. Schultz, R. K. Brown, J. M. Williams, and R. R. Schrock, *J. Am.*

Chem. Soc., **103**, 169 (1981).
42) G. Smith, R. R. Schrock, M. R. Churchill, and W. J. Youngs, *Inorg. Chem.*, **20**, 387 (1981).
43) M. D. Curtis, and J. Real, *Organometallics*, **4**, 940 (1985).
44) (a) F. A. Cotton, and W. J. Roth, *J. Am. Chem. Soc.*, **105**, 3734 (1983). (b) D. A. Lemenovskii, V. P. Fedin, Yu. L. Slovohotov, and Yu. T. Struchkov, *J. Organomet. Chem.*, **228**, 153 (1982).
45) (a) W. A. Herrmann, H. Biersack, M. L. Ziegler, and B. Balbach, *J. Organomet. Chem.*, **206**, C33 (1981). (b) Yu. V. Skripkin, I. L. Eremenko, A. A. Pasynskii, Yu. T. Struchkov, and V. E. Shklover, *J. Organomet. Chem.*, **267**, 285 (1984).
46) F. A. Cotton, M. P. Diebold, and W. J. Roth, *Inorg. Chem.*, **24**, 22 (1985).
47) L. J. Guggenberger, P. Meakin, and F. N. Tebbe, *J. Am. Chem. Soc.*, **96**, 5420 (1974).
48) W. R. Tikkanen, J. W. Egan, and J. L. Petersen, *Organometallics*, **3**, 1646 (1984).
49) (a) A. I. Gusev, and Yu. T. Struchkov, *Zh. Strukt. Khim.*, *10*, 107 (1969). (b) E. Hey, F. Weller, and K. Dehnickel, *Z. Anorg. Allg. Chem.*, **514**, 25 (1984). (c) A. A. Pasynskii, Yu. V. Skripkin, I. L. Eremenko, V. T. Kalinnikov, G. G. Aleksandrov, and Yu. T. Struchkov, *J. Organomet. Chem.*, **165**, 39 (1979).

Chapter 2. Diverse Reaction Courses in the Controlled Carbometallation of Heterocumulenes, Ketones, and Alkyne with Zirconium-Diene Complexes

Group 4A and group 5A early-transition-metal-diene complexes have received considerable current attention because of their unique M-C bonding properties (bent s-*cis* and novel s-*trans* coordination) and their high reactivities that have enabled a broad range of selective carbometalations to take place with both electrophiles (saturated and unsaturated aldehydes, ketones, esters, and nitriles) and unsaturated hydrocarbons (alkenes, dienes, alkynes).[1-10] Perhaps the most fascinating property of this class of diene complexes lies in their facile interconversions between σ^2,π-η^4-metallacyclo-3-pentene or π^2-η^4-s-*trans*-diene-metal species and transitory η^2-s-*cis*- or η^2-s-*trans*-metal-diene species generated during their versatile reactions.[1-18] This unusual behavior imparts a special utility to these diene complexes and a convenient means of revealing the chemical and structural features of early transition organometallics because the subtle differences existing these complexes and substrates can be amplified effectively on the regio- and stereochemistry of the reaction products.

2-1. Molecular Structures of Carbon Dioxide, Isocyanate, and Ketene 1:1 and 1:2 Inserted Compounds

The current major problems are to find (1) the essential factor(s) in determining the structures of the final products, i.e. (*Z*)-metallacycle (A), (σ,*anti*-η^3-allyl)metal (B), (*E*)-metallacycle (C), or (σ,*syn*-η^3-allyl)metal species (D) for which the X,Y, and Z groups assume the sp^3 or sp^2 configuration, (2) factor(s) in controlling the reaction courses single and double carbometalations, (3) a correlation between the geometry of the coordinated dienes (s-*cis* or s-*trans*) and the stereochemistry of the products, and (4) the effect of alkyl substitution at the diene ligand on the regiochemistry of the products.

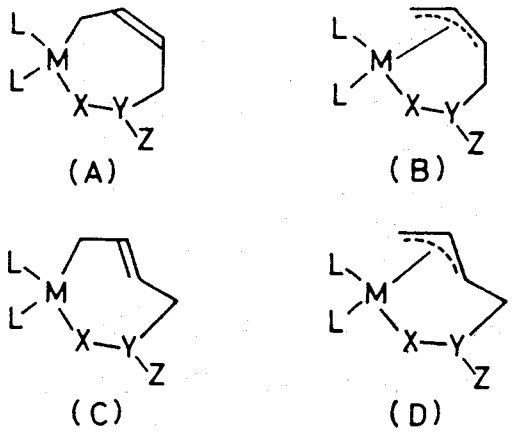

X=O, N, CR, CHR
Y=C, CR, CRR′,
Z=O, OR, NR, NRR′, CRR′, CR_3

In order to obtain a sound experimental basis for the mechanistic considerations, the molecular structures of the 1:1 adducts of $Zr(C_5Me_5)_2$(s-*trans*-butadiene) (**1**) with CO_2 (**2**) and *t*-BuNCO (**3a**), 1:2 adduct of $Zr(C_5Me_5)_2$(s-*cis*-isoprene) with PhN=C=O (**4a**), and the 1:1 adduct of $Zr(C_5Me_5)_2$(s-*trans*-butadiene) with Ph_2C=C=O (**5**) have been determined by X-ray diffraction method.

2-1-1. Reaction courses for the addition of carbon dioxide to diene complexes

Zirconium-diene complexes were found to readily react with carbon dioxide under atmospheric pressure in hydrocarbon solvents. The mode of insertion changes drastically depending upon the bulkiness of the ancillary ligand (C_5H_5 or C_5Me_5) along with the geometry (s-*cis* or s-*trans*) of the coordinated dienes. These reactions can be classified into three groups on the basis of the reaction stoichiometry (1:1, 1:2, or 2:1 ratio). The present experiments provide important information about the effects of the configuration (sp^2 or sp^3) of Y on the stereochemistry of the products.

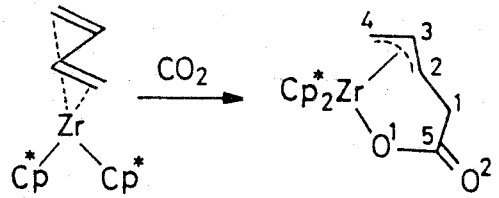

1 2

Molecular structure of the 1:1 adduct (**2**) of ZrCp*(s-*trans*-butadiene) and CO_2 has been determined by X-ray diffraction method. The crystal data and parameters for structure determination are summarized in Table 2-1. Final atomic coordinates are listed in Table 2-2, and selected interatomic distances and angles are in Table 2-3. The molecular structure is given in Fig. 2-1 along with the numbering scheme. The butadiene unit is bound to the metal in a twisted *syn*-η^3-allyl fashion. The torsional angle around the C(2)-C(3) bond (150.3°) thereby deviates largely from 180°. The zirconium atom is tetracoordinated if the Cp and allyl groups are each considered to occupy only one coordination site. The OC(=O) group was found to assume the expected ester-type structure, where one oxygen atom, O(1), links to the metal while the other is bent away from the metal. The geometrical distortion around the *syn*-η^3-allyl group brings about substantial lengthening of the Zr-C(2) bond (2.709Å) relative to the Zr-C(4) (2.403Å) and Zr-C(3) (2.483Å) bonds. The Zr-C(2) bond of this molecule is longer than the corresponding bond between Zr and terminal carbon of η^3-allyl groups (2.442-2.624Å in $ZrCp(\eta^3\text{-allyl})_2(\eta^1\text{-allyl})$.[19] All of these Zr-C bonds are remarkably longer as expected than the Zr-C single bonds (2.21-2.27Å) reported for $[ZrCp_2Me.THF]^+$,[20] $ZrCp_2Me_2$,[21] $ZrCp_2(C_6H_4)$,[22] $ZrCp_2Cl(CH_2OCH_3)$,[23] and $ZrCp_2(RC{\equiv}CH)$.[24] The Zr-O bond length (2.144Å) is nearly comparable with those for $[Cp_2Zr(OCH_2CH_2CH_2)]_2$ (2.190Å)[25] and $Cp_2Zr[OC(=M(CO)_5)CH_2CHCHCH_2]$ (M=Cr, 2.138Å)[26]but longer than the Zr-O bonds (1.95-1.97Å) in $[ZrCp_2O]_3$,[27] $ZrCp^*_2Cl(OH)$,[28] and $ZrCp^*_2(OH)_2$.[29] The C(5)-O(2) (1.212Å) and C(5)-O(1) bonds (1.299Å) exhibit normal lengths.

Table 2-1. Crystal Data and Experimental Parameters for X-Ray Structure Determination of $(\eta^5\text{-}C_5Me_5)_2Zr(C_4H_6).CO_2$ (**2**)

Formula	$C_{25}H_{36}O_2Zr$
Formula weight	459.8
Crystal system	monoclinic
Space group	$P2_1/n$
Temp., °C	20
a,[a] Å	8.816(1)
b, Å	28.916(3)
c, Å	9.388(1)
β, deg	108.89(1)
V, Å^3	2264.2(5)
Z	4
D_{calcd}, g cm^{-3}	1.348
$F(000)$, e	904
μ(MoKα), cm^{-1}	5.0
Crystal size, mm	0.35x0.25x0.25
2θ range,[b] deg	4<2θ<55
Scan width, deg in 2θ	2.0+0.70tanθ
Scan speed, deg min^{-1}	4.0
Background count, s	5
Reflections measured	5202
Reflections observed[c]	3851
Radiation damage	no
No. of variables	398
GOF[d]	1.40
R[e]	0.060
R_w[f]	0.084

[a]Least-squares refinement of the θ values for 25 reflections with 2θ>25°. [b]Intensity data were collected on a Rigaku four-circle diffractometer using graphite-monochromatized MoKα radiation by the θ-2θ scan method. [c]$|F_o|>3\sigma(F_o)$. [d]$[\Sigma w(|F_o|-|F_c|)^2/(n-m)]^{1/2}$, where n and m are the No. of reflections used and variables refined, respectively. [e]$R=\Sigma(|F_o|-|F_c|)/\Sigma|F_o|$. [f]$R_w=[\Sigma w(|F_o|-|F_c|)^2/\Sigma w|F_o|^2]^{1/2}$, $w=[\sigma^2(F_o)+g(F_o)^2]^{-1}$, and $g=0.003$.

Table 2-2. Final Atomic Coordinates and Equivalent Isotropic Temperature Factors for Nonhydrogen Atoms in $(\eta^5\text{-}C_5Me_5)Zr(C_4H_6).CO_2$ (2) with Estimated Standard Deviations in Parentheses[a]

atom	x	y	z	B_{eq}, Å^2
Zr	0.26404 (6)	0.376030 (16)	0.30637 (5)	2.33
O(1)	0.2319 (5)	0.30466 (14)	0.2418 (5)	2.6
O(2)	0.2701 (7)	0.23493 (18)	0.1619 (18)	5.4
C(1)	0.4973 (9)	0.2855 (3)	0.2420 (10)	4.3
C(2)	0.5361 (10)	0.3299 (4)	0.3205 (16)	8.0
C(3)	0.5391 (10)	0.3698 (4)	0.2909 (16)	7.3
C(4)	0.5187 (8)	0.4137 (3)	0.3539 (8)	3.2
C(5)	0.3203 (8)	0.2726 (3)	0.2117 (8)	3.2
C(11)	0.1297 (7)	0.3491 (3)	0.4918 (7)	2.6
C(12)	0.2875 (7)	0.3325 (2)	0.5539 (6)	2.5
C(13)	0.3918 (7)	0.3699 (3)	0.5992 (6)	3.0
C(14)	0.2963 (8)	0.4115 (3)	0.5657 (7)	2.9
C(15)	0.1348 (8)	0.3983 (3)	0.5056 (7)	2.7
C(16)	−0.0201 (8)	0.3201 (3)	0.4417 (9)	3.8
C(17)	0.3321 (9)	0.2825 (3)	0.5790 (8)	4.0
C(18)	0.5661 (9)	0.3678 (4)	0.6979 (8)	5.1
C(19)	0.3581 (11)	0.4602 (3)	0.6127 (9)	4.7
C(20)	−0.0028 (10)	0.4290 (3)	0.5074 (9)	4.8
C(21)	0.1304 (7)	0.4455 (2)	0.1455 (7)	2.6
C(22)	0.2295 (8)	0.4271 (3)	0.0684 (7)	3.1
C(23)	0.1732 (10)	0.3822 (3)	0.0167 (7)	3.9
C(24)	0.0331 (9)	0.3743 (3)	0.0566 (7)	3.8
C(25)	0.0041 (7)	0.4135 (3)	0.1344 (7)	2.8
C(26)	0.1408 (10)	0.4948 (3)	0.2051 (8)	4.4
C(27)	0.3498 (11)	0.4529 (4)	0.0224 (11)	5.6
C(28)	0.2294 (14)	0.3528 (4)	−0.0852 (9)	6.9
C(29)	−0.0753 (12)	0.3334 (3)	0.0078 (11)	7.3
C(30)	−0.1545 (9)	0.4244 (4)	0.1552 (10)	5.5

[a]Positional parameters are in fraction of cell edges and B_{eq} is the equivalent isotropic temperature factors calculated from the corresponding anisotropic thermal parameters.

Table 2-3. Interatomic Bond Distances (Å) and Angles (°) in (η^5-$C_5Me_5)_2Zr(C_4H_6).CO_2$ (**2**) with Estimated Standard Deviations in Parentheses

(a) Bond Distances

Zr–O(1)	2.144 (4)	C(11)–C(12)	1.408 (8)
Zr–C(2)	2.709 (15)	C(11)–C(15)	1.427 (9)
Zr–C(3)	2.483 (14)	C(11)–C(16)	1.506 (10)
Zr–C(4)	2.403 (7)	C(12)–C(13)	1.394 (9)
Zr–C(11)	2.524 (6)	C(12)–C(17)	1.497 (10)
Zr–C(12)	2.592 (6)	C(13)–C(14)	1.443 (9)
Zr–C(13)	2.618 (6)	C(13)–C(18)	1.517 (11)
Zr–C(14)	2.571 (7)	C(14)–C(15)	1.404 (9)
Zr–C(15)	2.567 (6)	C(14)–C(19)	1.524 (11)
Zr–C(21)	2.559 (6)	C(15)–C(20)	1.508 (11)
Zr–C(22)	2.612 (7)	C(21)–C(22)	1.406 (9)
Zr–C(23)	2.581 (9)	C(21)–C(25)	1.425 (9)
Zr–C(24)	2.560 (7)	C(21)–C(26)	1.523 (10)
Zr–C(25)	2.576 (6)	C(22)–C(23)	1.419 (11)
O(1)–C(5)	1.299 (8)	C(22)–C(27)	1.472 (12)
O(2)–C(5)	1.212 (9)	C(23)–C(24)	1.421 (11)
C(2)–C(3)	1.187 (21)	C(23)–C(28)	1.479 (15)
C(3)–C(4)	1.436 (16)	C(24)–C(25)	1.415 (10)
C(1)–C(2)	1.465 (17)	C(24)–C(29)	1.497 (13)
C(1)–C(5)	1.539 (11)	C(25)–C(30)	1.505 (11)

(b) Bond Angles

O(1)–Zr–C(4)	121.2 (2)	C(13)–C(14)–C(19)	125.4 (6)
Zr–O(1)–C(5)	135.6 (4)	C(15)–C(14)–C(19)	126.0 (6)
Zr–C(2)–C(1)	110.4 (8)	C(11)–C(15)–C(14)	107.7 (5)
Zr–C(2)–C(3)	66.3 (10)	C(11)–C(15)–C(20)	125.9 (6)
C(2)–C(3)–C(4)	138.2 (14)	C(14)–C(15)–C(20)	123.4 (6)
Zr–C(4)–C(3)	76.0 (6)	C(22)–C(21)–C(25)	108.6 (5)
C(1)–C(2)–C(3)	138.8 (14)	C(22)–C(21)–C(26)	124.7 (6)
C(2)–C(1)–C(5)	111.3 (8)	C(25)–C(21)–C(23)	125.9 (6)
O(1)–C(5)–O(2)	123.7 (7)	C(21)–C(22)–C(23)	108.4 (6)
O(1)–C(5)–C(1)	115.5 (6)	C(21)–C(22)–C(27)	125.9 (6)
O(2)–C(5)–C(1)	120.7 (7)	C(23)–C(22)–C(27)	124.7 (7)
C(12)–C(11)–C(15)	107.8 (5)	C(22)–C(23)–C(24)	107.1 (7)
C(12)–C(11)–C(16)	126.0 (6)	C(22)–C(23)–C(28)	126.4 (8)
C(15)–C(11)–C(16)	125.6 (6)	C(24)–C(23)–C(28)	125.5 (8)
C(11)–C(12)–C(13)	109.1 (5)	C(23)–C(24)–C(25)	109.1 (6)
C(11)–C(12)–C(17)	124.7 (6)	C(23)–C(24)–C(29)	124.6 (7)
C(13)–C(12)–C(17)	126.0 (6)	C(25)–C(24)–C(29)	125.9 (7)
C(12)–C(13)–C(14)	107.4 (5)	C(21)–C(25)–C(24)	106.8 (6)
C(12)–C(13)–C(18)	126.4 (6)	C(21)–C(25)–C(30)	126.3 (6)
C(14)–C(13)–C(18)	124.7 (6)	C(24)–C(25)–C(30)	124.4 (6)
C(13)–C(14)–C(15)	107.8 (6)		

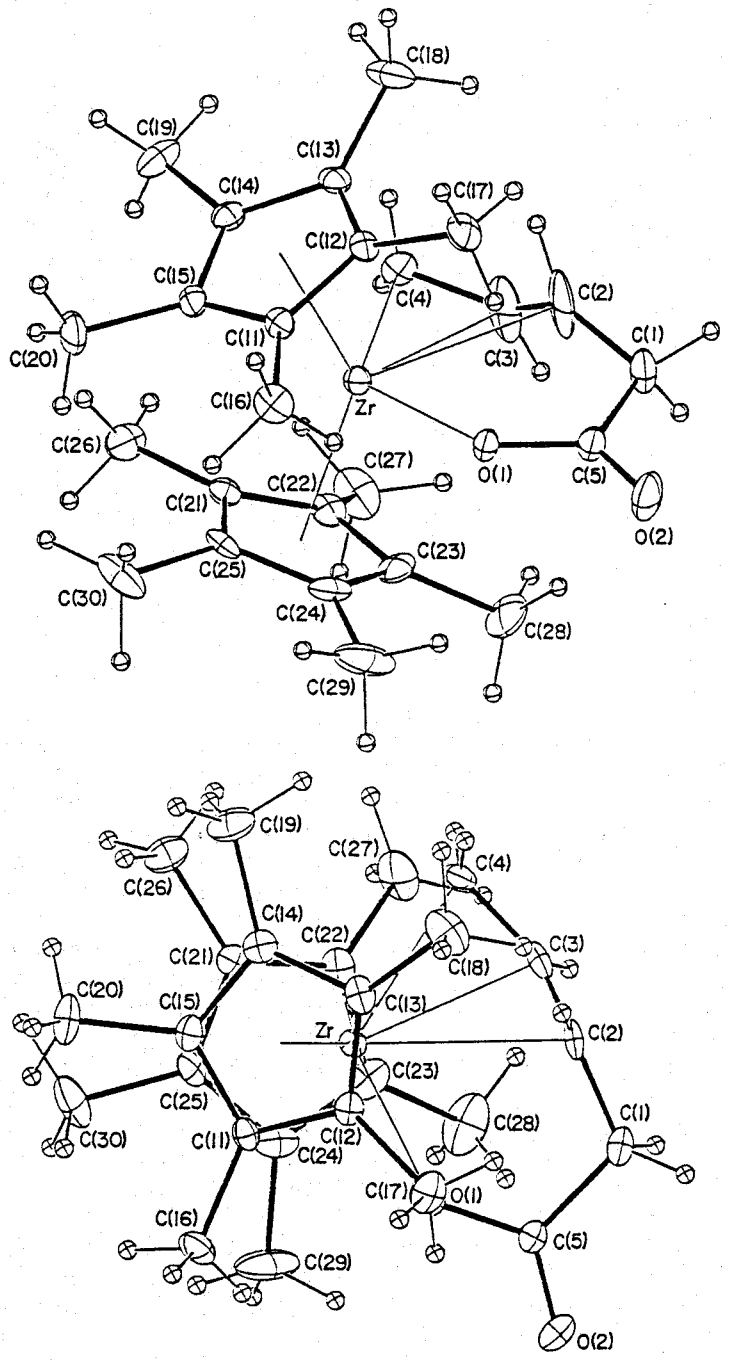

Fig. 2-1. Molecular structure of $(\eta^5\text{-}C_5Me_5)_2Zr(C_4H_6).CO_2$ (**2**).

The O(1)=C(5)-C(1) angle (115.5°) of **2** exceeds the angles of 106-107° found for ketone inserted oxametallacycles,[4] reflecting the sp^2 configuration of the C(5) carbon in **2**. Although the $CH_2CHCHCH_2CO_2$ group in **2** interacts with the metal at both of its ends, O(1), O(2), C(5), and C(1) atoms show almost no perturbation from coplanarity (the dihedral angle between the O(1)-C(5)-O(2) and O(2)-C(5)-C(1) planes is only 0.6°); i.e., the C(5) carbon has a strain-free sp^2 configuration. The σ,*syn*-η^3-allyl-type coordination of the diene unit causes an expansion of O(1)-Zr-C(4) angle to 121.2° from those (89-90°) for ketone-inserted (*Z*)-oxazirconacyclo-4-heptenes.[4] The whole geometry of the present CO_2 adduct resembles well those for iron and nickel derivatives $(PR_3)_3Fe[C_5H_8C(=O)O]$[26] and (TMEDA)Ni[$CH_2C(CH_3)C(CH_3)CH_2C(=O)O$].[30]

2-1-2. Reaction courses for the addition of isocyanates to diene complexes

Reactions of alkyl or phenyl isocyanate with a series of zirconium-diene complexes have been explored in order to find what differences, if any, might be observed relative to the isoelectronic CO_2 reactions.

The exact molecular structure of the 1:1 adduct of isocyanate was obtained by the X-ray analysis of the $ZrCp^*_2$(s-*trans*-C_4H_6)/*t*-BuNCO adduct **3a**. The crystal data and parameters for structure determination are summarized in Table 2-4. Final atomic coordinates are listed in Table 2-5, and selected bond distances and angles are in Table 2-6, respectively. The ORTEP drawings are illustrated in Fig. 2-2 with the numbering schemes. The molecular structure is best described as pseudotetrahedral about the metal with the twisted *syn*-η^3-allyl unit occupying one of the tetrahedral coordination sites. The *t*-BuNCO molecule has been inserted into the Zr-C(1) bond at its CO moiety, and the N-*t*-Bu group is bent away from the metal. Thus the whole geometry of **3a** is comparable with that of the CO_2-inserted complex **2**.

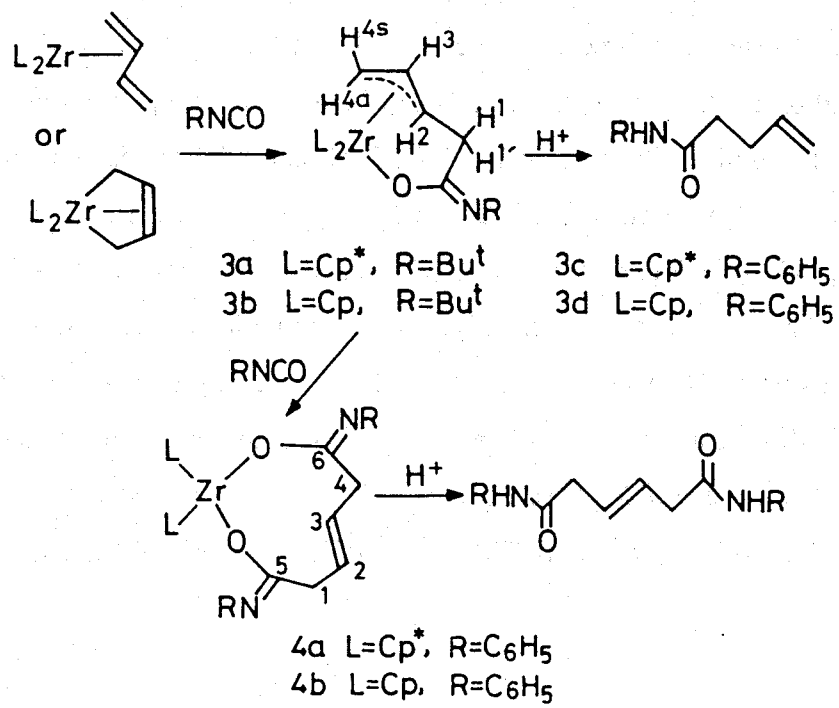

The most striking structural feature of **3a** emerges in the C(3)-C(4) and Zr-C(4) bonds. The C(3)-C(4) bond (1.449Å) is the longest among the (η^3-allyl)zirconium family (Table 2-7) while the C(2)-C(3) bond distance (1.332Å) is among the shortest. The Zr-C(4) bond (2.420Å) is shorter while the Zr-C(2) bond (2.671Å) is longer than those of typical (η^3-allyl)zirconium complexes.[31-33] These results indicate a substantial participation of the limiting (*E*)-oxazirconacyclo-4-heptene structure (C) in **3a** rather than the limiting (σ,η^3-allyl)zirconium form (D) as defined earlier. The deviation of C(1), C(2), C(3), and C(4) from the planar *trans* structure makes the torsional angle around the C(2)-C(3) bond, 158.9°, a little larger than the corresponding angle for **2** (150.3°).

The angle O-C(5)-C(1) of **3a**, ϕ_1 defined by X-Y-C(1) in C or D, almost equals that (115.5°) of the CO_2-inserted compound **2** (Table 2-7) but is remarkably larger than the ϕ_1 values (106.3-109.2°) for ketone-inserted oxametallacycles of geometry A reflecting the sp_2 configuration of the Y carbon

Table 2-4. Crystal Data and Experimental Parameters for X-Ray Structure Determination of $(\eta^5\text{-}C_5Me_5)_2Zr(C_4H_6).(t\text{-}BuNCO)$ (**3a**) and $(\eta^5\text{-}C_5Me_5)_2Zr(C_4H_6).(C_6H_5NCO)_2$ (**4a**)

Complex	**3a**	**4a**
Formula	$C_{29}H_{45}NOZr$	$C_{38}H_{46}N_2O_2Zr$
Formula weight	514.9	654.0
Crystal system	orthorhombic	orthorhombic
Space group	*Pbca*	$P2_12_12_1$
Temp., °C	20	20
a,[a] Å	14.458(2)	9.082(2)
b, Å	16.677(3)	17.275(3)
c, Å	22.446(3)	22.301(4)
V, Å^3	5411.9(14)	3498.9(13)
Z	8	4
D_{calcd}, g cm^{-3}	1.264	1.241
F(000), e	2192	1376
μ(MoKα), cm^{-1}	4.2	3.0
Crystal size, mm	0.45x0.40x0.30	0.60x0.30x0.25
2θ range,[b] deg	4<2θ<55	4<2θ<50
Scan width, deg in 2θ	2.0+0.70tanθ	2.0+0.70tanθ
Scan speed,deg min^{-1}	4.0	4.0
Background count, s	5	5
Reflections measured	6206	3478
Reflections observed[c]	3755	1831
Radiation damage	no	no
No. of variables	470	178
GOF[d]	0.82	0.67
R[e]	0.076	0.131
R_w[f]	0.099	0.144

[a]Least-squares refinement of the θ values for 25(**3a**) or 40 (**4a**) reflections with 2θ>25°. [b]Intensity data were collected on a Rigaku four-circle diffractometer; graphite-monochromatized MoKα radiation, θ-2θ scan method. [c] $|F_o|>3\sigma(F_o)$. [d] $[\Sigma w(|F_o|-|F_c|)^2/(n-m)]^{1/2}$, where *n* and *m* are the No. of reflections used and variables refined, respectively. [e] $R=\Sigma(|F_o|-|F_c|)/\Sigma|F_o|$. [f] $R_w=[\Sigma w(|F_o|-|F_c|)^2/\Sigma w|F_o|^2]^{1/2}$, $w=[\sigma^2(F_o)+g(F_o)^2]^{-1}$, and $g=0.003$.

Table 2-5. Final Atomic Coordinates and Equivalent Isotropic Temperature Factors for Nonhydrogen Atoms in $(\eta^5\text{-}C_5Me_5)_2Zr(C_4H_6).(t\text{-}BuNCO)$ (**3a**) with Estimated Standard Deviations in Parentheses[a]

atom	x	y	z	B_{eq}, Å^2
Zr	0.07922 (5)	0.18401 (4)	0.15106 (3)	3.31
O	0.1481 (4)	0.1262 (3)	0.0774 (2)	2.7
N	0.2008 (5)	0.0204 (4)	0.0161 (3)	3.8
C(1)	0.0839 (8)	−0.0070 (6)	0.0884 (4)	4.0
C(2)	0.0579 (7)	0.0250 (6)	0.1479 (5)	3.8
C(3)	−0.0214 (7)	0.0617 (6)	0.1610 (4)	4.0
C(4)	−0.0334 (7)	0.1143 (6)	0.2118 (4)	3.9
C(5)	0.1529 (6)	0.0515 (5)	0.0580 (4)	3.4
C(6)	0.2626 (7)	0.0643 (6)	−0.0239 (4)	4.1
C(7)	0.3241 (7)	0.1287 (6)	0.0041 (4)	4.8
C(8)	0.3288 (8)	−0.0012 (7)	−0.0508 (5)	5.9
C(9)	0.2030 (8)	0.1001 (7)	−0.0741 (5)	5.4
C(11)	0.0349 (6)	0.3268 (5)	0.1120 (4)	3.3
C(12)	−0.0418 (6)	0.2972 (5)	0.1460 (4)	3.6
C(13)	−0.0825 (6)	0.2330 (5)	0.1137 (4)	3.8
C(14)	−0.0271 (6)	0.2197 (5)	0.0630 (4)	3.4
C(15)	0.0470 (6)	0.2772 (5)	0.0624 (4)	3.2
C(16)	0.0778 (7)	0.4087 (5)	0.1184 (5)	4.7
C(17)	−0.0853 (7)	0.3364 (6)	0.2010 (5)	4.9
C(18)	−0.1778 (7)	0.1977 (6)	0.1238 (6)	5.3
C(19)	−0.0486 (8)	0.1609 (6)	0.0129 (4)	4.8
C(20)	0.1133 (7)	0.2912 (6)	0.0120 (5)	4.7
C(21)	0.2404 (6)	0.1518 (5)	0.1967 (4)	3.1
C(22)	0.1798 (6)	0.1359 (5)	0.2436 (3)	3.1
C(23)	0.1363 (6)	0.2078 (5)	0.2607 (4)	3.6
C(24)	0.1740 (6)	0.2705 (5)	0.2251 (4)	3.4
C(25)	0.2360 (6)	0.2344 (5)	0.1835 (4)	3.2
C(26)	0.3044 (7)	0.0916 (6)	0.1675 (4)	4.3
C(27)	0.1745 (8)	0.0589 (6)	0.2794 (4)	5.2
C(28)	0.0743 (7)	0.2222 (7)	0.3150 (5)	5.3
C(29)	0.1676 (7)	0.3587 (6)	0.2421 (5)	5.1
C(30)	0.2979 (7)	0.2798 (6)	0.1396 (4)	4.5

[a]Positional parameters are in fraction of cell edges and B_{eq} is the equivalent isotropic temperature factors calculated from the corresponding anisotropic thermal parameters.

Table 2-6. Interatomic Bond Distances (Å) and Angles (°) in (η^5-$C_5Me_5)_2Zr(C_4H_6)$.(*t*-BuNCO) (**3a**) with Estimated Standard Deviations in Parentheses

(a) Bond Distances

Zr–O	2.157 (5)	C(6)–C(8)	1.572 (14)
Zr–C(2)	2.671 (10)	C(6)–C(9)	1.540 (14)
Zr–C(3)	2.515 (9)	C(11)–C(12)	1.434 (12)
Zr–C(4)	2.420 (9)	C(11)–C(15)	1.398 (11)
Zr–C(11)	2.618 (8)	C(11)–C(16)	1.507 (13)
Zr–C(12)	2.577 (9)	C(12)–C(13)	1.421 (12)
Zr–C(13)	2.614 (9)	C(12)–C(17)	1.532 (13)
Zr–C(14)	2.574 (8)	C(13)–C(14)	1.411 (12)
Zr–C(15)	2.567 (8)	C(13)–C(18)	1.516 (14)
Zr–C(21)	2.602 (8)	C(14)–C(15)	1.437 (11)
Zr–C(22)	2.659 (7)	C(14)–C(19)	1.523 (13)
Zr–C(23)	2.625 (8)	C(15)–C(20)	1.501 (13)
Zr–C(24)	2.591 (8)	C(21)–C(22)	1.395 (11)
Zr–C(25)	2.525 (8)	C(21)–C(25)	1.411 (11)
O–C(5)	1.321 (9)	C(21)–C(26)	1.514 (12)
N–C(5)	1.279 (11)	C(22)–C(23)	1.407 (11)
N–C(6)	1.463 (11)	C(22)–C(27)	1.517 (13)
C(5)–C(1)	1.553 (13)	C(23)–C(24)	1.423 (11)
C(1)–C(2)	1.486 (14)	C(23)–C(28)	1.534 (14)
C(2)–C(3)	1.332 (13)	C(24)–C(25)	1.427 (11)
C(3)–C(4)	1.449 (13)	C(24)–C(29)	1.523 (12)
C(6)–C(7)	1.530 (13)	C(25)–C(30)	1.530 (12)

(b) Bond Angles

O–Zr–C(4)	121.8 (3)	C(12)–C(13)–C(14)	107.2 (7)
Zr–O–C(5)	134.3 (5)	C(12)–C(13)–C(18)	126.4 (8)
C(5)–N–C(6)	125.4 (7)	C(14)–C(13)–C(18)	125.2 (8)
O–C(5)–N	130.9 (8)	C(13)–C(14)–C(15)	109.0 (7)
O–C(5)–C(1)	114.4 (7)	C(13)–C(14)–C(19)	125.5 (8)
N–C(5)–C(1)	114.6 (7)	C(15)–C(14)–C(19)	125.1 (8)
C(5)–C(1)–C(2)	109.4 (8)	C(11)–C(15)–C(14)	107.2 (7)
Zr–C(2)–C(1)	110.6 (6)	C(11)–C(15)–C(20)	126.0 (8)
Zr–C(2)–C(3)	68.7 (6)	C(14)–C(15)–C(20)	125.8 (8)
C(1)–C(2)–C(3)	125.6 (9)	C(22)–C(21)–C(25)	108.4 (7)
C(2)–C(3)–C(4)	123.8 (9)	C(22)–C(21)–C(26)	125.8 (7)
Zr–C(4)–C(3)	76.6 (5)	C(25)–C(21)–C(26)	125.7 (7)
N–C(6)–C(7)	117.1 (7)	C(21)–C(22)–C(23)	108.9 (7)
N–C(6)–C(8)	105.1 (7)	C(21)–C(22)–C(27)	126.3 (7)
N–C(6)–C(9)	107.5 (7)	C(23)–C(22)–C(27)	123.7 (7)
C(7)–C(6)–C(8)	107.0 (7)	C(22)–C(23)–C(24)	107.6 (7)
C(7)–C(6)–C(9)	110.7 (8)	C(22)–C(23)–C(28)	127.6 (8)
C(8)–C(6)–C(9)	109.2 (8)	C(24)–C(23)–C(28)	123.8 (8)
C(12)–C(11)–C(15)	108.5 (7)	C(23)–C(24)–C(25)	107.3 (7)
C(12)–C(11)–C(16)	125.4 (8)	C(23)–C(24)–C(29)	123.0 (7)
C(15)–C(11)–C(16)	124.1 (8)	C(25)–C(24)–C(29)	127.5 (7)
C(11)–C(12)–C(13)	107.9 (7)	C(21)–C(25)–C(24)	107.6 (7)
C(11)–C(12)–C(17)	126.9 (8)	C(21)–C(25)–C(30)	126.3 (7)
C(13)–C(12)–C(17)	124.2 (8)	C(24)–C(25)–C(30)	125.4 (7)

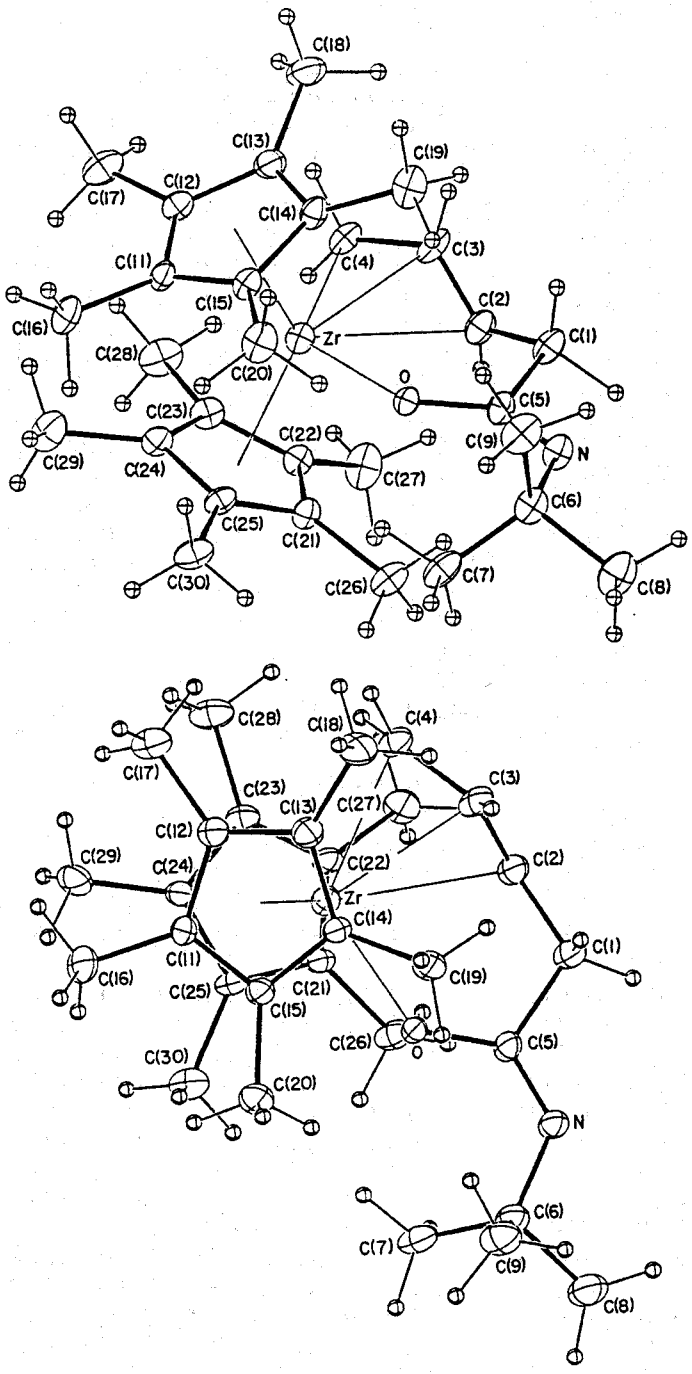

Fig. 2-2. Molecular structure of $(\eta^5\text{-}C_5Me_5)_2Zr(C_4H_6).(t\text{-BuNCO})$ (**3a**).

Table 2-7. Summary of Zr-C and C-C Bond Distances (Å) and Angles (°) of X-Y-C(1) (ϕ_1) and X-Y-Z (ϕ_2) for the 1:1 Adducts of Zirconium-Diene and Related Complexes

complexes	confor-matn[a]	Zr–C(4)	Zr–C(3)	Zr–C(2)	C(3)–C(4)	C(2)–C(3)	ϕ_1	ϕ_2	ref
$Cp^*_2Zr[CH_2CH{=}CHCH_2C(=O)O]$ (2)	D	2.403	2.483	(2.709)	1.436	(1.187)	115.5	123.7	this work
$Cp^*_2Zr[CH_2CH{=}CHCH_2C(=N\text{-}t\text{-}Bu)O]$ (3a)	D	2.420	2.575	2.671	1.449	1.332	114.4	130.9	this work
$Cp_2Zr[CH_2CH{=}CHCH_2C(=CoCp(CO))O]$	D	2.423	2.492	2.614	1.403	1.304	111.5	122.0	30
$Cp_2Zr(CH_2CH{=}CHCH_2CH_2CH_2)$	D	2.461	2.481	2.641	*b*	*b*	*b*	*b*	8
$Cp_2Zr[CH_2C(CH_3){=}CHCH_2C(CH_3){=}C(CH_3)]$[c]	D	2.427	2.595	2.522	1.421	1.361	124.5	118.4	d
$(C_8H_8)Zr(CH_2CH{=}CHCH_2CH_2CH{=}CHCH_2)$		2.823 2.826	2.529 2.534	2.379 2.391	1.360 1.362	1.446 1.439			32
$Cp^*_2Zr[CH_2CH{=}CHCH_2C(i\text{-}C_3H_7)_2O]$	A	2.294	3.144	3.702	1.482	1.313	106.6	106.7 110.0	4
$Cp^*_2Zr[CH_2CH{=}C(CH_3)CH_2C(i\text{-}C_3H_7)_2O]$[c]	A	2.311	3.177	3.729	1.494	1.324	106.3	106.6 109.0	4
$Cp_2Zr[CH_2CH{=}CHCH_2C(C_6H_5)_2O]$	A	2.311	3.051	3.612	1.468	1.351	107.2	110.1 107.7	8

[a] Conformations are given in the Introduction. [b] Atomic coordinates are not given. [c] Numbering system is as follows: C(4), allyl terminal; C(3), $C(CH_3)$ carbon; C(2), isoprene C(3) carbon.

[a)]Conformations are given in **2-1**. [b)]Atomic coordinates are not given. [c)]Numbering system is as follows: C(4), allyl terminal; C(3), $C(CH_3)$ carbon; C(2), isoprene C(3) carbon. [d)]O. Eisenstein and Y. Jean, *J. Am. Chem. Soc.*, **107**, 1177 (1985).

for the former and the sp^3 configuration for the latter. The angle ϕ_2 defined by X-Y-Z, the sp^2 carbon bonded angle O(1)-C(5)-N for **3a** and O(1)-C(5)-O(2) for **2**, also exceed the sp^3 carbon bonded angles (106-110°) as found for ketone inserted compound.[4] The deviation of the O, C(5), N, and C(1) atoms from coplanarity leads to a dihedral angle between the O-C(5)-N and C(5)-N-C(1) planes of 4.7°, indicating the presence of only a small ring strain in this fragment. These results inform me that the magnitude of the angle ϕ_1 serves as a crucial factor in determining the gross geometry of the final products, A or D, when X is an oxygen atom. However, replacement of the oxygen atom at X with a CH_2, CHR, or CR= group invariably leads to complexes of structure D, regardless of the configuration (sp^2 or sp^3) of the X group.[6,10] This is due to the lengthening of the Zr-X single bond along with increased Lewis acidity of the Zr-C bonded complexes.

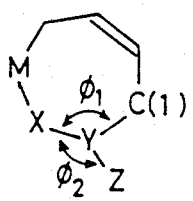

(A)

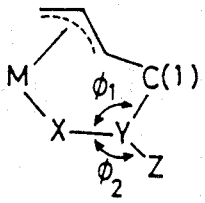

(D)

Phenylisocyanate has increased electrophilicity as compared with *t*-BuNCO, and hence this molecule can take part in both single and double insertions into $ZrCp^*_2$(s-*trans*-butadiene) (**1**) and $ZrCp_2$(s-*cis*-butadiene) (**3**). The 1:1 addition gives **3c** or **3d** of σ,*syn*-η^3-allyl structure while the 1:2 addition leads to nine-membered 1,3-dioxametallacycles **4a** and **4b** of *E* geometry. Acid cleavage of **4a** and **4b** gave the expected (*E*)-dicarboxylic acid amides quantitatively.

The X-ray analysis of two mole adduct of $OCNC_6H_5$ to $ZrCp^*_2$(s-*trans*-butadiene)(**4a**) was also undertaken to obtain unambiguous evidence regarding the macrocyclic structure of the doubly inserted isocyanate compounds. The

crystal data and experimental parameters for structure determination are summarized in Table 2-4. Final atomic coordinates are listed in Table 2-8, and interatomic bond distances and angles are in Table 2-9. The gross geometry of **4a** is depicted in Fig. 2-3 along with numbering scheme. The total accuracy of the molecular structure is severely affected by the low quality of the X-ray data, especially at the higher diffraction angles. However, the ORTEP plot clearly confirms the nine-membered 1,3-dioxazircona-6-nonene structure and the *E* geometry of the olefinic C(2)-C(3) bond. Each of the two phenyl isocyanate molecules is bound through carbon to one opposite end of the butadiene unit and is bound to the metal through its oxygen atom. The whole molecule has an approximate twofold symmetry. passing through the C(2)-C(3) bond and Zr atom. The torsional angle around C(2)-C(3) bond is 161°, deviating significantly from 180°. Seven of the atoms involved in the nine-membered ring are lie in a plane to within 0.06Å, while the other two atoms, C(2) and C(3), deviate from coplanarity by 0.17 and 0.30Å, respectively, on opposite sides. This is the first X-ray structure of such nine-membered early-transition-metal compounds. In the case of related 12-membered-ring macrocyclic titanium compounds, $[TiCp_2OC(O)CR{=}CRC(O)O]_2$, both planar and nonplanar conformations have been reported.[34] The Zr-O bond distances (2.00(2) and 2.01(2)Å) and the angles around the isocyanates, O(1)-C(5)-N(1) = 115(3)°, O(2)-C(6)-N(2) = 125(4)°, C(5)-N(1)-C(11) = 121(3)°, and C(6)-N(2)-C(21) = 123(3)°, are all reasonable. The O(1)-Zr-O(2) bite angle (98.7(8)°) in **4a** is significantly larger than the O-Zr-C angles for seven-membered oxazirconacycles (89.6-91.9°) and those for six-membered oxazirconacycles like $ZrCp_2(OCH_2CH_2SiMe_2CH_2)$ (91.0°),[35] $ZrCp_2[OC(=CH_2)SiMe_2CO(=CH_2)]$ (89.7°),[36] and $ZrCp^*_2[O(CH_2)_4]$ (84.1°).[37]

2-1-3. Abnormal addition of diphenylketene to diene complex

Table 2-8. Final Atomic Coordinates and Equivalent Isotropic Temperature Factors for Nonhydrogen Atoms in $(\eta^5\text{-}C_5Me_5)_2Zr(C_4H_6).(C_6H_5NCO)_2$ (**4a**) with Estimated Standard Deviations in Parentheses[a]

atom	*x*	*y*	*z*	B_{eq} (*B*), Å^2
Zr	0.0950 (3)	0.17137 (16)	0.21129 (11)	3.2[a]
O(1)	0.156 (3)	0.0821 (12)	0.1597 (9)	3.5
O(2)	0.143 (3)	0.2581 (12)	0.1544 (10)	4.1
N(1)	0.214 (4)	−0.0372 (16)	0.1416 (12)	4.3
N(2)	0.159 (3)	0.3827 (14)	0.1261 (11)	3.1
C(1)	0.258 (5)	0.056 (3)	0.0644 (17)	5.0
C(2)	0.279 (6)	0.144 (3)	0.059 (3)	8.6
C(3)	0.227 (5)	0.207 (3)	0.0488 (17)	5.5
C(4)	0.248 (5)	0.284 (3)	0.0563 (18)	6.0
C(5)	0.211 (4)	0.0313 (17)	0.1227 (13)	2.6
C(6)	0.181 (4)	0.320 (3)	0.1163 (15)	5.2
C(11)	0.273 (4)	−0.1024 (18)	0.1035 (14)	4.0
C(12)	0.190 (5)	−0.133 (3)	0.0563 (16)	5.0
C(13)	0.224 (6)	−0.194 (3)	0.028 (3)	8.6
C(14)	0.400 (6)	−0.223 (3)	0.0420 (17)	6.7
C(15)	0.469 (4)	−0.189 (2)	0.0883 (14)	4.6
C(16)	0.414 (4)	−0.1300 (16)	0.1204 (12)	3.4
C(21)	0.195 (4)	0.4415 (19)	0.0866 (14)	3.6
C(22)	0.341 (5)	0.468 (3)	0.0861 (17)	6.1
C(23)	0.384 (7)	0.539 (3)	0.050 (3)	9.7
C(24)	0.254 (5)	0.563 (3)	0.0143 (17)	5.3
C(25)	0.129 (4)	0.537 (2)	0.0060 (15)	4.8
C(26)	0.108 (5)	0.4749 (19)	0.0477 (14)	4.7
C(31)	−0.155 (4)	0.2368 (17)	0.2110 (17)	4.0
C(32)	−0.145 (3)	0.1980 (16)	0.1593 (12)	2.5
C(33)	−0.157 (4)	0.1216 (18)	0.1664 (13)	2.8
C(34)	−0.147 (3)	0.1088 (16)	0.2306 (11)	2.4
C(35)	−0.161 (4)	0.170 (3)	0.2605 (13)	4.1
C(36)	−0.172 (4)	0.320 (3)	0.2275 (16)	6.2
C(37)	−0.185 (6)	0.240 (3)	0.103 (3)	8.4
C(38)	−0.162 (5)	0.060 (3)	0.1132 (19)	7.1
C(39)	−0.159 (6)	0.021 (4)	0.256 (3)	9.8
C(40)	−0.204 (5)	0.188 (3)	0.3276 (16)	5.8
C(41)	0.272 (5)	0.109 (3)	0.2811 (18)	5.3
C(42)	0.189 (4)	0.1483 (16)	0.3156 (13)	3.3
C(43)	0.220 (5)	0.239 (2)	0.3024 (16)	5.1
C(44)	0.326 (5)	0.227 (3)	0.2579 (16)	5.0
C(45)	0.348 (5)	0.153 (3)	0.2496 (19)	6.4
C(46)	0.282 (6)	0.023 (3)	0.283 (3)	8.6
C(47)	0.107 (7)	0.126 (3)	0.378 (3)	9.3
C(48)	0.153 (5)	0.309 (3)	0.3269 (19)	8.7
C(49)	0.388 (7)	0.302 (4)	0.239 (3)	11.2
C(50)	0.478 (7)	0.132 (3)	0.199 (3)	11.2

[a]Positional parameters are in fraction of cell edges and B_{eq} is the equivalent isotropic temperature factors calculated from the corresponding anisotropic thermal parameters. B_{eq} is only for Zr and *B* for remaining atoms.

Table 2-9. Interatomic Bond Distances (Å) and Selected Bond Angles (°) in $(\eta^5\text{-}C_5Me_5)_2Zr(C_4H_6).(C_6H_5NCO)_2$ (**4a**) with Estimated Standard Deviations in Parentheses

(a) Bond distance

Zr	-	O(1)	2.004(20)	Zr	-	O(2)	2.011(20)
Zr	-	C(31)	2.537(37)	Zr	-	C(32)	2.511(27)
Zr	-	C(33)	2.639(30)	Zr	-	C(34)	2.489(27)
Zr	-	C(35)	2.569(42)	Zr	-	C(41)	2.487(39)
Zr	-	C(42)	2.511(28)	Zr	-	C(43)	2.604(35)
Zr	-	C(44)	2.527(39)	Zr	-	C(45)	2.473(43)
O(1)	-	C(5)	1.304(35)	O(2)	-	C(6)	1.407(46)
N(1)	-	C(5)	1.257(39)	N(1)	-	C(11)	1.509(41)
N(2)	-	C(6)	1.122(48)	N(2)	-	C(21)	1.383(40)
C(5)	-	C(1)	1.434(46)	C(1)	-	C(2)	1.538(63)
C(2)	-	C(3)	1.206(65)	C(3)	-	C(4)	1.345(57)
C(4)	-	C(6)	1.600(57)	C(11)	-	C(12)	1.404(48)
C(11)	-	C(16)	1.416(41)	C(12)	-	C(13)	1.253(61)
C(13)	-	C(14)	1.711(62)	C(14)	-	C(15)	1.347(51)
C(15)	-	C(16)	1.334(43)	C(21)	-	C(22)	1.407(49)
C(21)	-	C(26)	1.305(45)	C(22)	-	C(23)	1.514(62)
C(23)	-	C(24)	1.478(61)	C(24)	-	C(25)	1.230(50)
C(25)	-	C(26)	1.435(46)	C(31)	-	C(32)	1.337(45)
C(31)	-	C(35)	1.598(56)	C(31)	-	C(36)	1.486(56)
C(32)	-	C(33)	1.334(40)	C(32)	-	C(37)	1.496(54)
C(33)	-	C(34)	1.451(40)	C(33)	-	C(38)	1.592(52)
C(34)	-	C(35)	1.254(50)	C(34)	-	C(39)	1.625(59)
C(35)	-	C(40)	1.577(57)	C(41)	-	C(42)	1.276(48)
C(41)	-	C(45)	1.244(58)	C(41)	-	C(46)	1.483(64)
C(42)	-	C(43)	1.620(45)	C(42)	-	C(47)	1.626(54)
C(43)	-	C(44)	1.397(52)	C(43)	-	C(48)	1.463(59)
C(44)	-	C(45)	1.313(58)	C(44)	-	C(49)	1.479(66)
C(45)	-	C(50)	1.677(68)				

(b) Bond angle

O(1)	-Zr	-O(2)	98.7(8)	C(5)	-N(1)	-C(11)	121.4(26)
C(6)	-N(2)	-C(21)	123.0(32)	O(1)	-C(5)	-N(1)	115.3(26)
O(1)	-C(5)	-C(1)	118.9(27)	N(1)	-C(5)	-C(1)	125.7(29)
C(5)	-C(1)	-C(2)	114.0(32)	C(1)	-C(2)	-C(3)	148.8(48)
C(2)	-C(3)	-C(4)	143.5(46)	C(3)	-C(4)	-C(6)	115.7(35)
O(2)	-C(6)	-N(2)	125.1(37)	O(2)	-C(6)	-C(4)	107.5(30)
N(2)	-C(6)	-C(4)	127.3(38)	N(1)	-C(11)	-C(12)	121.0(28)
N(1)	-C(11)	-C(16)	115.0(25)	C(12)	-C(11)	-C(16)	123.9(29)
C(11)	-C(12)	-C(13)	124.3(38)	C(12)	-C(13)	-C(14)	112.6(39)
C(13)	-C(14)	-C(15)	116.1(33)	C(14)	-C(15)	-C(16)	125.2(32)
C(11)	-C(16)	-C(15)	116.6(27)	N(2)	-C(21)	-C(22)	118.0(29)
N(2)	-C(21)	-C(26)	127.4(30)	C(22)	-C(21)	-C(26)	114.6(31)
C(21)	-C(22)	-C(23)	120.9(34)	C(22)	-C(23)	-C(24)	107.6(36)
C(23)	-C(24)	-C(25)	135.9(38)	C(24)	-C(25)	-C(26)	107.0(31)
C(21)	-C(26)	-C(25)	133.0(31)				

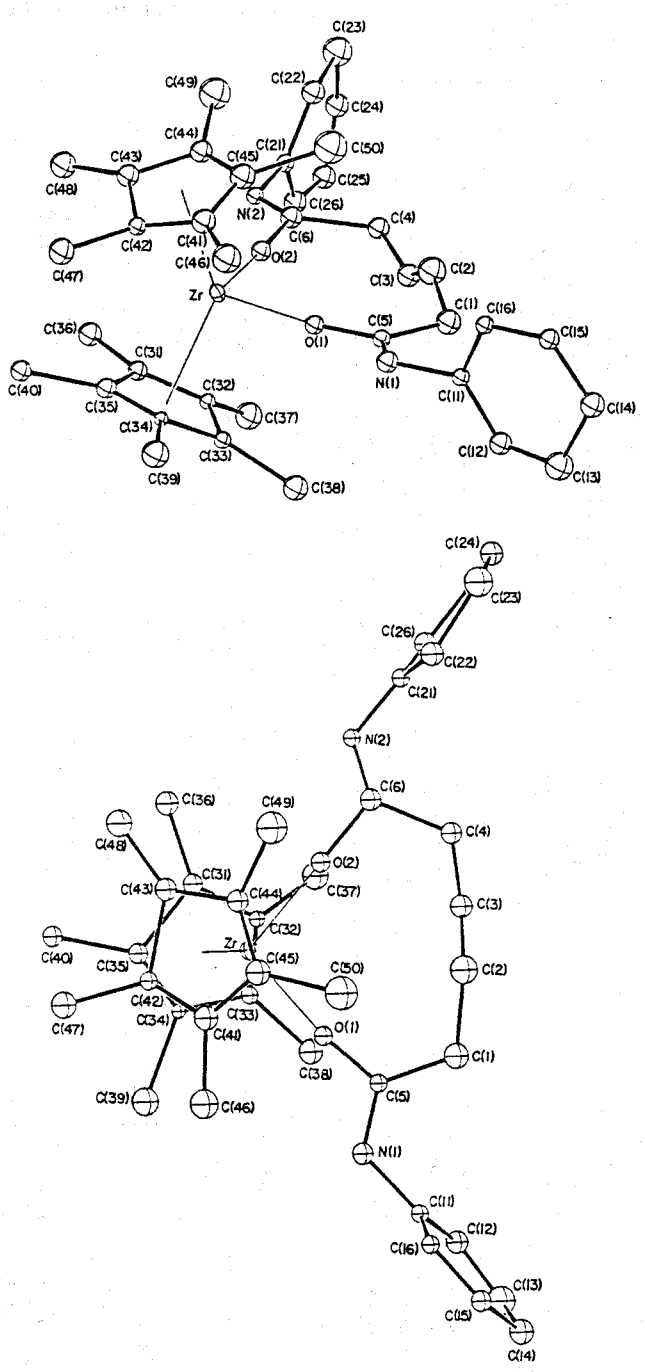

Fig. 2-3. Molecular structure of $(\eta^5\text{-}C_5Me_5)_2Zr(C_4H_6).(C_6H_5NCO)_2$ (**4a**).

A bulky ketene, diphenylketene, was found to undergo a fundamentally different type of cycloaddition reaction. The stoichiometric addition of $ZrCp^*_2$(isoprene) to diphenylketene provides a novel six-membered oxametallacycle (**5**) as the sole observable product in 95% yield whose structure was established by the X-ray analysis.

The crystal data and experimental parameters for structure determination are summarized in Table 2-10. Final atomic coordinates are listed in Table 2-11, and interatomic bond distances and angles in Table 2-12. The X-ray structural studies on the diphenylketene inserted complex **5** provide clear evidence for the six-membered oxametallacyclic framework as illustrated in Fig. 2-4, which revealed that the diphenylketene is bound to the metal through its oxygen atom and bound to the C(3) carbon atom of the isoprene unit at its central carbon C(6). Consequently the molecule contains a six-membered ring. The molecule involves olefinic bonds at the C(1)-C(2) and the C(6)-C(7) positions, and hence the Zr, C(1), C(2), C(3), C(5), and H(1) atoms as well as the O, C(6), C(7), and C(3) atoms are both nearly coplanar. A dihedral angle of 29.1° is formed between these two planes. The O-C(6) bond distance (1.345Å) is a little shorter than a typical C-O single bond. The bond angles around the C(3) atom indicate the normal sp^3 configuration. The bite angle (82.3°) defined by O-Zr-C(1) is slightly smaller than that of ketone-inserted seven-membered oxametallacycles (90-92°), reflecting the smaller ring size of **5**, but larger than that of five-membered oxametallacycle (72.2°).[25)]

2-2. Regio- and Stereoselective Courses for Insertion of Ketones into s-*cis*- and s-*trans*-Diene Complexes of Zirconium Leading to (*Z*)-1,2-Oxazirconacyclohept-4-enes

The unusual versatility of organozirconium complexes has led to many important developments in organic synthesis. $(\eta^5\text{-}C_5H_5)_2Zr$(s-*cis*-isoprene)

Table 2-10. Crystal Data and Experimental Parameters for X-Ray Structure Determination of $(\eta^5\text{-}C_5Me_5)_2Zr(isoprene)((C_6H_5)_2C{=}C{=}O)$ (**5**)

Formula	$C_{39}H_{48}OZr$
Formula weight	624.0
Crystal system	monoclinic
Space group	$P2_1/c$
Temp., °C	20
a,[a] Å	12.282(3)
b, Å	16.082(3)
c, Å	17.981(4)
β, deg	108.56(3)
V, Å^3	3367.1(15)
Z	4
D_{calcd}, g cm^{-3}	1.231
$F(000)$, e	1728
μ(MoKα), cm^{-1}	4.1
Crystal size, mm	0.60x0.25x0.20
2θ range,[b] deg	4<2θ<55
Scan width, deg in 2θ	2.0+0.70tanθ
Scan speed, deg min^{-1}	4.0
Background count, s	5
Reflections measured	7724
Reflections observed[c]	5431
Radiation damage	no
No. of variables	563
GOF[d]	1.14
R[e]	0.066
R_w[f]	0.088

[a] Least-squares refinement of the θ values for 40 reflections with 2θ>25°. [b] Intensity data were collected on a Rigaku four-circle diffractometer using graphite-monochromatized MoKα radiation by the θ-2θ scan method. [c] $|F_o|>3\sigma(F_o)$. [d] $[\Sigma w(|F_o|-|F_c|)^2/(n-m)]^{1/2}$, where n and m are the No. of reflections used and variables refined, respectively. [e] $R=\Sigma(|F_o|-|F_c|)/\Sigma|F_o|$. [f] $R_w=[\Sigma w(|F_o|-|F_c|)^2/\Sigma w|F_o|^2]^{1/2}$, $w=[\sigma^2(F_o)+g(F_o)^2]^{-1}$, and g=0.003.

Table 2-11. Final Atomic Coordinates and Equivalent Isotropic Temperature Factors for Nonhydrogen Atoms in $(\eta^5\text{-}C_5Me_5)_2Zr(isoprene)\text{-}((C_6H_5)_2C{=}C{=}O)$ (**5**) with Estimated Standard Deviations in Parentheses[a]

atom	x	y	z	B_{eq}, Å^2
Zr	0.20758 (4)	0.12059 (3)	0.33551 (3)	2.76
O(1)	0.2473 (3)	0.1052 (2)	0.2368 (2)	2.3
C(1)	0.0558 (5)	0.0432 (4)	0.2705 (4)	2.7
C(2)	0.0364 (5)	0.0087 (4)	0.1994 (4)	2.6
C(3)	0.1080 (5)	0.0191 (4)	0.1442 (4)	2.7
C(4)	0.0447 (6)	0.0795 (5)	0.0770 (4)	3.9
C(5)	−0.0694 (6)	−0.0458 (5)	0.1635 (4)	4.1
C(6)	0.2307 (5)	0.0482 (4)	0.1796 (3)	2.4
C(7)	0.3180 (5)	0.0267 (4)	0.1518 (4)	2.9
C(21)	0.1493 (5)	0.2626 (4)	0.2706 (3)	2.7
C(22)	0.2328 (5)	0.2768 (4)	0.3451 (4)	3.1
C(23)	0.1790 (6)	0.2569 (4)	0.4025 (4)	3.4
C(24)	0.0693 (6)	0.2265 (4)	0.3632 (4)	3.4
C(25)	0.0496 (5)	0.2311 (4)	0.2818 (4)	3.1
C(26)	0.1644 (7)	0.2867 (5)	0.1933 (4)	4.5
C(27)	0.3461 (7)	0.3180 (5)	0.3576 (5)	5.2
C(28)	0.2254 (8)	0.2833 (5)	0.4887 (4)	5.5
C(29)	−0.0224 (7)	0.2034 (6)	0.4010 (5)	5.8
C(30)	−0.0642 (6)	0.2162 (5)	0.2184 (5)	4.8
C(31)	0.3893 (5)	0.0416 (4)	0.4068 (4)	3.1
C(32)	0.3624 (6)	0.0897 (4)	0.4660 (4)	3.4
C(33)	0.2619 (6)	0.0560 (4)	0.4755 (4)	3.3
C(34)	2.2243 (6)	−0.0101 (4)	0.4232 (4)	3.5
C(35)	0.3032 (5)	−0.0195 (4)	0.3806 (4)	2.9
C(36)	0.4946 (6)	0.0535 (6)	0.3824 (5)	4.9
C(37)	0.4443 (8)	0.1505 (5)	0.5177 (5)	5.9
C(38)	0.2137 (9)	0.0747 (6)	0.5413 (5)	6.8
C(39)	0.1285 (8)	−0.0695 (6)	0.4205 (6)	6.3
C(40)	0.2992 (7)	−0.0881 (5)	0.3215 (4)	4.4
C(41)	0.3089 (6)	−0.0407 (4)	0.0937 (4)	3.6
C(42)	0.2811 (7)	−0.1230 (5)	0.1066 (5)	4.8
C(43)	0.2827 (8)	−0.1875 (6)	0.0535 (6)	6.3
C(44)	0.3110 (8)	−0.1686 (6)	−0.0121 (6)	6.4
C(45)	0.3413 (8)	−0.0902 (6)	−0.0268 (5)	5.9
C(46)	0.3415 (7)	−0.0246 (5)	0.0265 (4)	5.0
C(51)	0.4315 (5)	0.0684 (5)	0.1806 (4)	3.5
C(52)	0.5325 (6)	0.0210 (6)	0.2001 (4)	5.2
C(53)	0.6390 (8)	0.0600 (10)	0.2295 (6)	8.0
C(54)	0.6446 (9)	0.1452 (10)	0.2393 (6)	9.0
C(55)	0.5457 (9)	0.1957 (7)	0.2176 (6)	7.4
C(56)	0.4404 (6)	0.1544 (5)	0.1871 (4)	4.5

[a]Positional parameters are in fraction of cell edges and B_{eq} is the equivalent isotropic temperature factors calculated from the corresponding anisotropic thermal parameters.

Table 2-12. Interatomic Bond Distances (Å) and Selected Bond Angles (°) in $(\eta^5\text{-}C_5Me_5)_2Zr(isoprene)((C_6H_5)_2C{=}C{=}O)$ (5) with Estimated Standard Deviations in Parentheses

	(a) Bond Distances		
Zr–O	2.000 (4)	C(23)–C(28)	1.532 (11)
Zr–C(1)	2.236 (6)	C(24)–C(25)	1.408 (9)
Zr–C(21)	2.561 (6)	C(24)–C(29)	1.535 (11)
Zr–C(22)	2.531 (6)	C(25)–C(30)	1.515 (10)
Zr–C(23)	2.579 (7)	C(31)–C(32)	1.437 (9)
Zr–C(24)	2.564 (6)	C(31)–C(35)	1.410 (8)
Zr–C(25)	2.581 (6)	C(31)–C(36)	1.504 (10)
Zr–C(31)	2.533 (6)	C(32)–C(33)	1.408 (9)
Zr–C(32)	2.555 (6)	C(32)–C(37)	1.495 (11)
Zr–C(33)	2.605 (6)	C(33)–C(34)	1.397 (9)
Zr–C(34)	2.596 (6)	C(33)–C(38)	1.512 (13)
Zr–C(35)	2.551 (6)	C(34)–C(35)	1.420 (9)
C(1)–C(2)	1.344 (8)	C(34)–C(39)	1.505 (11)
C(2)–C(3)	1.530 (8)	C(35)–C(40)	1.522 (10)
C(2)–C(5)	1.529 (9)	(C41)–C(42)	1.405 (10)
C(3)–C(4)	1.553 (9)	C(41)–C(46)	1.411 (10)
C(3)–C(6)	1.511 (8)	C(42)–C(43)	1.414 (12)
C(6)–C(7)	1.364 (8)	C(43)–C(44)	1.366 (14)
O–C(6)	1.345 (6)	C(44)–C(45)	1.365 (14)
C(7)–C(41)	1.485 (9)	C(45)–C746)	1.424 (13)
C(7)–C(51)	1.484 (9)	C(51)–C(52)	1.402 (12)
C(21)–C(22)	1.422 (8)	C(51)–C(53)	1.389 (10)
C(21)–C(25)	1.397 (8)	C(52)–C(53)	1.394 (18)
C(21)–C(26)	1.512 (10)	C(53)–C(54)	1.380 (22)
C(22)–C(23)	1.429 (9)	C(54)–C(55)	1.409 (19)
C(22)–C(27)	1.493 (11)	C(55)–C(56)	1.402 (13)
C(23)–C(24)	1.396 (9)		
	(b) Bond Angles		
O–Zr–C(1)	82.3 (2)	C(2)–C(3)–C(4)	109.0 (5)
Zr–O–C(6)	138.0 (3)	C(2)–C(3)–C(6)	117.6 (5)
Zr–C(1)–C(2)	126.4 (4)	C(4)–C(3)–C(6)	108.6 (5)
C(1)–C(2)–C(3)	127.3 (5)	O–C(6)–C(3)	114.9 (5)
C(1)–C(2)–C(5)	120.5 (5)	O–C(6)–C(7)	120.5 (5)
C(3)–C(2)–C(5)	112.1 (5)	C(3)–C(6)–C(7)	124.3 (5)

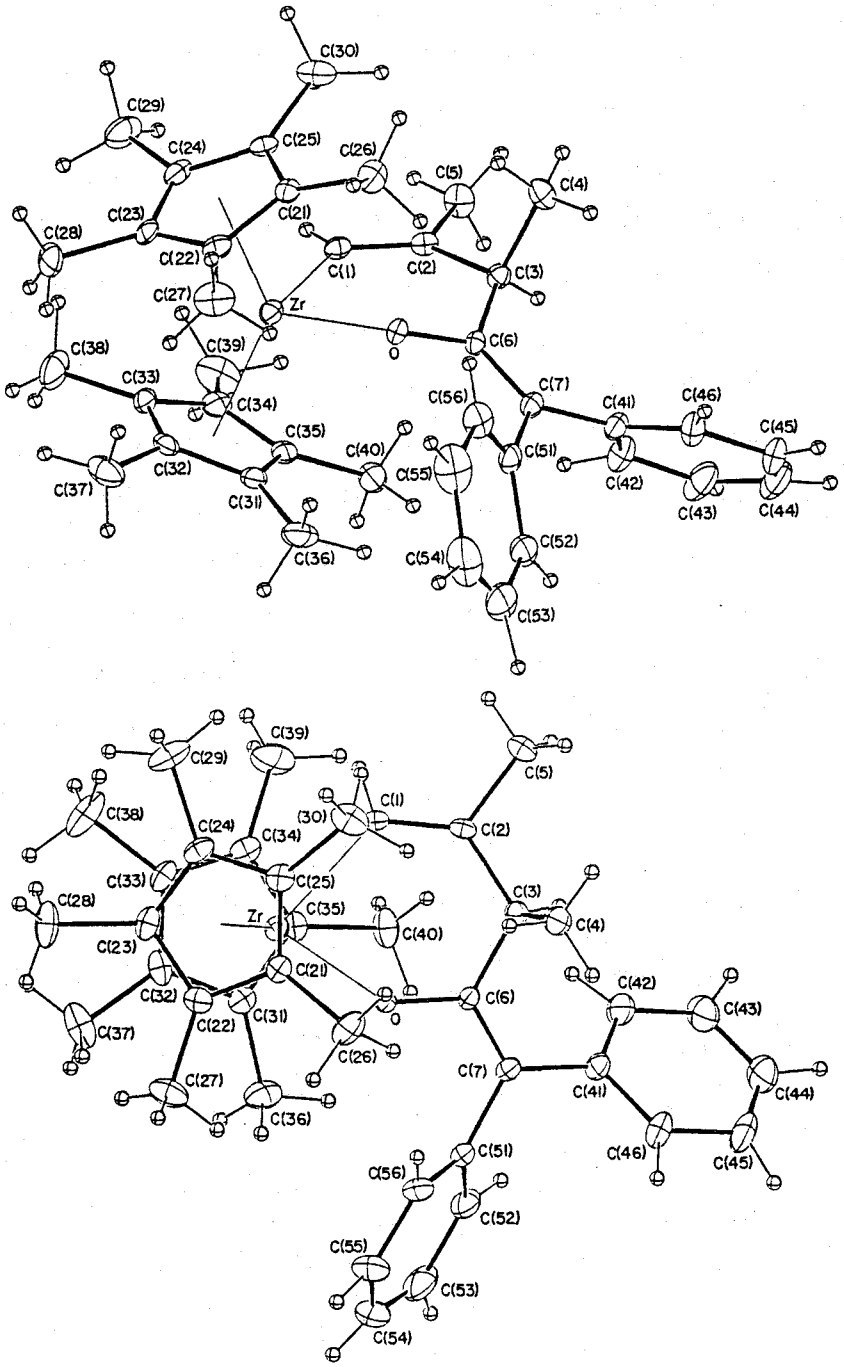

Fig. 2-4. Molecular structure of $(\eta^5\text{-}C_5Me_5)_2Zr(isoprene)((C_6H_5)_2C{=}C{=}O)$ (**5**).

readily reacts with saturated or unsaturated ketones, aldehydes or esters; these reactions result in the regioselective C-C bond formation at the C_1 atom of the coordinated isoprene.[5,38] Stereochemical pathways for this reaction are of interest in understanding the unique chemical properties of the zirconium complexes. Two pathways are conceivable: (a) insertion of carbonyl compound to the M-C bond with retention of the s-*cis* diene conformation and b) insertion after conversion to the s-*trans*-diene coordination. Selective preparation of the s-*cis* and the s-*trans* zirconium-diene complexes is necessary to settle this problem. Though preparations of the s-*cis* and s-*trans* isomers of $(\eta^5\text{-}C_5H_5)_2Zr$(butadiene) complexes were reported,[12,14,39-41] purification of the respective isomers is difficult due to the existence of rapid equilibration between them. A thermally stable s-*trans* isomer of the butadiene complex was found to be obtained exclusively when the C_5H_5 ligand was replaced with C_5Me_5 ligand. The corresponding isoprene complexes, $(\eta^5\text{-}C_5R_5)_2Zr$(isoprene) (R=H, Me), assume the s-*cis*-diene coordination irrespective of the ligand. These findings prompted me to examine the reaction of carbonyl compounds with the s-*cis*- and the s-*trans*-diene complexes to define the stereochemical course by means of the X-ray structure analysis and chemical characterization.

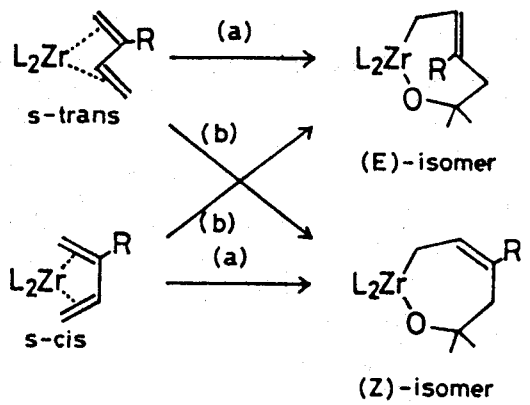

1a R=H, L=C_5Me_5
1b R=Me, L=C_5Me_5
1c R=H, L=C_5H_5
1d R=Me, L=C_5H_5

6 R=H, L=C_5Me_5
7 R=Me, L=C_5Me_5

Single crystals of 1,2-oxazirconacyclohept-4-enes (**6** and **7**) were prepared by the 1:1 reaction of $(C_5Me_5)_2Zr$(s-*trans*-butadiene)(**1a**) or $(C_5Me_5)_2Zr$(s-*cis*-isoprene)(**1d**) with 2,4-dimethyl-3-pentanone at 30°C in benzene to define the stereochemistry of the insertion reaction in terms of X-ray crystal structure analysis.

The crystal data and experimental parameters for structure determination for **6** and **7** are summarized in Table 2-13. Final atomic coordinates are listed in Tables 2-14 (**6**) and 2-15 (**7**), and interatomic bond distances and angles are in Tables 2-16 (**6**) and 2-17 (**7**), respectively. The molecular structures of **6** and **7** are shown in Figs. 2-5 and 2-6. The molecular structure of **6** shows that the 2,4-dimethyl-3-pentanone inserts regioselectively into the bond between zirconium and one of terminal carbon atoms of butadiene [Zr-C(4) bond]. The molecular structure of **7** shows that the insertion of ketone with $(C_5Me_5)_2Zr$(isoprene) occurred into the bond between zirconium and C_1 atom of isoprene [C(4) atom in Fig. 2-6]. Thus, the insertion occurred regioselectively into the sterically hindered Zr-C(4) bond rather than into the less hindered Zr-C(1) bond.

The overall geometry of complexes **6** and **7** is essentially the same. The zirconium atom is coordinated with two C_5Me_5 ligands and bonded with the C(1) atom of the diene part and the oxygen atom of the ketone part in a pseudo-tetrahedral manner. The Zr-C(1) lengths, 2.294Å in **6** and 2.311Å in **7**, are similar to the Zr-C(alkyl) distances in $(\eta^5\text{-}C_9H_7)_2ZR(CH_3)_2$ [2.255Å],[42] $(\eta^5\text{-}C_5H_5)_2Zr(CH_2SiMe_3)_2$ [2.279Å],[43] and $(\eta^5\text{-}C_5H_5)_2Zr(CH_2CMe_3)_2$ [2.288Å],[44] and also to the Zr-C(terminal) distance in $(\eta^5\text{-}C_5H_5)_2Zr$(2,3-dimethylbutadiene) [2.300Å].[12] The Zr-O distances are 1.961Å and 1.964Å for **6** and **7**, respectively. These distances are slightly shorter than the expected Zr-O single bond distance estimated from the sum of the covalent radii for zirconium (1.45-1.48Å) and oxygen (0.66Å). The Zr-O-C(5) angles have relatively large values of 155.2° for **6** and 156.5° for **7**, respectively. The C(2)-C(3) bond distances,

Table 2-13. Crystal Data and Experimental Parameters for X-Ray Structure Determination of $(\eta^5\text{-}C_5Me_5)_2ZrOC(i\text{-}Pr)_2CH_2CH{=}CHCH_2$ (**6**) and $(\eta^5\text{-}C_5Me_5)_2ZrOC(i\text{-}Pr)_2CH_2CMe{=}CHCH_2$ (**7**)

Complex	**6**	**7**
Formula	$C_{31}H_{50}OZr$	$C_{32}H_{52}OZr$
Formula weight	530.0	544.0
Crystal system	monoclinic	monoclinic
Space group	$P2_1/n$	$P2_1/n$
Temp., °C	20	20
a,[a] Å	11.650(2)	10.279(3)
b, Å	17.791(3)	30.177(4)
c, Å	13.612(2)	9.955(2)
β, deg	92.20(2)	108.67(2)
V, Å^3	2819.3(9)	2925.3(11)
Z	4	4
D_{calcd}, g cm^{-3}	1.248	1.235
$F(000)$, e	1136	1168
μ(MoKα), cm^{-1}	4.06	3.93
Crystal size, mm	0.60x0.50x0.30	0.45x0.40x0.35
2θ range,[b] deg	4<2θ<55	4<2θ<50
Scan width, deg in 2θ	2.0+0.70tanθ	2.0+0.70tanθ
Scan speed,deg min^{-1}	4.0	4.0
Background count, s	4	4
Reflections measured	6478	5134
Reflections observed[c]	4308	3526
Radiation damage	no	no
No. of variables	331	336
GOF[d]	1.080	1.332
R[e]	0.111	0.104
R_w[f]	0.219	0.094

[a)]Least-squares refinement of the θ values for 25 (**6**) or 34 (**7**) reflections with 2θ>25°. [b)]Intensity data were collected on a Rigaku four-circle diffractometer; graphite-monochromatized MoKα radiation, θ-2θ scan method. [c)]non-zero reflections. [d)]$[\Sigma w(|F_o|-|F_c|)^2/(n-m)]^{1/2}$, where n and m are the No. of reflections used and variables refined, respectively. [e)]$R=\Sigma(|F_o|-|F_c|)/\Sigma|F_o|$. [f)]$R_w=[\Sigma w(|F_o|-|F_c|)^2/\Sigma w|F_o|^2]^{1/2}$, $w=[\sigma^2(F_o)+g(F_o)^2]^{-1}$, and g=0.003.

Table 2-14. Final Atomic Coordinates and Equivalent Isotropic Temperature Factors for Nonhydrogen Atoms in $(\eta^5\text{-}C_5Me_5)_2ZrOC(i\text{-}Pr)_2\text{-}CH_2CH{=}CHCH_2$ (**6**) with Estimated Standard Deviations in Parentheses[a]

Atom	*x*	*y*	*z*	B_{eq}/Å^2
Zr	0.29990(8)	0.37823(5)	0.28324(7)	2.70
O	0.4643(6)	0.3586(4)	0.2706(5)	2.7
C(1)	0.2565(9)	0.3052(6)	0.1480(8)	2.9
C(2)	0.3397(12)	0.3180(7)	0.0701(8)	4.2
C(3)	0.4495(10)	0.3012(7)	0.0703(8)	3.4
C(4)	0.5157(10)	0.2640(6)	0.1533(9)	3.4
C(5)	0.5627(9)	0.3203(6)	0.2337(7)	2.7
C(7)	0.6405(10)	0.3760(7)	0.1848(8)	3.6
C(8)	0.7485(13)	0.3443(9)	0.1346(12)	5.9
C(9)	0.6788(12)	0.4458(8)	0.2484(11)	5.1
C(10)	0.6173(10)	0.2738(7)	0.3220(8)	3.6
C(11)	0.6932(16)	0.2037(10)	0.2918(13)	7.4
C(12)	0.6806(11)	0.3203(9)	0.4003(10)	4.9
C(21)	0.3321(9)	0.4989(6)	0.1804(7)	2.6
C(22)	0.3269(9)	0.5192(6)	0.2810(8)	2.7
C(23)	0.2107(9)	0.5129(5)	0.3094(8)	2.8
C(24)	0.1473(10)	0.4849(7)	0.2284(9)	3.6
C(25)	0.2215(9)	0.4765(6)	0.1485(7)	2.8
C(26)	0.4290(11)	0.5135(7)	0.1137(9)	4.1
C(27)	0.4246(11)	0.5520(7)	0.3451(10)	4.2
C(28)	0.1652(12)	0.5525(8)	0.3987(9)	4.6
C(29)	0.0155(11)	0.4804(10)	0.2156(14)	6.3
C(30)	0.1782(12)	0.4634(8)	0.0444(9)	4.7
C(31)	0.2696(9)	0.2508(6)	0.3802(8)	2.9
C(32)	0.3198(9)	0.3033(6)	0.4481(7)	2.6
C(33)	0.2374(10)	0.3610(6)	0.4623(8)	3.0
C(34)	0.1383(9)	0.3432(6)	0.4055(8)	2.8
C(35)	0.1623(9)	0.2779(7)	0.3520(8)	3.1
C(36)	0.3175(11)	0.1742(6)	0.3526(10)	4.3
C(37)	0.4298(11)	0.2936(8)	0.5111(8)	4.3
C(38)	0.2501(13)	0.4163(7)	0.5477(8)	4.3
C(39)	0.0195(11)	0.3755(8)	0.4195(11)	4.9
C(40)	0.0689(11)	0.2348(9)	0.2911(11)	5.0

[a]Positional parameters are in fraction of cell edges and B_{eq} is the equivalent isotropic temperature factors calculated from the corresponding anisotropic thermal parameters.

Table 2-15. Final Atomic Coordinates and Equivalent Isotropic Temperature Factors for Nonhydrogen Atoms in $(\eta^5\text{-}C_5Me_5)_2ZrOC(i\text{-}Pr)_2\text{-}CH_2CMe{=}CHCH_2$ (7) with Estimated Standard Deviations in Parentheses[a]

Atom	x	y	z	B_{eq}/Å$^{2\ 10)}$
Zr	0.02683(11)	0.13713(4)	0.37664(12)	2.66
O	-0.1373(8)	0.1066(3)	0.2551(8)	2.3
C(1)	-0.0573(14)	0.2031(4)	0.2646(13)	3.1
C(2)	-0.1129(14)	0.1974(4)	0.1074(14)	3.0
C(3)	-0.2218(14)	0.1745(5)	0.0330(12)	3.0
C(4)	-0.3165(13)	0.1500(5)	0.0994(13)	3.3
C(5)	-0.2719(12)	0.1027(5)	0.1513(13)	2.8
C(6)	-0.2675(18)	0.1743(6)	-0.1306(14)	5.2
C(7)	-0.2618(13)	0.0745(5)	0.0276(13)	3.1
C(8)	-0.3996(17)	0.0671(6)	-0.0929(17)	6.0
C(9)	-0.1885(16)	0.0270(5)	0.0728(16)	4.4
C(10)	-0.3715(12)	0.0869(5)	0.2335(15)	3.5
C(11)	-0.5284(16)	0.0977(7)	0.1595(21)	6.1
C(12)	-0.3535(19)	0.0364(6)	0.2781(17)	5.2
C(21)	0.1464(12)	0.1140(5)	0.1925(13)	2.6
C(22)	0.1937(12)	0.0862(5)	0.3090(12)	2.6
C(23)	0.2824(13)	0.1108(5)	0.4272(14)	3.1
C(24)	0.2819(12)	0.1544(5)	0.3806(14)	3.0
C(25)	0.2003(12)	0.1568(5)	0.2379(15)	3.3
C(26)	0.0780(15)	0.1018(6)	0.0423(14)	4.3
C(27)	0.1765(14)	0.0354(5)	0.3086(15)	3.8
C(28)	0.3827(17)	0.0890(6)	0.5552(15)	5.7
C(29)	0.3754(17)	0.1929(6)	0.4608(21)	6.1
C(30)	0.2047(17)	0.1975(6)	0.1461(17)	5.3
C(31)	-0.1037(13)	0.1646(5)	0.5519(12)	2.9
C(32)	-0.0714(14)	0.1205(5)	0.5833(12)	2.9
C(33)	0.0720(14)	0.1151(5)	0.6397(13)	3.1
C(34)	0.1308(13)	0.1569(5)	0.6482(12)	3.2
C(35)	0.0237(14)	0.1893(5)	0.5868(12)	3.0
C(36)	-0.2440(13)	0.1872(6)	0.5028(14)	4.4
C(37)	-0.1723(18)	0.0838(5)	0.5886(16)	4.7
C(38)	0.1419(18)	0.0728(6)	0.7079(16)	5.0
C(39)	0.2734(15)	0.1711(7)	0.7392(17)	5.4
C(40)	0.0375(17)	0.2383(5)	0.5914(16)	4.4

[a]Positional parameters are in fraction of cell edges and B_{eq} is the equivalent isotropic temperature factors calculated from the corresponding anisotropic thermal parameters.

Table 2-16. Interatomic Bond Distances (Å) in $(\eta^5\text{-}C_5Me_5)_2ZrOC(i\text{-}Pr)_2CH_2CH{=}CHCH_2$ (**6**) and $(\eta^5\text{-}C_5Me_5)_2ZrOC(i\text{-}Pr)_2CH_2CMe{=}CHCH_2$ (**7**)

	6	**7**		**6**	**7**
Zr -O	1.961(7)	1.964(8)	C(24)-C(25)	1.423(16)	1.401(20)
Zr -C(1)	2.294(10)	2.311(14)	C(21)-C(26)	1.498(16)	1.481(21)
C(1) -C(2)	1.482(17)	1.494(20)	C(22)-C(27)	1.523(16)	1.542(19)
C(1) -H(11)	0.89(10)	1.01(12)	C(23)-C(28)	1.519(17)	1.509(22)
C(1) -H(12)	1.00(10)	1.16(12)	C(24)-C(29)	1.541(21)	1.556(25)
C(2) -C(3)	1.313(17)	1.324(20)	C(25)-C(30)	1.504(17)	1.541(23)
C(2) -H(2)	0.97(11)	0.93(10)	C(31)-C(32)	1.425(14)	1.384(19)
C(3) -C(4)	1.499(16)	1.530(19)	C(31)-C(35)	1.380(15)	1.449(19)
C(3) -C(6)		1.545(22)	C(32)-C(33)	1.423(14)	1.408(19)
C(3) -H(3)	1.19(10)		C(33)-C(34)	1.400(15)	1.389(20)
C(4) -C(5)	1.567(15)	1.536(18)	C(34)-C(35)	1.405(15)	1.452(19)
C(4) -H(41)	1.20(11)	1.04(12)	C(31)-C(36)	1.524(17)	1.527(21)
C(4) -H(42)	0.90(10)	1.02(11)	C(32)-C(37)	1.524(17)	1.530(22)
C(5) -O	1.440(12)	1.442(14)	C(33)-C(38)	1.525(18)	1.515(23)
C(5) -C(7)	1.514(15)	1.529(18)	C(34)-C(39)	1.518(17)	1.517(23)
C(5) -C(10)	1.573(15)	1.576(19)	C(35)-C(40)	1.546(18)	1.487(22)
C(7) -C(8)	1.560(20)	1.552(22)	Zr -C(21)	2.598(10)	2.608(13)
C(7) -C(9)	1.569(18)	1.614(20)	Zr -C(22)	2.527(10)	2.549(12)
C(7) -H(7)	0.92(11)	1.13(11)	Zr -C(23)	2.641(10)	2.635(13)
C(10)-C(11)	1.592(22)	1.577(25)	Zr -C(24)	2.687(12)	2.660(14)
C(10)-C(12)	1.518(19)	1.583(24)	Zr -C(25)	2.669(10)	2.649(15)
C(10)-H(10)	1.04(10)	1.19(12)	Zr -C(31)	2.654(10)	2.652(13)
C(21)-C(22)	1.420(14)	1.388(18)	Zr -C(32)	2.613(10)	2.614(13)
C(21)-C(25)	1.401(14)	1.420(20)	Zr -C(33)	2.589(11)	2.596(14)
C(22)-C(23)	1.427(14)	1.442(18)	Zr -C(34)	2.635(10)	2.638(14)
C(23)-C(24)	1.395(16)	1.394(19)	Zr -C(35)	2.597(11)	2.626(14)

Table 2-17. Interatomic Bond Angles (°) in $(\eta^5\text{-}C_5Me_5)_2ZrOC(i\text{-}Pr)_2CH_2CH{=}CHCH_2$ (**6**) and $(\eta^5\text{-}C_5Me_5)_2ZrOC(i\text{-}Pr)_2CH_2CMe{=}CHCH_2$ (**7**)

			6	**7**				**6**	**7**
O	-Zr	-C(1)	90.8(4)	89.6(5)	C(5)	-C(10)	-C(12)	114.9(10)	113.6(12)
Zr	-O	-C(5)	155.2(7)	156.5(8)	C(5)	-C(10)	-H(10)	114(6)	104(6)
Zr	-C(1)	-C(2)	110.9(8)	111.4(9)	C(11)	-C(10)	-C(12)	110.4(11)	109.9(13)
Zr	-C(1)	-H(11)	97(6)	119(7)	C(11)	-C(10)	-H(10)	95(6)	104(6)
Zr	-C(1)	-H(12)	109(6)	109(6)	C(12)	-C(10)	-H(10)	106(6)	109(6)
C(2)	-C(1)	-H(11)	116(6)	103(7)	C(22)	-C(21)	-C(25)	107.4(10)	106.7(12)
C(2)	-C(1)	-H(12)	107(6)	117(6)	C(22)	-C(21)	-C(26)	126.9(10)	128.2(13)
H(11)	-C(1)	-H(12)	117(9)	98(9)	C(25)	-C(21)	-C(26)	124.5(10)	124.0(13)
C(1)	-C(2)	-C(3)	128.9(12)	128.1(13)	C(21)	-C(22)	-C(23)	108.5(10)	109.4(12)
C(1)	-C(2)	-H(2)	124(7)	128(6)	C(21)	-C(22)	-C(27)	126.2(10)	126.1(12)
C(3)	-C(2)	-H(2)	103(7)	104(6)	C(23)	-C(22)	-C(27)	124.8(10)	123.8(12)
C(2)	-C(3)	-C(4)	125.1(11)	123.5(13)	C(22)	-C(23)	-C(24)	107.1(10)	106.3(12)
C(2)	-C(3)	-C(6)		120.6(13)	C(22)	-C(23)	-C(28)	122.9(10)	123.2(13)
C(4)	-C(3)	-C(6)		115.7(12)	C(24)	-C(23)	-C(28)	127.5(11)	128.4(13)
C(2)	-C(3)	-H(3)	116(5)		C(23)	-C(24)	-C(25)	108.8(10)	108.9(13)
C(4)	-C(3)	-H(3)	118(5)		C(23)	-C(24)	-C(29)	127.1(12)	126.7(14)
C(3)	-C(4)	-C(5)	113.6(9)	115.5(11)	C(25)	-C(24)	-C(29)	122.7(12)	123.5(14)
C(3)	-C(4)	-H(41)	110(5)	109(6)	C(21)	-C(25)	-C(24)	108.2(10)	108.7(13)
C(3)	-C(4)	-H(42)	108(7)	109(6)	C(21)	-C(25)	-C(30)	127.4(10)	128.2(14)
C(5)	-C(4)	-H(41)	118(5)	107(6)	C(24)	-C(25)	-C(30)	123.0(10)	121.4(14)
C(5)	-C(4)	-H(42)	110(7)	109(6)	C(32)	-C(31)	-C(35)	107.2(10)	107.9(12)
H(41)	-C(4)	-H(42)	96(8)	106(9)	C(32)	-C(31)	-C(36)	127.0(10)	129.5(13)
O	-C(5)	-C(4)	106.6(8)	106.3(10)	C(35)	-C(31)	-C(36)	125.5(10)	122.4(13)
O	-C(5)	-C(7)	110.0(8)	109.0(10)	C(31)	-C(32)	-C(33)	107.4(10)	110.2(12)
O	-C(5)	-C(10)	106.7(8)	106.6(10)	C(31)	-C(32)	-C(37)	127.3(10)	126.0(13)
C(4)	-C(5)	-C(7)	108.1(10)	109.7(11)	C(33)	-C(32)	-C(37)	124.3(10)	122.6(13)
C(4)	-C(5)	-C(10)	108.5(10)	106.4(11)	C(32)	-C(33)	-C(34)	108.0(10)	107.5(13)
C(7)	-C(5)	-C(10)	116.6(9)	118.2(10)	C(32)	-C(33)	-C(38)	121.4(10)	124.1(14)
C(5)	-C(7)	-C(8)	117.6(10)	115.0(11)	C(34)	-C(33)	-C(38)	128.3(11)	127.1(13)
C(5)	-C(7)	-C(9)	115.9(10)	114.6(11)	C(33)	-C(34)	-C(35)	107.3(10)	109.2(12)
C(5)	-C(7)	-H(7)	102(7)	109(6)	C(33)	-C(34)	-C(39)	125.5(10)	127.7(13)

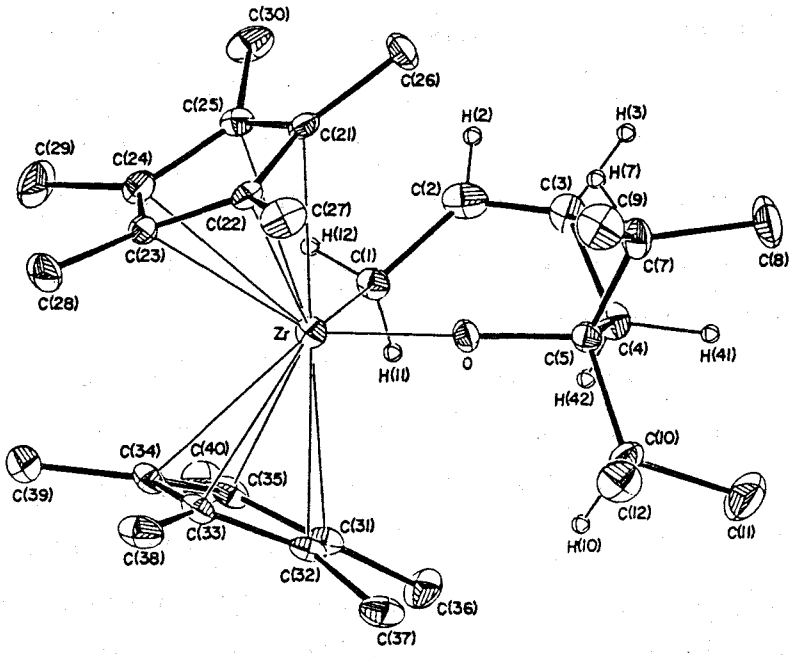

Fig. 2-5. Molecular structure of $(\eta^5\text{-}C_5Me_5)_2ZrOC(i\text{-}Pr)_2CH_2CH{=}CHCH_2$ (**6**).

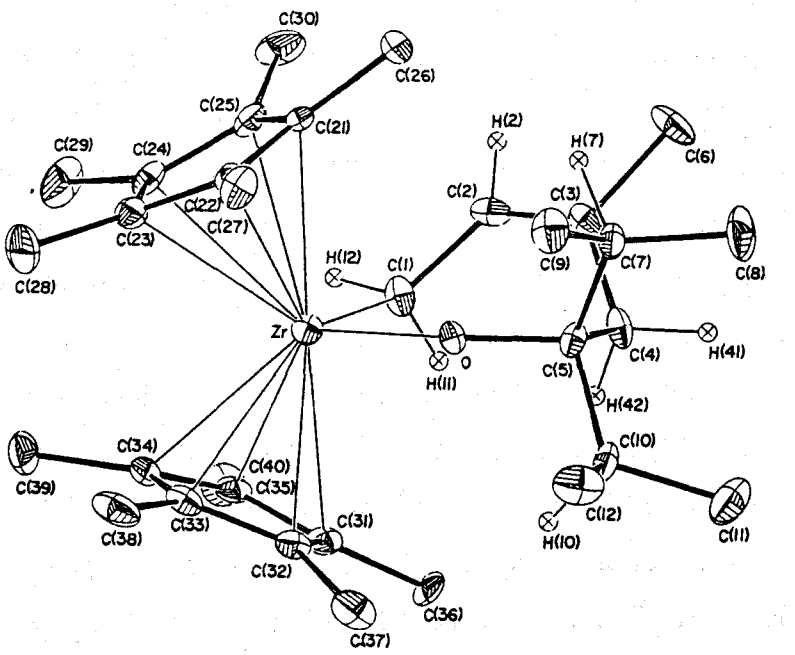

Fig. 2-6. Molecular structure of $(\eta^5\text{-}C_5Me_5)_2ZrOC(i\text{-}Pr)_2CH_2CMe{=}CHCH_2$ (**7**).

1.313Å in **6** and 1.324Å in **7**, show that these bonds are the localized carbon-carbon double bonds, whose standard value is 1.337±6Å. The interatomic distances between zirconium and C(2) and/or C(3) atoms [Zr-C(2):3.144Å in **6**, 3.177Å in **7**; Zr-C(3): 3.702Å in **6**, 3.729Å in **7**] indicate that there is no direct interaction between zirconium and the C(2)-C(3) double bond. Thus, the oxametallacycloheptene part in these complexes is described as having the 1,2-oxazirconacyclohept-4-ene structure.

The characteristic views of the molecular structure of **7** are shown in Figs. 2-7 and 2-8. The corresponding views of **6** are essentially the same as those of **7** in these Figures. The most interesting features in the oxametallacycloheptene part in these complexes are the conformations of C(1)-C(2)-C(3)-C(4) moieties, which correspond to the 1,3-dienes in the original complexes into which the ketone inserts. The torsional angles about C(2)-C(3) double bonds, C(1)-C(2)-C(3)-C(4), are 0.0° in **6** and 2.3° in **7**, respectively. Thus, the C(1) to C(4) moiety takes the *s-cis* structure in both complexes. The oxametallacycloheptene parts in **6** and **7** are divided into two planar moieties, the plane of diene moiety [C(1) to C(4), including also C(6) in **7**] and the approximate plane defined by C(1), Zr, O, C(5), and C(4) with the maximum atomic deviations from the plane of 0.088Å in **6** and 0.051Å in **7**, the dihedral angles being 62.7° in **6** and 61.1° in **7**, respectively. All the methyl groups in 2,4-dimethyl-3-pentanone moieties locate away from the oxametallacycloheptene part to release the possible nonbonded interatomic repulsions in both complexes.

The mean distances between zirconium and carbon atoms of C_5Me_5 ligands are 2.623Å in **6** and 2.621Å in **7**, and those between zirconium and the centroids of C_5Me_5 ligands [d_1 and d_2 in Fig. 2-8] are 2.331Å in both complexes. These distances are slightly longer than the corresponding distances in $(\eta^5\text{-}C_5H_5)_2ZrCl_2$[44] of 2.522Å and 2.20Å or those in $(\eta^5\text{-}C_5H_5)_2Zr(CHPh_2)$[45] of 2.513Å and 2.22Å. The CCP(1)-Zr-CCP(2) [CCP(1) and CCP(2), which are the centroids of C(21) to C(25) and C(31) and C(35)] angles [θ_1 in Fig. 2-8],

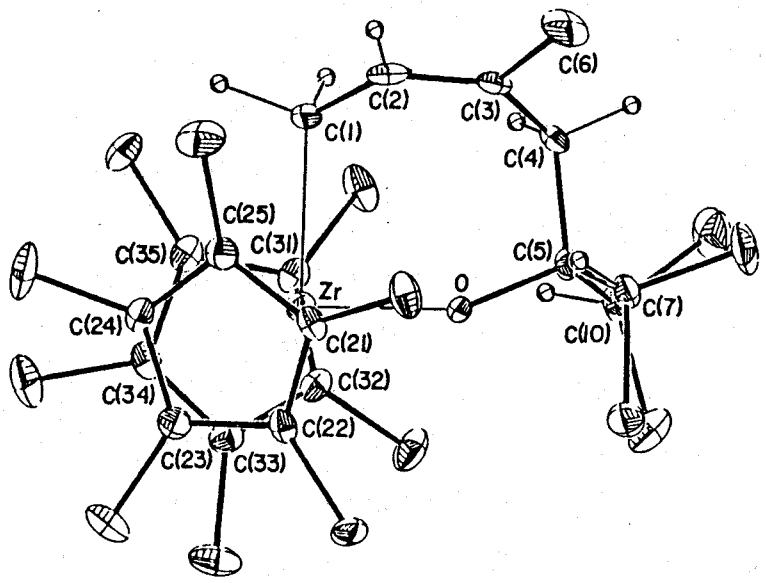

Fig. 2-7. Molecular structure of **7** projected onto the plane defined by Zr, O, and C(1) atoms.

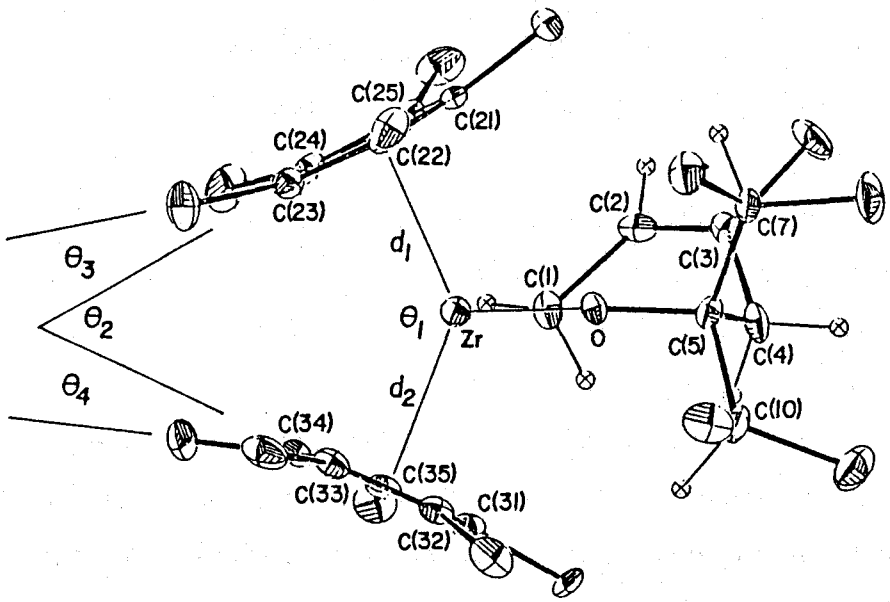

Fig. 2-8. Molecular structure of **7** viewed along the plane defined by Zr, O, and C(1) atoms.

129.0° in **6** and 129.4° in **7**, are similar to those in $(\eta^5\text{-}C_5H_5)_2Zr(CHPh_2)$[45] [128.4°], $(\eta^5\text{-}C_5H_5)_2ZrF_2$[46][127.8°], and $(\eta^5\text{-}C_5H_5)_2Zr$(2,3-dimethylbutadiene)[12] [124°]. Figure 2-7 shows that the two C_5Me_5 ligands are in a staggered conformation so as to release the non-bonded repulsion between the methyl groups of facing C_5Me_5 ligands. However, all the methyl groups in C_5Me_5 ligands in **6** and **7** bend back from the zirconium atom with the angular deviations from the C_5 plane [θ_3 or θ_4 in Fig. 2-8] of 3.7 to 16.1° [av. 10.2°] on CP(1) [ring defined by C(21) to C(25)] and of 7.2 to 15.2° [av. 10.2°] in CP(2) [ring defined by C(31) to C(35)] for **6**, and of 6.1 to 14.6° [av. 9.9°] in CP(1) and of 5.9 to 15.7° [av. 9.6°] in CP(2) for **7**, respectively. Some short contacts are found between these methyl groups, resulting in the large angular deviations from the C_5 rings: C(28)...C(38) 3.288Å, θ_3 16.1° [C(28)], θ_4 12.2° [C(38)] in **6**, and 3.329Å, θ_3 14.6° [C(28)], θ_4 8.1° [C(38)] in **7**; C(29)...C(39) 3.344Å, θ_3 9.5° [C(29)], θ_4 15.2° [C(39)] in **6**, and 3.327Å, θ_3 7.3° [C(29)], θ_4 15.7° [C(39)] in **7**. Some short contacts are also found between the methyl groups in the C_5Me_5 ligands and the oxametallacycloheptene part; C(1)...C(30) 3.262Å in **6** and 3.273Å in **7**; C(9)...C(26) 3.588Å in **6** and 3.635Å in **7**; and C(12)...C(37) 3.372Å in **6** and 3.374Å in **7**. The shortest nonbonded contact of the methyl group on C(3) in **7** is the C(6)...C(7) of 3.392Å.

The comparison between the molecular structures of **6** and **7** showed that these complexes take essentially the same structure in spite of the different coordination modes of the 1,3-diene in $(\eta^5\text{-}C_5Me_5)_2Zr$(butadiene) and $(\eta^5\text{-}C_5Me_5)_2Zr$(isoprene).

It is evident from the X-ray work that both the s-*cis*-diene and the s-*trans*-diene complexes gave oxametallocycloheptenes with (*Z*)-structure. Thus, the insertion of ketone caused the conversion of butadiene from s-*trans* to s-*cis* and the retention of isoprene in s-*cis* structure. The interconversion occurs presumably *via* 1,2-η^2-diene metal species with 16e configuration and the process *via* 1,4-η^2-diene metal species (16e) can be ruled out.

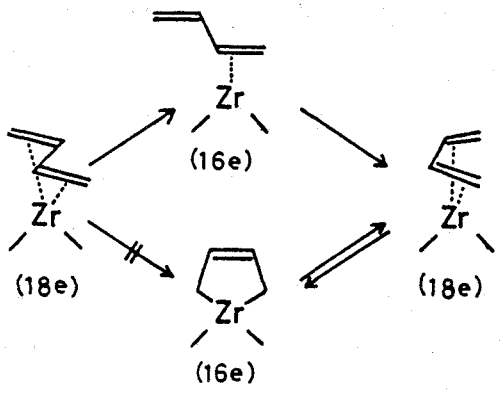

Since the Zr-η^4-diene complex has 18e configuration and leaves no vacant coordination site, the insertion of 2,4-dimethyl-3-pentanone may take place after its conversion to zirconacyclopent-3-ene structure with 16e configuration. Direct conversion of η^2-diene species to metallacyclopentene can not be ruled out when a ketone is present in the system. An MO calculation predicts that wedged $(C_5H_5)_2M$ fragment has three in-plane orbitals of d-character.[47] The $2a_1$ and b_2 orbitals are used for forming the zircona ring and the remaining vacant orbital ($1a_1$) may be used for the coordination of the ketone. Therefore, a zircona ring coordinated through oxygen atom of carbonyl group may be postulated as the intermediate. Insertion of ketone will then take place *via* four-centered transition state.

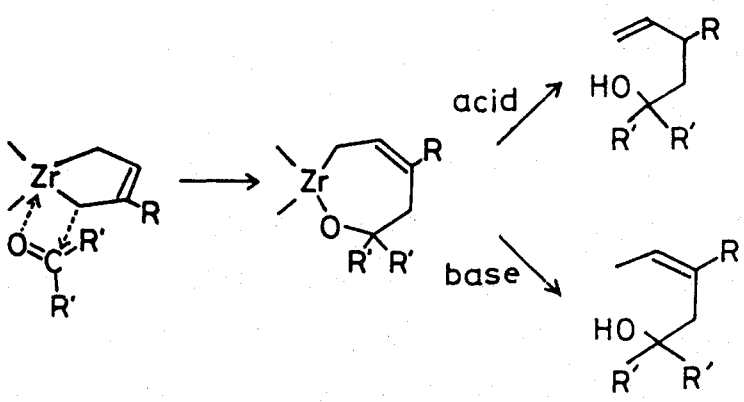

Hydrolysis of **7** with protic acid (aq HCl) gave 2,5-dimethyl-3-isopropyl-6-hepten-3-ol but hydrolysis with bases such as NaOH and Et_2NH gave (*Z*)-2,5-dimethyl-3-isopropyl-5-hepten-3-ol quantatively, in line with the X-ray structure. The high regioselectivity observed in the formation of **7** is explained by the inductive effect of the methyl group of isoprene, which causes the higher negative charge on the C_1 atom.

Other ketones, such as 2-propanone or 3-pentanone, and aldehydes such as ethanal or propanal, also react with **1a-1d** in the same fashion. Therefore, the present reaction mechanism seems applicable in general for these reactions.

2-3 Unique Structure of $(\eta^5\text{-}C_5H_5)_2Zr(CH_2C(CH_3)CHCH_2C(CH_3)=C(CH_3))$ Prepared by Regioselective Insertion of 2-Butyne to $Zr(\eta^5\text{-}C_5H_5)_2$(Isoprene)

The 1,3-diene complexes of Group 4 metals (Ti, Zr, Hf) are known to have reactive metal-carbon bonds, which insert compounds with unsaturated C-O, C-C and C-N bonds into the metal-carbon bond to lead to regioselective carbon-carbon bond formation.[5,6,48,49] $ZrCp_2$(isoprene), thus, inserts ketones or aldehydes at an unusual position [Zr-C(1) bond] to give a sterically hindered product, while the corresponding magnesium-diene complexes and allylic zirconium complexes generally react with ketones or aldehydes at the Zr-C(3) bond.[5,50] In contrast to the reaction of carbonyl compounds, insertion of olefins, dienes or alkynes occurred into the Zr-C(4) bond regioselectively.[6]

The determination of the molecular structures of these complexes provides clear evidences for the regioselective C-C bond formation. The X-ray structure analysis of the insertion product obtained from $Zr(\eta^5\text{-}C_5Me_5)_2$(isoprene) and diisopropyl ketone showed a 7-membered ring oxametallacyclic structure where the ketone is inserted into the Zr-C(1) bond.[51] Here, the molecular structure of a novel regioselective insertion product of 2-butyne with $ZrCp_2$(isoprene) has been determined by the X-ray diffraction

method.

Crystal data and experimental parameters for structure determination are summarized in Table 2-18. Final atomic coordinates are listed in Table 2-19, and interatomic bond distances and angles in Table 2-20. The X-ray structure analysis revealed a unique 1-3-η; 6-η-(2*E*,5*Z*)-2,5-dimethyl-2,5-heptadien-1,6-diyl ligand bound to $Zr(\eta 5\text{-}C_5H_5)_2$ species. The molecular structure obtained is shown in Fig. 2-9. Note that the 2-butyne molecule was inserted into the Zr-C(4) bond of $ZrCp_2$(isoprene) making bonds between Zr and C(7) [2.367Å], and C(6) and C(4) [1.511Å]. The C(6)-C(7) bond distance of 1.347Å agrees with the normal double bond distance of 1.337±6Å.[52] The 2-butyne moiety [C(6), C(7), C(8) and C(9)] locates roughly on the plane composed of Zr, C(1) and C(4) with the maximum atomic deviation of 0.23Å.

The most important feature of this molecule is in the structure of the isoprene moiety. The Zr-C(1), Zr-C(2) and Zr-C(3) distances are 2.427, 2.595 and 2.522Å, respectively, while Zr-C(4) distance of 3.466Å is far from the bonding distance. The C(1)-C(2), C(2)-C(3) and C(3)-C(4) distances are 1.421, 1.361 and 1.485Å, respectively. These distances indicate a π-allyl type coordination of the isoprene moiety to the Zr atom. The present complex takes a π-allylic structure also in solution.[53] The structure of the starting material, $ZrCp_2$(isoprene), has been reported to have the conventional s-*cis* structure in an benzene solution.[40] Thus, the (s-*cis*-η^4-diene)metal or metallacyclo-3-pentene structures changed to the (π-allyl)metal structure. Because of this structural change, the conformation of the isoprene moiety changed from s-*cis* to s-*trans*, the torsional angle around C(2)-C(3) bond, C(1)-C(2)-C(3)-C(4), being 166.4°. The dihedral angle between the planes defined by Zr, C(1) and C(3), and by C(1), C(2), C(3) and C(5) is 114.1°.

The bond distances between the Zr atom and carbon atoms of Cp(1) [C(11) to C(15)] and Cp(2) [C(21) to C(25)] range from 2.507 to 2.565Å [av. 2.538Å], and 2.530 to 2.584Å [av. 2.559Å], respectively. The Cp(1)centroid-Zr-

Table 2-18. Crystal Data and Experimental Parameters for X-Ray Structure Determination of $(\eta^5\text{-}C_5H_5)_2Zr[(CH_2C(CH_3)CHCH_2\text{-}C(CH_3)=C(CH_3)]$

Formula	$C_{19}H_{24}Zr$
Formula weight	343.6
Crystal system	orthorhombic
Space group	$P2_12_12_1$
Temp., °C	20
a,[a] Å	21.828(6)
b, Å	8.280(2)
c, Å	8.842(2)
V, Å^3	1598.1(7)
Z	4
D_{calcd}, g cm^{-3}	1.428
$F(000)$, e	712
μ(MoKα), cm^{-1}	6.7
Crystal size, mm	0.63x0.38x0.15
2θ range,[b] deg	4<2θ<66
Scan width, deg in 2θ	2.0+0.70tanθ
Scan speed, deg min^{-1}	4.0
Background count, s	5
Reflections measured	3402
Reflections observed[c]	2734
Radiation damage	no
No. of variables	242
GOF[d]	1.127
R[e]	0.067
R_w[f]	0.082

[a)]Least-squares refinement of the θ values for 25 reflections with 2θ>25°. [b)]Intensity data were collected on a Rigaku four-circle diffractometer using graphite-monochromatized MoKα radiation by the θ-2θ scan method. [c)]non-zero reflections. [d)]$[\Sigma w(|F_o|-|F_c|)^2/(n-m)]^{1/2}$, where n and m are the No. of reflections used and variables refined, respectively. [e)]$R=\Sigma(|F_o|-|F_c|)/\Sigma|F_o|$. [f)]$R_w=[\Sigma w(|F_o|-|F_c|)^2/\Sigma w|F_o|^2]^{1/2}$, $w=[\sigma^2(F_o)+g(F_o)^2]^{-1}$, and g=0.003.

Table 2-19. Final Atomic Coordinates and Equivalent Isotropic Temperature Factors for Nonhydrogen Atoms in $(\eta^5\text{-}C_5H_5)_2Zr[(CH_2C(CH_3)\text{-}CHCH_2C(CH_3)=C(CH_3)]$ with Estimated Standard Deviations in Parentheses[a]

atom	*x*	*y*	*z*	B_{eq}, Å^2
ZR	0.14838(3)	0.22181(8)	0.08964(7)	2.65
C(1)	0.1138(4)	0.0261(10)	0.2752(10)	3.20
C(2)	0.0578(4)	0.1078(9)	0.2468(9)	3.06
C(3)	0.0395(3)	0.1209(8)	0.1001(9)	2.54
C(4)	-0.0084(4)	0.2227(11)	0.0284(9)	2.98
C(5)	0.0244(5)	0.1943(12)	0.3727(10)	3.8
C(6)	0.0210(4)	0.3311(9)	-0.0884(9)	2.62
C(7)	0.0823(4)	0.3502(9)	-0.0851(9)	2.76
C(8)	-0.0237(4)	0.4107(13)	-0.1976(10)	4.0
C(9)	0.1105(5)	0.4607(12)	-0.2057(10)	3.8
C(11)	0.2152(5)	0.4641(13)	0.1359(11)	4.5
C(12)	0.2230(4)	0.3585(12)	0.2630(9)	3.7
C(13)	0.1664(5)	0.3682(15)	0.3404(9)	5.0
C(14)	0.1262(5)	0.4601(11)	0.2667(11)	3.9
C(15)	0.1564(6)	0.5233(11)	0.1427(12)	4.8
C(21)	0.1740(5)	0.1046(12)	-0.1703(9)	3.7
C(22)	0.1678(4)	-0.0292(10)	-0.0773(11)	3.6
C(23)	0.2151(5)	-0.0266(12)	0.0304(11)	4.1
C(24)	0.2511(4)	0.1070(14)	0.0035(11)	4.3
C(25)	0.2247(5)	0.1916(13)	-0.1238(10)	4.3

[a]Positional parameters are in fraction of cell edges and B_{eq} is the equivalent isotropic temperature factors calculated from the corresponding anisotropic thermal parameters. B_{eq} is only for Zr and *B* for remaining atoms.

Table 2-20. Interatomic Bond Distances (Å) and Selected Bond Angles (°) in $(\eta^5\text{-}C_5H_5)_2Zr[(CH_2C(CH_3)CHCH_2C(CH_3)=C(CH_3)]$ with Estimated Standard Deviations in Parentheses

Bond distance (Å)

Zr	- C(1)	2.427(8)	Zr	- C(2)	2.595(7)
Zr	- C(3)	2.522(7)	Zr	- C(7)	2.367(7)
C(1)	- C(2)	1.421(11)	C(2)	- C(3)	1.361(10)
C(2)	- C(5)	1.511(12)	C(3)	- C(4)	1.485(11)
C(4)	- C(6)	1.511(11)	C(6)	- C(7)	1.347(10)
C(6)	- C(8)	1.522(12)	C(7)	- C(9)	1.534(12)
C(11)	- C(12)	1.434(14)	C(11)	- C(15)	1.376(15)
C(12)	- C(13)	1.414(15)	C(13)	- C(14)	1.332(15)
C(14)	- C(15)	1.382(14)	C(21)	- C(22)	1.387(13)
C(21)	- C(25)	1.383(13)	C(22)	- C(23)	1.404(13)
C(23)	- C(24)	1.378(14)	C(24)	- C(25)	1.445(14)
Zr	- CP(1)	2.247	Zr	- CP(2)	2.266

Bond angle (°)

C(1)	-Zr	-C(7)	123.5(2)	C(2)	-Zr	-C(7)	92.8(2)
C(3)	-Zr	-C(7)	66.3(2)	C(1)	-C(2)	-C(3)	117.3(7)
C(1)	-C(2)	-C(5)	120.7(7)	C(3)	-C(2)	-C(5)	121.5(7)
C(2)	-C(3)	-C(4)	131.2(7)	C(3)	-C(4)	-C(6)	109.3(6)
C(4)	-C(6)	-C(7)	118.5(6)	C(4)	-C(6)	-C(8)	114.7(6)
C(7)	-C(6)	-C(8)	126.8(7)	C(6)	-C(7)	-C(9)	117.0(6)
CP(1)	-Zr	-CP(2)	128.1				

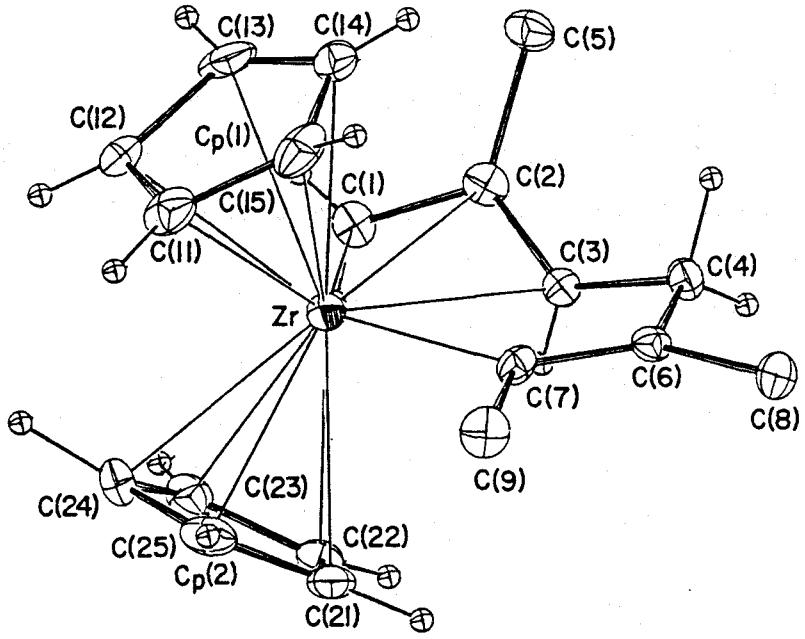

Fig. 2-9. Molecular structure of $(\eta^5\text{-}C_5H_5)_2Zr[(CH_2C(CH_3)CHCH_2\text{-}C(CH_3)=C(CH_3)]$.

Cp(2)centroid angle is 128.1°, which is similar to those in $ZrCp_2$(s-*cis*-2,3-dimethylbutadiene) [124°][12] and $ZrCp_2$(s-*trans*-1,4-diphenylbutadiene) [125.0 and 129.4°].[54]

Similar structures to the present complex have been deduced from the ^1H NMR spectra for a series of olefin insertion products, $(\eta^5\text{-}C_5H_5)_2Zr(CH_2C(CH_3)CHCH_2)CRR'CH_2$ where R, R' are H, CH_3, C_2H_5, C_3H_7 or C_4H_9.[55]

References

1) H. Yasuda and A. Nakamura, *Angew. Chem., Int. Ed. Engl.*, **26**, 723 (1987).

2) H. Yasuda, K. Tatsumi, and A. Nakamura, *Acc. Chem. Res.*, **18**, 120 (1985).

3) M. Akita, Y. Matsuoka, K. Asami, H. Yasuda, and A. Nakamura, *J. Organomet. Chem.*, **327**, 193 (1987).

4) Y. Kai, N. Kanehisa, K. Miki, N. Kasai, M. Akita, H. Yasuda, and A. Nakamura, *Bull. Chem. Soc. Jpn.*, **56**, 3735 (1983).

5) H. Yasuda, Y. Kajihara, K. Mashima, K. Nagasuna, and A. Nakamura, *Chem. Lett.*, **1981**, 671.

6) H. Yasuda, Y. Kajiwara, K. Nagasuna, K. Mashima, and A. Nakamura, *Chem. Lett.*, **1981**, 719.

7) H. Yasuda, T. Okamoto, K. Mashima, and A. Nakamura, *J. Organomet. Chem.*, **363**, 61 (1989).

8) G. Erker, K. Engel, J. L. Atwood, and W. E. Hunter, *Angew. Chem., Int. Ed. Engl.*,**22** 494 (1983).

9) G. Erker and U. Dorf, *Angew. Chem., Int. Ed. Engl.*, **22**, 777 (1983).

10) G. Erker, K. Engel, U. Dorf, J. L. Atwood, and W. Hunter, *Angew. Chem., Int. Ed. Engl.*, **21**, 914 (1985).

11) G. Erker, C. Kruger, and G. Muller, *Adv. Organomet. Chem.*, **24**, 1 (1985).

12) G. Erker, J. Wicher, K. Engel, F. Rosenfeldt, W. Dietrich, and C. Kruger, *J. Am. Chem. Soc.*, **102**, 6346 (1980).

13) H. Yasuda, Y. Kajihara, K. Mashima, K. Nagasuna, K. Lee, and A. Nakamura, *Organometallics*, **1**, 388 (1982).

14) H. Yasuda, K. Mashima, K. Lee, and A. Nakamura, *Chem. Lett.*, **1981**, 519.

15) S. Datta, S. S. Wreford, R. R. Beatty, and T. J. MeNeese, *J. Am. Chem. Soc.*, **101**, 1053 (1979).

16) R. R. Beatty, S. Datta, and S. S. Wreford, *Inorg. Chem.*, **18**, 3139 (1979).

17) S. Datta, M. B. Fisher, and S. S. Wreford, *J. Organomet. Chem.*, **188**, 353 (1980).

18) J. Blenkers, B. Hessen, F. van Bolhuis, A. Wagner, J. H. Teuben, *Organometallics*, **6**, 459 (1987).

19) G. Erker, K. Berg, K. Angermund, and C. Kruger, *Organometallics*, **6**, 2621 (1987).

20) R. F. Jordan, C. S. Bajgur, and B. Scott, *J. Am. Chem. Soc.*, **108**, 7410 (1986).

21) W. E. Hunter, D. C. Hrncir, R. Vann Bynum, R. A. Penttila, and J. L. Atwood, *Organometallics*, **2**, 750 (1983).
22) S. L. Buchwald, B. T. Watson and J. C. Huffman, *J. Am. Chem. Soc.*, **108**, 7411 (1986).
23) G. Erker, R. Schlund, and C. Kruger, *J. Chem. Soc., Chem. Commun.*, **1986**, 1403.
24) S. L. Buchwald, B. T. Watson, and J. C. Huffman, *J. Am. Chem. Soc.*, **109**, 2544 (1987).
25) H. Takaya, M. Yamakawa, and K. Mashima, *J. Chem. Soc., Chem. Commun.*, **1983**, 1283.
26) H. Hoberg, and K. Jennin, *J. Organomet. Chem.*, **322**, 193 (1987).
27) C. Fachinetti, C. Floriani, A. Chiese-Villa, and C. Guastini, *J. Am. Chem. Soc.*, **101**, 1767 (1979).
28) G. L. Hillhouse and J. E. Bercaw, *J. Am. Chem. Soc.*, **106**, 5472 (1984).
29) R. Boltolin, V. Patel, I. Mundy, N. J. Tator, and A. J. Carty, *J. Chem. Soc., Chem. Commun.*, **1985**, 456.
30) D. Walther, E. Dinjus, H. Gorls, J. Sirler, O. L. Lindquisit, and L. Andersen, *J. Organomet. Chem.*, **286**, 103 (1985).
31) (a) J. K. Becconsall and S. O'Brien, *J. Chem. Soc., Chem. Commun.*, **1966**, 302. (b) J. K. Becconsall and B. E. Job, *J. Chem. Soc.*, **A1967**, 423.
32) D. J. Brauer and C. Kruger, *Organometallics*, **1**, 207 (1982). (b) H.-J. Kablitz and G. Wilke, *J. Organomet. Chem*, **51**, 241 (1973).
33) D. J. Brauer and C. Kruger, *Organometallics*, **1**, 204 (1982).
34) H.-P. Klein, K. Doppert, and U. Thewalt, *J. Organomet. Chem.*, **280**, 203 (1985).
35) J. L. Petersen and W. R. Tikkanen, *Organometallics*, **3**, 1651 (1984).
36) J. L. Petersen and J. W. Jr. Egan, *Organometallics*, **6**, 2007 (1987).
37) K. Mashima, Dissertation, Osaka University, 1985.
38) M. Akita, H. Yasuda, and A. Nakamura, *Chem. Lett.*, **1983**, 217.
39) G. Erker, J. Wicher, K. Engel, and C. Kruger, *Chem. Ber.*, **115**, 3300 (1982).
40) H. Yasuda, Y. Kajihara, K. Mashima, K. Nagasuna, K. Lee, and A. Nakamura, *Organometallics*, **1**, 388 (1982).
41) H. Yasuda, Y. Kajihara, K. Mashima, K. Nagasuna, K. Lee, and A. Nakamura, *Organometallics*, **2**, 478 (1983).
42) J. L. Atwood, W. E. Hunter, D. C. Hrncir, E. Samuel, H. Alt, and M. D. Rausch, *Inorg. Chem.*, **14**, 1757 (1975).

43) J. Jeffery, M. F. Lappert, and N. T. Loung-Thi, *J. Chem. Soc., Chem. Commun.*, **1978**, 1081.
44) I. A. Ronova, N. V. Alekseev, N. I. Gapotcheko, and Yu. T. Struchkov, *J. Organomet. Chem.*, **25**, 149 (1970).
45) J. L. Atwood, G. K. Barker, J. Holton, W. E. Hunter, M. F. Lappert, and R. Pearce, *J. Am. Chem. Soc.*, 99, 6645 (1977).
46) M. A. Bush and G. A. Sim, *J. Chem. Soc., Sect. A*, **1971**, 2225.
47) J. W. Lauher and R. Hoffmann, *J. Am. Chem. Soc.*, 98, 1729 (1976).
48) G. Erker and K. Cropp, *J. Am. Chem. Soc.*, **101**, 3659 (1979).
49) D. B. Carr and J. Schwartz, *J. Am. Chem. Soc.*, **101**, 3521 (1979).
50) Y. Yamamoto and K. Maruyama, *Tetrahedran Lett.*, **1981**, 2895.
51) N. Kanehisa, Y. Kai, K. Miki, N. Kasai, M. Akita, H. Yasuda, and A. Nakamura, 45th Annual Meeting of the Chemical Society of Japan, Tokyo, April 1982, Abstr. No. 3B31.
52) "International Tables for X-Ray Crystallography," Kynoch Press, Vol. III, Birmingham (1968), P.276.
53) The previously reported ^{1}H-NMR data (Ref. 38a) are better understood by the 1-3-η;6-η-2,5-dimethyl-2,5-heptadiene-1,6-diyl structure based on the present X-ray work.
54) Y. Kai, N. Kanehisa, K. Miki, N. Kasai, K. Mashima, K. Nagasuna, H. Yasuda, and A. Nakamura, *J. Chem. Soc., Chem. Commun.*, **1982**, 191.
55) For example, ^{1}H-NMR data for isobutene insertion product (toluene-d_8 at 30°C); δ 1.39(d,H_1(*anti*),J_{gem}=4.6Hz), 1.98(d,H_1(*syn*)), 3.55(d of d,H_3,$J_{3,4}$=10.2,$J_{3,4}$=4.9Hz), 1.90(d,H_4,J_{gem}=12.0Hz), 2.06(d,$H_{4'}$), 1.56(s,CH_3 of isoprene unit), 1.20 and 1.41(s,CH_3 of isobutene unit), 5.01 and 5.36(s,C_5H_5), 0.87(s,CH_2,Zr-CH_2).

Chapter 3. Versatile Bonding Character of Bulky Phenoxy Ligands in Early Transition Metal Complexes

The use of bulky aryloxy or alkoxy metal compounds of group 4-6 as an alternative of cyclopentadienyl compounds, MX_nCp and MX_nCp_2, is of current interest in organometallic chemistry.[1-3] Aryloxy or alkoxy ligands are expected to have the structural features of smaller bulkiness in the metal coordination spheres compared with Cp ligands and flexible conformation around metal-OR [R=alkyl or phenyl] bonds.

The 1:1 reaction of $TiCl_4(THF)_2$ with 2,6-dimethylphenoxy(trimethyl)-silane in THF at 60°C for 2 h was found to afford a pure sample of a new compound, $TiCl_3[O\text{-}2,6\text{-}(CH_3)_2C_6H_3](THF)_2$ (**1**) in 90% yield releasing Me_3SiCl as monitored by NMR spectra. After the usual work-up, the resulting product was purified by recrystallization form THF/hexane to give red crystals of **1** in 79% yield (mp 122°C). Analogously, the corresponding zirconium and hafnium derivatives, $MCl_3[O\text{-}2,6\text{-}(CH_3)_2C_6H_3](THF)_2$ [**2**, M=Zr, mp 142°C(dec) and **3**, M=Hf, mp 161°C(dec)], were first obtained in high purity by refluxing the 1:1 mixture in THF for 6 h, and these were isolated as colorless crystals in 55-65% yields. Bis(phenoxy) derivatives, $MCl_2[O\text{-}2,6\text{-}(CH_3)_2C_6H_3]_2(THF)_2$, were also available by refluxing a mixture of the corresponding metal halides and $C_6H_3(CH_3)_2O\text{-}Si(CH_3)_3$ (1:2.5 ratio) in THF for 10 h. Recrystallization of the product from THF/hexane gave a titanium compound (**4**, mp. 85°C) as dark-red crystals and a zirconium derivative [**5**, mp 153°C(dec)] and a hafnium derivative (**6**, 170°C) as colorless crystals in ca. 75% yield. The present method[4] is found to be superior to the conventional methods (i.e. reaction with a substituted bulky phenoxysodium[5] or reaction of bulky phenols in the presence of an amine[6]) with respect to the easiness in handling, purity of both mono- and bis-(phenoxy)metal compounds and yield.

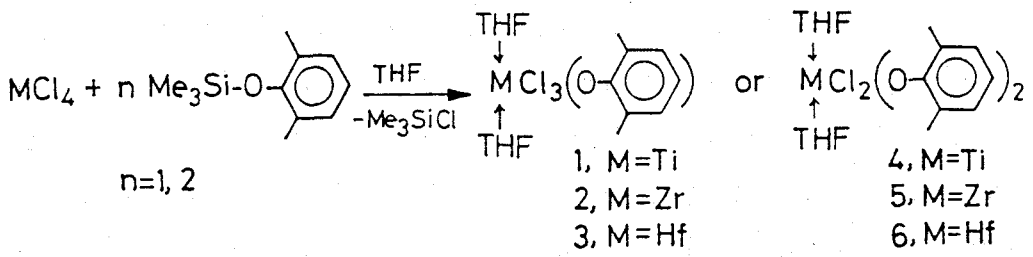

The present method is also useful for the synthesis of group 5 niobium and group 6 tungsten phenoxides. The 1:1 and 1:2 reactions of anhydrous $NbCl_5$ with 2,6-dimethylphenoxy(trimethyl)silane in toluene at 80 °C for 2-6 h followed by the addition of 20 equimol of THF gave $NbCl_4$[O-2,6-$(CH_3)_2C_6H_3$](THF) (**7**) and $NbCl_3$[O-2,6-$(CH_3)_2C_6H_3]_2$(THF) (**8**), respectively in quantitative yield. Direct addition of $NbCl_5$ to THF must be avoided since cationic ring opening polymerization of THF occurs promptly. Recrystallization of the products from THF/hexane provides **7** (mp 143 °C) and **8** (mp 178 °C) as red crystals in 82% and 75%, respectively. In essentially the same manner, both WCl_5[O-2,6-$(CH_3)_2C_6H_3$] (**9**, mp 151 °C) and WCl_4[O-2,6-$(CH_3)_2C_6H_3]_2$ (**10**, mp 166 °C) were successfully prepared as dark purple crystals for **9**, and dark blue crystals for **10** respectively.

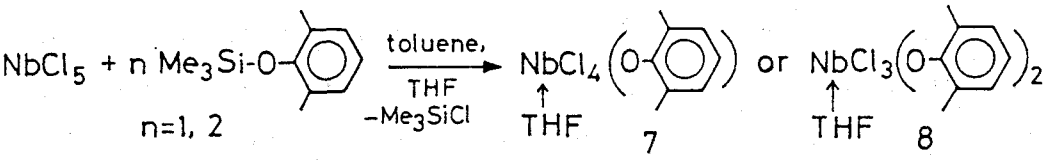

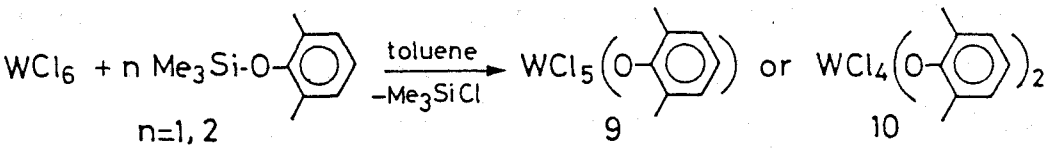

In order to elucidate the exact geometries of this series of early transition metal-phenoxides, the X-ray structure analyses have been proceeded on the complexes **1**, **4**, **5**, **7**, **8**, **9**, **10**, and $NbCl_3$[O-2,6-$(C_6H_5)_2C_6H_3]_2$(THF) (**8b**). Unit-cell parameters were determined at room temperature by a least-squares fit

of the 2θ values of strong higher-angle reflections observed on a four-circle diffractometer. The measurements of diffraction intensities have been carried out in the similar ways as described in the preceding complexes. Rotating anode X-ray generator was used for **7** and **9**, and sealed-off tube was used for other complexes. The data measurements for **7** and **9** were proceeded by the MSC/AFC software[7]. The experimental conditions for **7** and **9** are; θ-2θ scan technique, variable scan rate of 8-16°min^{-1} in θ depending on the peak intensity of each reflection, weak reflections were repeated up to three times, scan width of $\Delta\theta=1.0+0.30\tan\theta$, total background countings are 50% of the peak scan times, and for other complexes; θ-2θ scan technique, fixed scan rate of 2° min^{-1} in θ, scan width of $\Delta\theta=1.0+0.35\tan\theta$, fixed background counts 5 s on each end of scan. Three standard reflections were measured after every 150 reflections for **7** and **9** and 61 reflections for other complexes in order to monitor the radiation damage and any change in the crystal orientation. No significant intensity decay of the standard reflections was observed for all crystals. Absorption corrections were applied for **7** and **9**.

The determination and refinement of the crystal structures of **7** and **9** were carried out by using the TEXSAN software system[8] and those of other complexes by the preceding programs. All crystal structures were solved by heavy-atom method. Successive Fourier syntheses phased by the metal atoms found in Patterson maps clearly revealed the remaining nonhydrogen atoms. The structures were refined anisotropically by the full-matrix least-squares method [XRAY-76[9]] for crystals except **7** and **9**, the function minimized being $\Sigma w(\Delta F)^2$. All of the hydrogen atoms were located on difference Fourier maps and were included in the refinement with isotropic temperature factors. The applied weighting schemes were $w=4(F_o)^2/\sigma^2(F_o^2)$ for **7** and **9** and $w=[\sigma_{cs}^2(F_o)+g\times(F_o)^2]^{-1}$ for **1** (g=0.003), **4** (g=0.002), **5** (g=0.004), **8** (g=0.003), **8b** (g=0.003), and **10** (g=0.003). The computations for **7** and **9** were proceeded on VAXstation 3100 in Rigaku AFC-5R system in the Department of Applied

Chemistry, Faculty of Engineering, Osaka University while those for other complexes were carried out on ACOS-850 computer at the Research Center for Protein Engineering, Institute for Protein Research, Osaka University.

3-1. Stereochemistry of Monophenoxide with Groups 4 and 5 Early Transition Metals

Different kinds of early transition metal alkoxides have been prepared and the ligation of alkoxide have provided new aspects of these metals. However, a few example of monokisalkoxide complexes have been prepared because the reaction of alcohol with metal afforded the complied mixture of different number of alkoxide on a metal. It was found that a chlorine atom bound to group 4-6 transition metals can be replaced by the reaction with $ArOSiMe_3$ to afford monokisaryloxo complexes of type $MCl_n(OAr)$.

X-ray structure analyses have been proceeded on complexes **1** and **7**. Crystal data, data collection, and parameters for structure refinement of **1** and **7** are summarized in Tables 3-1 and 3-2, respectively. Fractional atomic coordinates and equivalent isotropic temperature factors for nonhydrogen atoms are listed in Tables 3-3 and 3-4. Interatomic bond distances and angles are listed in Tables 3-5 and 3-6. The molecular structures of **1** and **7** are shown in Fig. 3-1 by ORTEP drawings[10] together with the partial atomic labellings. In complex **1** the central atom Ti has six-coordinated geometry with two THF ligands in *cis* position and three chlorine atoms in *meridian* position. Complex **7** belongs to orthorhombic crystal system with space group *Cmcm*. Since four molecules are in the unit cell, the crystallographic molecular symmetry is *mm* (C_{2v}), and all the nonhydrogen atoms except chlorines are on a mirror plane. Therefore, phenoxy and THF ligands are in *trans*, and central Nb atom also has six-coordinated geometry. In complex **1**, the Cl(1)-Ti-Cl(2) angle is 166.9° and both Cl(1), Cl(2) atoms tilt away from the phenoxy ligand. In complex **7**, the

Table 3-1. Crystal Data and Experimental Parameters for X-Ray Structure Determination of $TiCl_3[O\text{-}2,6\text{-}(CH_3)_2C_6H_3](THF)_2$ (**1**)

Formula	$TiCl_3O_3C_{16}H_{25}$
Formula weight	419.7
Crystal system	orthorhombic
Space group	$Pna2_1$
Temp., °C	20
a,[a] Å	17.389(3)
b, Å	10.610(1)
c, Å	10.83582)
V, Å^3	1998.9(5)
Z	4
D_{calcd}, g cm^{-3}	1.394
$F(000)$, e	872
μ(MoKα), cm^{-1}	8.5
Crystal size, mm	0.45x0.38x0.5
2θ range,[b] deg	4<2θ<60
Scan width, deg in 2θ	1.0+0.35tanθ
Scan speed, deg min^{-1}	4
Background count, s	5
Reflections measured	3058
Reflections observed[c]	2345
Radiation damage	no
No. of variables	308
GOF[d]	2.793
R[e]	0.053
R_w[f]	0.074

[a]Least-squares refinement of the θ values for 25 reflections with 2θ>25°. [b]Intensity data were collected on a Rigaku four-circle diffractometer using graphite-monochromatized MoKα radiation by the θ-2θ scan method. [c]$|F_o|>3\sigma(F_o)$. [d]$[\Sigma w(|F_o|-|F_c|)^2/(n-m)]^{1/2}$, where n and m are the No. of reflections used and variables refined, respectively. [e]$R=\Sigma(|F_o|-|F_c|)/\Sigma|F_o|$. [f]$R_w=[\Sigma w(|F_o|-|F_c|)^2/\Sigma w|F_o|^2]^{1/2}$, $w=[\sigma^2(F_o)+g(F_o)^2]^{-1}$, and $g=0.003$.

Table 3-2. Crystal Data and Experimental Parameters for X-Ray Structure Determination of $NbCl_4[O\text{-}2,6\text{-}(CH_3)_2C_6H_3](THF)$ (7)

Formula	$NbCl_4O_2C_{12}H_{17}$
Formula weight	428.0
Crystal system	orthorhombic
Space group	*Cmcm*
Temp., °C	23
a,[a] Å	7.979(3)
b, Å	17.094(4)
c, Å	12.536(2)
V, Å^3	1709.7(8)
Z	4
D_{calcd}, g cm^{-3}	1.663
F(000), e	856
μ(MoKα), cm^{-1}	13.0
Crystal size, mm	0.25x0.40x0.30
2θ range,[b] deg	$6<2\theta<55$
Scan width, deg in 2θ	$1.630+0.30\tan\theta$
Scan speed, deg min^{-1}	8-16
Background count, s	50% of peak scan
Reflections measured	1146
Reflections observed[c]	702
Radiation damage	no
No. of variables	60
GOF[d]	2.27
R[e]	0.053
R_w[f]	0.038

[a]Least-squares refinement of the θ values for 25 reflections with $2\theta>25°$. [b]Intensity data were collected on a Rigaku four-circle diffractometer using graphite-monochromatized MoKα radiation by the θ-2θ scan method. [c]$|F_o|>3\sigma(F_o)$. [d]$[\Sigma w(|F_o|-|F_c|)^2/(n-m)]^{1/2}$, where *n* and *m* are the No. of reflections used and variables refined, respectively. [e]$R=\Sigma(|F_o|-|F_c|)/\Sigma|F_o|$. [f]$R_w=[\Sigma w(|F_o|-|F_c|)^2/\Sigma w|F_o|^2]^{1/2}$, $w=4F_o^2/\sigma^2(F_o^2)$.

Table 3-3. Final Atomic Coordinates and Equivalent Isotropic Temperature Factors for Nonhydrogen Atoms in $TiCl_3[O\text{-}2,6\text{-}(CH_3)_2C_6H_3](THF)_2$ (**1**) with Estimated Standard Deviations in Parentheses[a)]

Atom	x	y	z	B_{eq}
Ti	0.17659(5)	0.05375(9)	0	3.25
Cl(1)	0.12358(9)	-0.13336(14)	0.0729(3)	4.76
Cl(2)	0.21494(10)	0.26119(15)	-0.0346(3)	4.72
Cl(3)	0.13359(12)	0.0188(3)	-0.1956(3)	5.66
O(1)	0.2703(2)	-0.0058(4)	-0.0204(5)	4.0
O(3)	0.0650(2)	0.1342(4)	0.0432(6)	4.5
O(4)	0.1963(3)	0.0963(5)	0.1931(5)	4.1
C(11)	0.3450(3)	-0.0375(5)	-0.0360(7)	3.5
C(12)	0.3807(4)	-0.1093(6)	0.0559(7)	4.0
C(13)	0.4579(4)	-0.1430(8)	0.0382(9)	5.4
C(14)	0.4975(5)	-0.1006(9)	-0.0667(10)	6.3
C(15)	0.4614(5)	-0.0302(8)	-0.1540(9)	5.5
C(16)	0.3832(4)	0.0029(6)	-0.1437(7)	4.3
C(17)	0.3374(5)	-0.1546(9)	0.1665(8)	5.6
C(18)	0.3423(6)	0.0725(8)	-0.2437(9)	5.9
C(31)	-0.0090(4)	0.0720(7)	0.0190(12)	6.5
C(32)	-0.0673(5)	0.1744(8)	0.0208(12)	6.9
C(33)	-0.0343(5)	0.2665(9)	0.1095(13)	7.2
C(34)	0.0502(5)	0.2613(7)	0.0856(14)	7.2
C(41)	0.1516(6)	0.0483(13)	0.2980(9)	8.0
C(42)	0.1857(7)	0.1021(12)	0.4095(10)	7.2
C(43)	0.2672(6)	0.1393(10)	0.3735(9)	6.6
C(44)	0.2613(5)	0.1717(8)	0.2382(8)	5.3

[a)]Positional parameters are in fraction of cell edges and B_{eq} is the equivalent isotropic temperature factors calculated from the corresponding anisotropic thermal parameters.

Table 3-4. Final Atomic Coordinates and Equivalent Isotropic Temperature Factors for Nonhydrogen Atoms in $NbCl_4[O\text{-}2,6\text{-}(CH_3)_2C_6H_3](THF)$ (7) with Estimated Standard Deviations in Parentheses[a)]

atom	x	y	z	B_{eq}
Nb	0	0.10268(7)	1/4	3.73
Cl(1)	0.2075(2)	0.0905(1)	0.1179(1)	5.3
O(1)	0	0.2091(4)	1/4	4.2
O(2)	0	-0.0264(4)	1/4	3.7
C(11)	0	0.2907(7)	1/4	3.7
C(12)	0	0.3277(5)	0.3492(7)	4.3
C(13)	0	0.4102(6)	0.3446(8)	5.3
C(14)	0	0.4501(8)	1/4	6.0
C(15)	0	0.2843(5)	0.4519(7)	5.4
C(21)	0	-0.0753(5)	0.3460(7)	6.4
C(22)	0	-0.1555(6)	0.3081(7)	7.4

[a)]Positional parameters are in fraction of cell edges and B_{eq} is the equivalent isotropic temperature factors calculated from the corresponding anisotropic thermal parameters.

Table 3-5. Interatomic Bond Distances (Å) and Bond Angles (°) for Nonhydrogen Atoms in $TiCl_3[O\text{-}2,6\text{-}(CH_3)_2C_6H_3](THF)_2$ (**1**) with Estimated Standard Deviations in Parentheses

Bond distance

Ti	- Cl(1)	2.327(3)		Ti	- Cl(2)	2.330(3)	
Ti	- Cl(3)	2.277(3)		Ti	- O(1)	1.762(5)	
Ti	- O(3)	2.171(6)		Ti	- O(4)	2.168(5)	
O(1)	- C(11)	1.352(8)		O(3)	- C(31)	1.471(13)	
O(3)	- C(34)	1.447(15)		O(4)	- C(41)	1.468(14)	
O(4)	- C(44)	1.468(10)		C(11)	- C(12)	1.399(10)	
C(11)	- C(16)	1.410(10)		C(12)	- C(13)	1.403(12)	
C(12)	- C(17)	1.495(11)		C(13)	- C(14)	1.403(14)	
C(14)	- C(15)	1.359(14)		C(15)	- C(16)	1.408(12)	
C(16)	- C(18)	1.492(12)		C(31)	- C(32)	1.486(17)	
C(32)	- C(33)	1.486(19)		C(33)	- C(34)	1.494(20)	
C(41)	- C(42)	1.462(18)		C(42)	- C(43)	1.521(16)	
C(43)	- C(44)	1.510(13)					

Bond angle

Cl(1)	-Ti	-Cl(2)	166.9(1)	Cl(1)	-Ti	-Cl(3)	92.7(1)
Cl(1)	-Ti	-O(1)	95.9(2)	Cl(1)	-Ti	-O(3)	84.7(2)
Cl(1)	-Ti	-O(4)	85.0(1)	Cl(2)	-Ti	-Cl(3)	95.6(1)
Cl(2)	-Ti	-O(1)	93.1(2)	Cl(2)	-Ti	-O(3)	85.3(2)
Cl(2)	-Ti	-O(4)	85.0(1)	Cl(3)	-Ti	-O(1)	97.4(2)
Cl(3)	-Ti	-O(3)	88.4(2)	Cl(3)	-Ti	-O(4)	169.7(2)
O(1)	-Ti	-O(3)	174.2(2)	O(1)	-Ti	-O(4)	92.8(2)
O(3)	-Ti	-O(4)	81.4(2)	Ti	-O(1)	-C(11)	173.4(5)
Ti	-O(3)	-C(31)	124.5(6)	Ti	-O(3)	-C(34)	126.4(7)
C(31)	-O(3)	-C(34)	108.6(8)	Ti	-O(4)	-C(41)	126.3(6)
Ti	-O(4)	-C(44)	123.8(4)	C(41)	-O(4)	-C(44)	109.8(7)
O(1)	-C(11)	-C(12)	118.2(6)	O(1)	-C(11)	-C(16)	118.7(6)
C(12)	-C(11)	-C(16)	123.1(6)	C(11)	-C(12)	-C(13)	117.8(7)
C(11)	-C(12)	-C(17)	121.5(7)	C(13)	-C(12)	-C(17)	120.7(7)
C(12)	-C(13)	-C(14)	119.9(8)	C(13)	-C(14)	-C(15)	120.9(9)
C(14)	-C(15)	-C(16)	121.9(9)	C(11)	-C(16)	-C(15)	116.4(7)
C(11)	-C(16)	-C(18)	121.8(7)	C(15)	-C(16)	-C(18)	121.8(7)
O(3)	-C(31)	-C(32)	105.4(9)	C(31)	-C(32)	-C(33)	103.1(10)
C(32)	-C(33)	-C(34)	104.1(11)	O(3)	-C(34)	-C(33)	105.3(11)
O(4)	-C(41)	-C(42)	106.9(10)	C(41)	-C(42)	-C(43)	105.5(10)
C(42)	-C(43)	-C(44)	104.2(8)	O(4)	-C(44)	-C(43)	104.5(7)

Table 3-6. Interatomic Bond Distances (Å) and Bond Angles (°) for Nonhydrogen Atoms in $NbCl_4[O\text{-}2,6\text{-}(CH_3)_2C_6H_3](THF)$ (7) with Estimated Standard Deviations in Parentheses

(a) Bond Distances (Å)

Nb	- Cl(1)	2.351(2)		Nb	- O(1)	1.819(8)	
Nb	- O(2)	2.207(7)		O(1)	- C(11)	1.40(1)	
O(2)	- C(21)	1.465(9)		C(11)	- C(12)	1.396(9)	
C(12)	- C(13)	1.41(1)		C(12)	- C(15)	1.49(1)	
C(13)	- C(14)	1.37(1)		C(21)	- C(22)	1.45(1)	
C(22)	- C(22)	1.46(2)					

b) Bond Angles (°)

Cl(1)	-Nb	-Cl(1)^{ii}	89.6(1)		Cl(1)	-Nb	-Cl(1)^{iii}	89.5(1)
Cl(1)	-Nb	-Cl(1)^{iv}	169.8(1)		Cl(1)	-Nb	-O(1)	95.1(1)
Cl(1)	-Nb	-O(2)	84.9(1)		O(1)	-Nb	-O(2)	180.0
Nb	-O(1)	-C(11)$_{ii}$	180.0		Nb	-O(2)	-C(21)	124.8(4)
C(21)	-O(2)	-C(21)^{ii}	110.5(9)		O(1)	-C(11)	-C(12)	117.0(6)
C(12)	-C(11)	-C(12)^{ii}	126(1)		C(11)	-C(12)	-C(13)	114.6(9)
C(11)	-C(12)	-C(15)	123.0(8)		C(13)	-C(12)	-C(15)$_{ii}$	122.3(8)
C(12)	-C(13)	-C(14)	122(1)		C(13)	-C(14)	-C(13)^{ii}	120(1)
O(2)	-C(21)	-C(22)	105.7(8)		C(21)	-C(22)	-C(22)^{ii}	109.1(5)

Code for superscript

i	x,	y,	z
ii	x,	y,	1/2-z
iii	-x,	y,	z
iv	-x,	y,	1/2-z

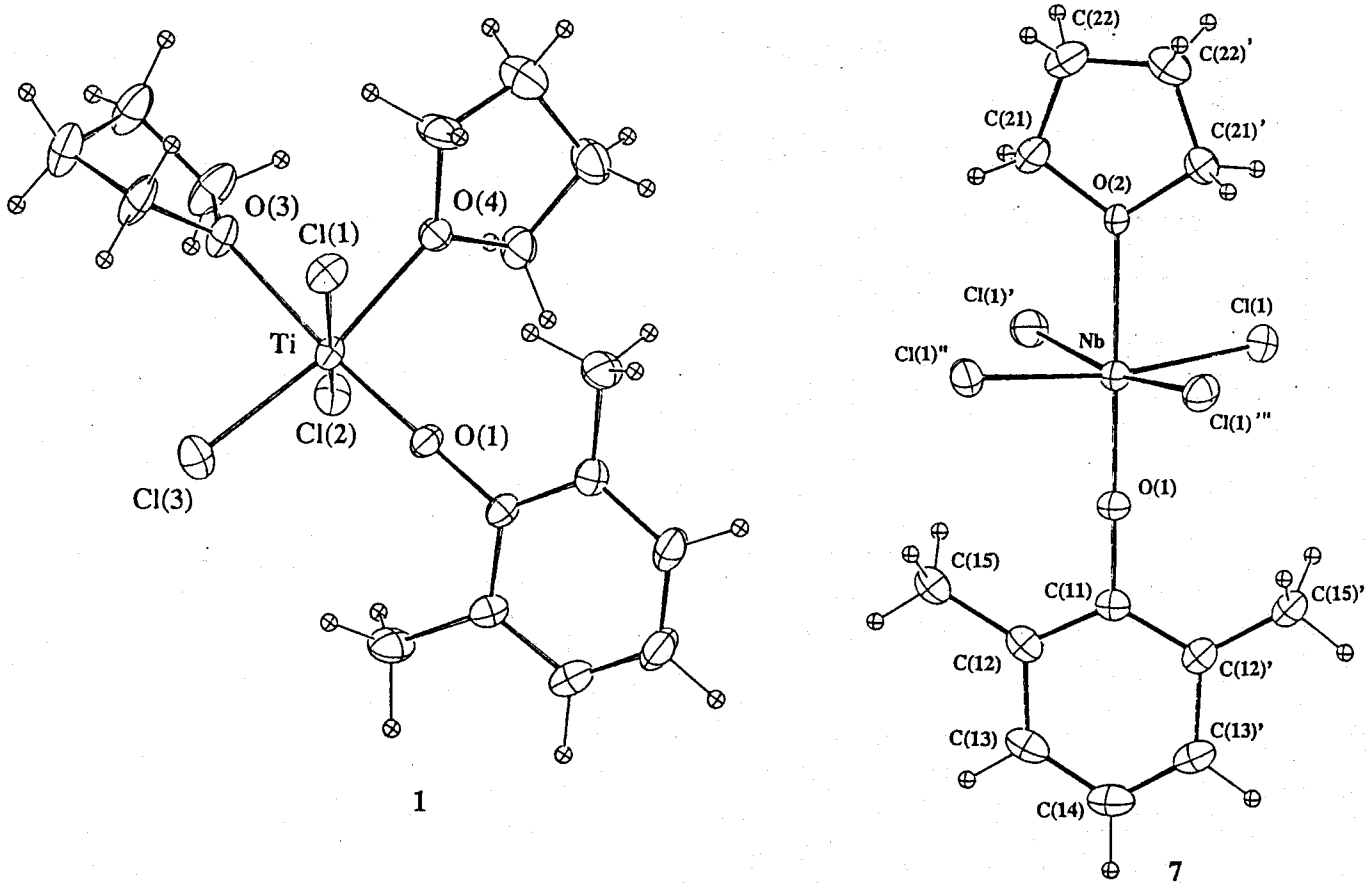

Fig. 3-1. Molecular structures of (a) $TiCl_3[O\text{-}2,6\text{-}(CH_3)_2C_6H_3]$ (**1**), and (b) $NbCl_4[O\text{-}2,6\text{-}(CH_3)_2C_6H_3](THF)$ (**7**).

Cl(1)-Nb-Cl(1) (*trans*) angles is 176.9° and also two chlorine atoms tilt away from the phenoxy ligand. Ti-Cl(3) (*trans* to THF) distance (2.277 Å) is slightly shorter than Ti-Cl(1) or Ti-Cl(2) (*trans* to each other); Ti-Cl(1), 2.327 Å and Ti-Cl(2), 2.330 Å. Nb-Cl(1) distance (2.351 Å) is slightly longer than Ti-Cl distances in complex **1** corresponding to the difference of covalent radii (Nb; 1.34 Å, Ti; 1.32 Å and Cl; 0.99 Å).

Central metal atoms Ti (in **1**), and Nb (in **7**) lie on the basal plane defined by O(1), O(3), O(4), Cl(3) atoms for **1** and by O(1) ,O(2), and two Cl atoms (*trans* to each other) for **7** respectively, and the sum of bond angles around the metal atoms in basal plane are 360.0° in both **1** and **7**. Ti-O(phenoxy) distance (1.762 Å) and Nb-O(phenoxy) distance (1.819 Å) are significant shorter than the sum of the covalent radii. These shortening may attained by the $p\pi$(oxygen)-$d\pi$(metal) contribution for the bond.

3-2. Stereochemistry of Bisphenoxide with Groups 4 and 5 Early Transition Metals

3-2-1. Molecular structures of $TiCl_2[O\text{-}2,6\text{-}(CH_3)_2C_6H_3]_2(THF)_2$ (4) and $ZrCl_2[O\text{-}2,6\text{-}(CH_3)_2C_6H_3]_2(THF)_2$ (5)

Crystal data, data collection, and parameters for structure refinement of **4** and **5** are summarized in Table 3-7. Fractional atomic coordinates and equivalent isotropic temperature factors for nonhydrogen atoms are listed in Tables 3-8 and 3-9. Interatomic bond distances and angles are summarized in Tables 3-10 and 3-11. The ORTEP views together with the partial atomic labellings in Fig. 3-2 show the comparative molecular structure of **4** and **5**. The complex **4** crystallized in the isomorphous lattice of complex **5**, therefore the main structural properties of **4** are similar to those found in **5**. However, the Zr-O(phenoxy) (1.906, 1.922 Å), Zr-O(THF) (2.292, 2.323 Å), Zr-Cl (2.458, 2.476

Table 3-7. Crystal Data and Experimental Parameters for X-Ray Structure Determination of $TiCl_2$(O-2,6-$(CH_3)_2C_6H_3)_2(THF)_2$(**4**) and $ZrCl_2$[O-2,6-$(CH_3)_2C_6H_3]_2(THF)_2$ (**5**).

Complex	**4**	**5**
Formula	$TiCl_2O_4C_{24}H_{34}$	$ZrCl_2O_4C_{24}H34$
Formula weight	505.3	548.7
Crystal system	monoclinic	monoclinic
Space group	*Cc*	*Cc*
Temp., °C	20	20
a,[a] Å	16.794(4)	16.660(9)
b, Å	13.498(2)	13.647(2)
c, Å	11.421(1)	11.589(2)
β, deg	90.72(1)	91.11(2)
V, $Å^3$	2588.8(7)	2634.0(8)
Z	4	4
D_{calcd}, g cm^{-3}	1.296	1.383
F(000), e	1064	1136
μ(MoKα), cm^{-1}	2.9	6.4
Crystal size, mm	0.63x0.38x0.30	0.20x0.25x0.20
2θ range,[b] deg	4<2θ<60	3<2θ<60
Scan width, deg in 2θ	1.0+0.35tanθ	1.103+0.35tanθ
Scan speed,deg min^{-1}	4.0	8.0-16.0
Background count, s	5	50% of peak scan
Reflections measured	3771	3997
Reflections observed[c]	1948	2266
Radiation damage	no	no
No. of variables	415	415
GOF[d]	3.040	4.579
R[e]	0.084	0.060
R_w[f]	0.092	0.086

[a)]Least-squares refinement of the θ values for 25 reflections with 2θ>25°. [b)]Intensity data were collected on a Rigaku four-circle diffractometer using graphite-monochromatized MoKα radiation by the θ-2θ scan method. [c)]non-zero reflections. [d)]$[\Sigma w(|F_o|-|F_c|)^2/(n-m)]^{1/2}$, where *n* and *m* are the No. of reflections used and variables refined, respectively. [e)]$R=\Sigma(|F_o|-|F_c|)/\Sigma|F_o|$. [f)]$R_w=[\Sigma w(|F_o|-|F_c|)^2/\Sigma w|F_o|^2]^{1/2}$, $w=[\sigma^2(F_o)+g(F_o)^2]^{-1}$, and g=0.003 for **4** and 0.004 for **5** respectively.

Table 3-8. Final Atomic Coordinates and Equivalent Isotropic Temerature Factors for Nonhydrogen Atoms in $TiCl_2[O\text{-}2,6\text{-}(CH_3)_2C_6H_3]_2(THF)_2$ (4) with Estimated Standard Deviations in Parentheses[a)]

Atom	x	y	z	B_{eq}
Ti	0.25	0.28505(15)	0.25	3.70
Cl(1)	0.2163(3)	0.2787(3)	0.4511(3)	5.48
Cl(2)	0.2493(3)	0.3073(3)	0.0462(4)	5.51
O(1)	0.2806(5)	0.1582(7)	0.2468(8)	4.8
O(2)	0.3451(5)	0.3423(7)	0.2717(8)	4.7
O(3)	0.1948(5)	0.4329(6)	0.2570(8)	4.8
O(4)	0.1247(5)	0.2431(7)	0.2233(8)	4.8
C(11)	0.2997(8)	0.0606(11)	0.2643(11)	4.3
C(12)	0.2662(8)	-0.0087(10)	0.1927(13)	4.8
C(13)	0.2837(10)	-0.1093(11)	0.2147(15)	6.5
C(14)	0.3336(10)	-0.1364(13)	0.3054(17)	7.0
C(15)	0.3682(10)	-0.0629(14)	0.3736(15)	6.8
C(16)	0.3552(8)	0.0389(10)	0.3554(12)	5.0
C(17)	0.2103(9)	0.0181(11)	0.0951(14)	5.8
C(18)	0.3940(9)	0.1171(12)	0.4284(13)	6.1
C(21)	0.4233(7)	0.3622(9)	0.2931(10)	4.0
C(22)	0.4808(9)	0.3189(10)	0.2196(13)	5.5
C(23)	0.5602(9)	0.3411(11)	0.2421(16)	6.4
C(24)	0.5815(9)	0.4027(13)	0.3377(16)	6.5
C(25)	0.5245(9)	0.4418(10)	0.4085(12)	5.8
C(26)	0.4427(8)	0.4245(11)	0.3852(12)	5.2
C(27)	0.4571(10)	0.2557(12)	0.1162(13)	6.7
C(28)	0.3806(9)	0.4674(12)	0.4648(12)	5.9
C(31)	0.2300(11)	0.5177(11)	0.1973(14)	7.0
C(32)	0.1858(16)	0.6056(13)	0.2382(16)	9.7
C(33)	0.1112(14)	0.5658(16)	0.292(2)	9.8
C(34)	0.1298(10)	0.4661(14)	0.3301(15)	7.8
C(41)	0.0727(10)	0.2731(14)	0.1225(14)	7.5
C(42)	-0.0107(10)	0.2397(14)	0.1551(19)	8.0
C(43)	0.0053(10)	0.1511(14)	0.2339(16)	8.0
C(44)	0.0819(9)	0.1742(12)	0.2946(15)	6.8

[a)]Positional parameters are in fraction of cell edges and B_{eq} is the equivalent isotropic temperature factors calculated from the corresponding anisotropic thermal parameters.

Table 3-9. Final Atomic Coordinates and Equivalent Isotropic Temerature Factors for Nonhydrogen Atoms in $ZrCl_2[O\text{-}2,6\text{-}(CH_3)_2C_6H_3]_2(THF)_2$ (**5**) with Estimated Standard Deviations in Parentheses[a)]

Atom	x	y	z	B_{eq}
Zr	0.25	0.28577(7)	0.25	4.25
Cl(1)	0.2107(3)	0.2825(3)	0.4549(3)	5.39
Cl(2)	0.2493(3)	0.3084(4)	0.0397(4)	5.47
O(1)	0.2819(5)	0.1518(6)	0.2506(8)	4.2
O(2)	0.3513(5)	0.3476(7)	0.2763(8)	4.2
O(3)	0.1908(6)	0.4359(7)	0.2536(8)	4.5
O(4)	0.1189(6)	0.2424(8)	0.2168(8)	4.5
C(11)	0.3025(7)	0.0552(9)	0.2698(10)	3.7
C(12)	0.2725(8)	-0.0153(10)	0.1990(12)	4.5
C(13)	0.2915(9)	-0.1128(10)	0.2226(15)	5.8
C(14)	0.3406(11)	-0.1352(12)	0.3133(17)	6.6
C(15)	0.3738(10)	-0.0648(13)	0.3801(15)	6.1
C(16)	0.3568(10)	0.0343(11)	0.3593(12)	5.2
C(17)	0.2170(9)	0.0104(12)	0.0972(15)	5.4
C(18)	0.3941(10)	0.1171(13)	0.4329(13)	6.2
C(21)	0.4302(7)	0.3702(9)	0.2991(11)	4.1
C(22)	0.4892(8)	0.3285(10)	0.2293(13)	4.9
C(23)	0.5679(9)	0.3515(13)	0.2540(16)	6.0
C(24)	0.5887(9)	0.4115(13)	0.3482(16)	6.3
C(25)	0.5286(9)	0.4511(11)	0.4150(14)	5.4
C(26)	0.4491(8)	0.4313(10)	0.3912(11)	4.5
C(27)	0.4677(10)	0.2667(12)	0.1272(15)	6.1
C(28)	0.3827(10)	0.4737(13)	0.4650(14)	6.1
C(31)	0.2270(11)	0.5210(11)	0.1948(14)	6.2
C(32)	0.1830(19)	0.6051(13)	0.2384(18)	9.5
C(33)	0.1119(18)	0.5744(16)	0.293(3)	10.0
C(34)	0.1226(13)	0.4678(15)	0.323(2)	8.6
C(41)	0.0688(11)	0.2665(14)	0.1157(18)	6.7
C(42)	-0.0129(11)	0.2322(16)	0.1435(19)	7.2
C(43)	-0.0013(10)	0.1483(16)	0.2256(18)	7.3
C(44)	0.0747(10)	0.1746(13)	0.2924(17)	6.3

[a)]Positional parameters are in fraction of cell edges and B_{eq} is the equivalent isotropic temperature factors calculated from the corresponding anisotropic thermal parameters.

Table 3-10. Interatomic Bond Distances (Å) and Bond Angles (°) for Nonhydrogen Atoms in $TiCl_2[O\text{-}2,6\text{-}(CH_3)_2C_6H_3]_2(THF)_2$ (4) with Estimated Standard Deviations in Parentheses

Bond distance

Ti	- Cl(1)	2.374(4)	Ti	- Cl(2)	2.347(4)
Ti	- O(1)	1.788(9)	Ti	- O(2)	1.788(9)
Ti	- O(3)	2.202(9)	Ti	- O(4)	2.197(9)
O(1)	- C(11)	1.369(16)	O(2)	- C(21)	1.360(14)
O(3)	- C(31)	1.461(19)	O(3)	- C(34)	1.455(20)
O(4)	- C(41)	1.492(20)	O(4)	- C(44)	1.434(19)
C(11)	- C(12)	1.360(19)	C(11)	- C(16)	1.418(19)
C(12)	- C(13)	1.411(22)	C(12)	- C(17)	1.493(21)
C(13)	- C(14)	1.374(25)	C(14)	- C(15)	1.384(26)
C(15)	- C(16)	1.405(23)	C(16)	- C(18)	1.490(20)
C(21)	- C(22)	1.413(18)	C(21)	- C(26)	1.382(18)
C(22)	- C(23)	1.388(22)	C(22)	- C(27)	1.506(22)
C(23)	- C(24)	1.415(24)	C(24)	- C(25)	1.367(22)
C(25)	- C(26)	1.416(20)	C(26)	- C(28)	1.508(20)
C(31)	- C(32)	1.478(31)	C(32)	- C(33)	1.503(34)
C(33)	- C(34)	1.446(29)	C(41)	- C(42)	1.523(28)
C(42)	- C(43)	1.520(28)	C(43)	- C(44)	1.487(25)

Bond angle

Cl(1)	-Ti	-Cl(2)	165.0(2)	Cl(1)	-Ti	-O(1)	93.3(3)
Cl(1)	-Ti	-O(2)	96.0(3)	Cl(1)	-Ti	-O(3)	83.8(3)
Cl(1)	-Ti	-O(4)	83.4(2)	Cl(2)	-Ti	-O(1)	95.8(3)
Cl(2)	-Ti	-O(2)	94.3(3)	Cl(2)	-Ti	-O(3)	85.6(3)
Cl(2)	-Ti	-O(4)	84.4(2)	O(1)	-Ti	-O(2)	99.2(4)
O(1)	-Ti	-O(3)	171.7(4)	O(1)	-Ti	-O(4)	91.4(4)
O(2)	-Ti	-O(3)	88.8(4)	O(2)	-Ti	-O(4)	169.3(4)
O(3)	-Ti	-O(4)	80.6(3)	Ti	-O(1)	-C(11)	170.0(9)
Ti	-O(2)	-C(21)	165.7(8)	Ti	-O(3)	-C(31)	121.4(8)
Ti	-O(3)	-C(34)	128.3(9)	C(31)	-O(3)	-C(34)	109.7(11)
Ti	-O(4)	-C(41)	125.9(9)	Ti	-O(4)	-C(44)	125.0(8)
C(41)	-O(4)	-C(44)	108.8(11)	O(1)	-C(11)	-C(12)	118.6(12)
O(1)	-C(11)	-C(16)	117.2(12)	C(12)	-C(11)	-C(16)	124.1(13)
C(11)	-C(12)	-C(13)	118.1(13)	C(11)	-C(12)	-C(17)	122.2(13)
C(13)	-C(12)	-C(17)	119.6(13)	C(12)	-C(13)	-C(14)	120.9(15)
C(13)	-C(14)	-C(15)	118.7(17)	C(14)	-C(15)	-C(16)	123.7(16)
C(11)	-C(16)	-C(15)	114.2(13)	C(11)	-C(16)	-C(18)	122.8(12)
C(15)	-C(16)	-C(18)	122.9(13)	O(2)	-C(21)	-C(22)	118.5(10)
O(2)	-C(21)	-C(26)	118.3(11)	C(22)	-C(21)	-C(26)	123.2(11)
C(21)	-C(22)	-C(23)	117.6(13)	C(21)	-C(22)	-C(27)	121.6(12)
C(23)	-C(22)	-C(27)	120.7(13)	C(22)	-C(23)	-C(24)	120.2(15)
C(23)	-C(24)	-C(25)	120.8(15)	C(24)	-C(25)	-C(26)	120.6(14)
C(21)	-C(26)	-C(25)	117.5(12)	C(21)	-C(26)	-C(28)	122.4(12)
C(25)	-C(26)	-C(28)	119.9(12)	O(3)	-C(31)	-C(32)	105.9(15)
C(31)	-C(32)	-C(33)	105.5(19)	C(32)	-C(33)	-C(34)	106.1(18)
O(3)	-C(34)	-C(33)	106.0(15)	O(4)	-C(41)	-C(42)	105.2(14)
C(41)	-C(42)	-C(43)	102.8(16)	C(42)	-C(43)	-C(44)	104.8(15)
O(4)	-C(44)	-C(43)	108.0(13)				

Table 3-11. Interatomic Bond Distances (Å) and Bond Angles (°) for Nonhydrogen Atoms in $ZrCl_2[O\text{-}2,6\text{-}(CH_3)_2C_6H_3]_2(THF)_2$ (**5**) with Estimated Standard Deviations in Parentheses

Bond distance

Zr	-	Cl(1)	2.476(5)	Zr	-	Cl(2)	2.456(5)
Zr	-	O(1)	1.904(8)	Zr	-	O(2)	1.906(9)
Zr	-	O(3)	2.275(9)	Zr	-	O(4)	2.288(10)
O(1)	-	C(11)	1.379(14)	O(2)	-	C(21)	1.372(15)
O(3)	-	C(31)	1.481(20)	O(3)	-	C(34)	1.467(24)
O(4)	-	C(41)	1.463(22)	O(4)	-	C(44)	1.480(21)
C(11)	-	C(12)	1.354(18)	C(11)	-	C(16)	1.393(20)
C(12)	-	C(13)	1.393(22)	C(12)	-	C(17)	1.525(22)
C(13)	-	C(14)	1.355(26)	C(14)	-	C(15)	1.346(26)
C(15)	-	C(16)	1.402(24)	C(16)	-	C(18)	1.539(23)
C(21)	-	C(22)	1.406(19)	C(21)	-	C(26)	1.386(18)
C(22)	-	C(23)	1.372(23)	C(22)	-	C(27)	1.490(22)
C(23)	-	C(24)	1.403(25)	C(24)	-	C(25)	1.387(24)
C(25)	-	C(26)	1.374(20)	C(26)	-	C(28)	1.526(21)
C(31)	-	C(32)	1.458(36)	C(32)	-	C(33)	1.419(42)
C(33)	-	C(34)	1.504(36)	C(41)	-	C(42)	1.481(29)
C(42)	-	C(43)	1.499(30)	C(43)	-	C(44)	1.514(28)

Bond angle

Cl(1)	-Zr	-Cl(2)	163.3(2)	Cl(1)	-Zr	-O(1)	93.3(3)
Cl(1)	-Zr	-O(2)	96.0(3)	Cl(1)	-Zr	-O(3)	82.9(3)
Cl(1)	-Zr	-O(4)	83.5(3)	Cl(2)	-Zr	-O(1)	96.9(3)
Cl(2)	-Zr	-O(2)	95.2(3)	Cl(2)	-Zr	-O(3)	84.9(3)
Cl(2)	-Zr	-O(4)	83.1(3)	O(1)	-Zr	-O(2)	100.3(4)
O(1)	-Zr	-O(3)	170.4(3)	O(1)	-Zr	-O(4)	91.0(3)
O(2)	-Zr	-O(3)	88.9(3)	O(2)	-Zr	-O(4)	168.7(4)
O(3)	-Zr	-O(4)	79.9(3)	Zr	-O(1)	-C(11)	170.8(8)
Zr	-O(2)	-C(21)	166.6(8)	Zr	-O(3)	-C(31)	121.1(9)
Zr	-O(3)	-C(34)	128.1(10)	C(31)	-O(3)	-C(34)	110.2(13)
Zr	-O(4)	-C(41)	127.2(10)	Zr	-O(4)	-C(44)	123.1(9)
C(41)	-O(4)	-C(44)	109.3(12)	O(1)	-C(11)	-C(12)	119.6(11)
O(1)	-C(11)	-C(16)	118.1(11)	C(12)	-C(11)	-C(16)	122.2(12)
C(11)	-C(12)	-C(13)	118.6(13)	C(11)	-C(12)	-C(17)	121.1(12)
C(13)	-C(12)	-C(17)	120.3(13)	C(12)	-C(13)	-C(14)	120.0(16)
C(13)	-C(14)	-C(15)	121.3(18)	C(14)	-C(15)	-C(16)	120.7(17)
C(11)	-C(16)	-C(15)	116.8(14)	C(11)	-C(16)	-C(18)	120.8(13)
C(15)	-C(16)	-C(18)	122.3(14)	O(2)	-C(21)	-C(22)	118.4(11)
O(2)	-C(21)	-C(26)	119.1(11)	C(22)	-C(21)	-C(26)	122.5(12)
C(21)	-C(22)	-C(23)	117.5(13)	C(21)	-C(22)	-C(27)	121.7(13)
C(23)	-C(22)	-C(27)	120.6(14)	C(22)	-C(23)	-C(24)	121.1(16)
C(23)	-C(24)	-C(25)	119.5(16)	C(24)	-C(25)	-C(26)	121.0(15)
C(21)	-C(26)	-C(25)	118.4(13)	C(21)	-C(26)	-C(28)	120.3(12)
C(25)	-C(26)	-C(28)	121.3(13)	O(3)	-C(31)	-C(32)	104.2(17)
C(31)	-C(32)	-C(33)	110.7(24)	C(32)	-C(33)	-C(34)	106.8(23)
O(3)	-C(34)	-C(33)	104.7(18)	O(4)	-C(41)	-C(42)	105.6(15)
C(41)	-C(42)	-C(43)	105.7(17)	C(42)	-C(43)	-C(44)	103.9(17)
O(4)	-C(44)	-C(43)	105.5(14)				

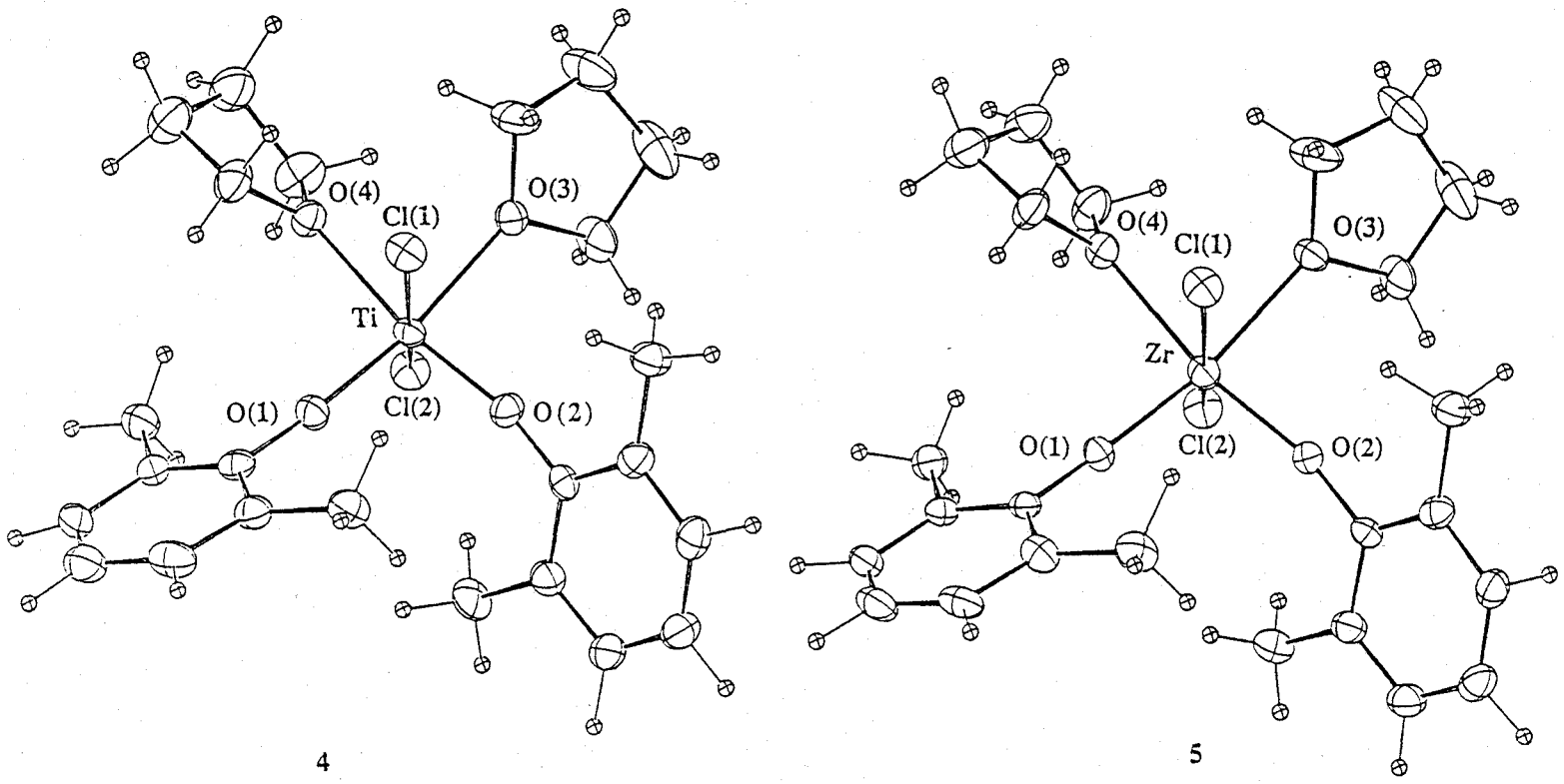

Fig. 3-2. Molecular structures of (a) $TiCl_2[O\text{-}2,6\text{-}(CH_3)_2C_6H_3]_2(THF)_2$ (**4**), and (b) $ZrCl_2[O\text{-}2,6\text{-}(CH_3)_2C_6H_3](THF)_2$ (**5**).

Å) in **5** are longer than those in **4** reflecting the larger covalent radius of Zr (1.45 Å) than Ti (1.32 Å). In Both complexes the central metal atoms have six-coordinated geometries with two phenoxy ligands in *cis*, THF ligands also in *cis*, and Cl atoms in *trans* position. Two Cl-M-Cl (M=Ti, Zr) angles (165.0° for **4**, 163.3° for **5**) show the deformation of two chloride ligands from the exact *trans* position, and also two chlorine atoms tilt away form phenoxy ligands. Central metal atoms lie on the basal plane defined by O(1), O(2), O(3) and O(4) atoms for **4** and **5**, and the sum of the bond angle around the metal atoms in basal plane are 360.0° for **4** and 360.1° for **5**, respectively. O(THF)-M-O(THF) angles (80.6° for **4** and 79.9° for **5**) are much smaller than 90°in both complexes, while the O(phenoxy)-M-O(phenoxy) angles (99.2° for 4 and 100.3° for **5**) are much larger than 90°. Zr-Cl distances (2.476 and 2.456 Å) are slightly longer than Ti-Cl distances (2.374 Å and 2.347 Å) and Zr-O(phenoxy) distances (1.904 Å and 1.906 Å) are slightly longer than Ti-O(phenoxy) distances (1.788 and 1.788 Å) and also Zr-O(THF) distances (2.275 and 2.288 Å) are slightly longer than Ti-O(THF) distances (2.202 and 2.197 Å). These aspects correspond to the metal covalent radii (Zr;1.45, Ti;1.32 Å).

3-2-2. Molecular Structures of $NbCl_3[O\text{-}2,6\text{-}(CH_3)_2C_6H_3]_2(THF)$ (8) and $NbCl_3[O\text{-}2,6\text{-}(C_6H_5)_2C_6H_3]_2(THF)$ (8b)

Crystal data, data collection, and parameters for structure refinement of **8** and **8b** are summarized in Table 3-12. Fractional atomic coordinates and equivalent isotropic temperature factors for nonhydrogen atoms in **8** and **8b** are listed in Tables 3-13 and 3-14. Interatomic bond distances and angles in **8** and **8b** are summarized in Tables 3-15 and 3-16. ORTEP views in Fig. 3-3 show the comparative molecular structures of **8** and **8b** together with the partial atomic labellings. In both complexes, the central metal atoms have six-coordinated geometries with two phenoxy groups in *cis* and chlorine atoms occupy *meridian*

Table 3-12. Crystal Data and Experimental Parameters for X-Ray Structure Determination of $NbCl_3$(O-2,6-$(CH_3)_2C_6H_3)_2$(THF)(**8**) and $NbCl_3$[O-2,6-$(C_6H_5)_2C_6H_3]_2$(THF)(**8b**)

Complex	**8**	**8b**
Formula	$NbCl_3O_3C_{20}H_{26}$	$NbCl_3O_3C_{40}H_{34}$ + 1/2(hexane)
Formula weight	513.7	762.0(805.1)
Crystal system	triclinic	triclinic
Space group	$P\bar{1}$	$P\bar{1}$
Temp., °C	20	20
a,[a] Å	9.639(9)	10.996(5)
b, Å	15.396(6)	18.009(4)
c, Å	8.763(4)	10.643(3)
α, deg	98.68(4)	90.30(2)
β, deg	98.61(9)	102.36(3)
γ, deg	75.45(6)	102.63(2)
V, Å^3	1235.8(15)	2006.0(12)
Z	2	2
D_{calcd}, g cm^{-3}	1.379	1.261(1.332)
F(000), e	524	780
μ(MoKα), cm^{-1}	8.1	5.3
2θ range,[b] deg	3<2θ<60	3<2θ<60
Scan width, deg in 2θ	0.84+0.35tanθ	1.732+0.35tanθ
Scan speed,deg min^{-1}	8.0-16.0	8-16.0
Background count, s	50% of peak scan	50% of peak scan
Reflections measured	7218	12196
Reflections observed[c]	4483	8023
Radiation damage	no	no
No. of variables	349	616
GOF[d]	4.937	6.781
R[e]	0.080	0.091
R_w[f]	0.130	0.143

[a)]Least-squares refinement of the θ values for 25 reflections with 2θ>25°. [b)]Intensity data were collected on a Rigaku four-circle diffractometer using graphite-monochromatized MoKα radiation by the θ-2θ scan method. [c)]non-zero reflections. [d)]$[\Sigma w(|F_o|-|F_c|)^2/(n-m)]^{1/2}$, where n and m are the No. of reflections used and variables refined, respectively. [e)]$R=\Sigma(|F_o|-|F_c|)/\Sigma|F_o|$. [f)]$R_w=[\Sigma w(|F_o|-|F_c|)^2/\Sigma w|F_o|^2]^{1/2}$, $w=[\sigma^2(F_o)+g(F_o)^2]^{-1}$, and g=0.003.

Table 3-13. Final Atomic Coordinates and Equivalent Isotropic Temperature Factors for Nonhydrogen Atoms in $NbCl_3[O\text{-}2,6\text{-}(CH_3)_2C_6H_3]_2(THF)$ (8) with Estimated Standard Deviations in Parentheses[a)]

Atom	x	y	z	B_{eq}
Nb	0.72962(8)	0.31630(5)	0.14411(9)	3.31
Cl(1)	0.7812(4)	0.44889(17)	0.0846(3)	4.42
Cl(2)	0.6400(3)	0.18751(17)	0.1640(4)	4.40
Cl(3)	0.5030(3)	0.4054(2)	0.2165(4)	4.90
O(1)	0.8168(7)	0.3248(4)	0.3443(7)	3.3
O(2)	0.8891(6)	0.2426(4)	0.0575(7)	3.0
O(3)	0.6164(6)	0.3107(5)	-0.0925(7)	3.3
C(11)	0.8966(9)	0.3294(7)	0.4858(9)	3.3
C(12)	0.8839(10)	0.4145(7)	0.5707(11)	3.6
C(13)	0.9699(13)	0.4202(9)	0.7126(12)	4.7
C(14)	1.0637(13)	0.3414(10)	0.7673(12)	5.2
C(15)	1.0707(11)	0.2586(9)	0.6789(13)	4.7
C(16)	0.9855(10)	0.2509(7)	0.5360(11)	3.7
C(17)	0.7807(13)	0.4979(8)	0.5153(13)	4.9
C(18)	0.9886(13)	0.1607(8)	0.4426(14)	5.2
C(21)	1.0127(8)	0.1835(6)	0.0183(10)	2.9
C(22)	1.1447(10)	0.2034(7)	0.0849(11)	3.3
C(23)	1.2727(11)	0.1419(9)	0.0438(14)	4.9
C(24)	1.2673(14)	0.0660(9)	-0.0572(16)	5.8
C(25)	1.1321(13)	0.0486(8)	-0.1243(15)	5.1
C(26)	1.0063(10)	0.1087(6)	-0.0889(11)	3.6
C(27)	1.1536(12)	0.2869(8)	0.1969(13)	5.0
C(28)	0.8612(12)	0.0915(7)	-0.1670(12)	4.5
C(31)	0.6733(11)	0.3338(8)	-0.2255(11)	4.2
C(32)	0.5766(13)	0.3022(10)	-0.3688(13)	5.7
C(33)	0.4419(13)	0.3069(12)	-0.3116(14)	6.7
C(34)	0.4732(12)	0.2938(12)	-0.1402(14)	5.7

[a)]Positional parameters are in fraction of cell edges and B_{eq} is the equivalent isotropic temperature factors calculated from the corresponding anisotropic thermal parameters.

Table 3-14. Final Atomic Coordinates and Equivalent Isotropic Temperature Factors for Nonhydrogen Atoms in $NbCl_3[O\text{-}2,6\text{-}(C_6H_5)_2C_6H_3]_2(THF)$ (**8b**) with Estimated Standard Deviations in Parentheses[a)]

Atom	x	y	z	B_{eq}
Nb	0.40489(7)	0.19644(4)	0.48516(6)	2.79
Cl(1)	0.2182(2)	0.20413(13)	0.55533(18)	3.48
Cl(2)	0.5788(3)	0.16310(13)	0.4191(2)	3.63
Cl(3)	0.4726(3)	0.13843(15)	0.68088(19)	4.44
O(1)	0.4884(5)	0.2923(3)	0.5603(5)	2.4
O(2)	0.3465(5)	0.2228(3)	0.3154(4)	2.4
O(3)	0.2959(6)	0.0789(4)	0.4207(6)	3.7
C(11)	0.5191(7)	0.3398(4)	0.6697(6)	2.3
C(12)	0.6267(8)	0.3386(4)	0.7641(6)	2.6
C(13)	0.6448(8)	0.3801(5)	0.8819(7)	3.0
C(14)	0.5580(9)	0.4196(5)	0.9033(7)	3.6
C(15)	0.4549(9)	0.4227(5)	0.8046(8)	3.6
C(16)	0.4334(7)	0.3849(4)	0.6866(7)	2.5
C(21)	0.3232(8)	0.2132(5)	0.1842(6)	2.7
C(22)	0.4222(8)	0.2414(5)	0.1218(7)	3.2
C(23)	0.3984(9)	0.2229(6)	-0.0104(7)	4.0
C(24)	0.2873(10)	0.1811(7)	-0.0767(7)	4.5
C(25)	0.1856(9)	0.1559(6)	-0.0146(7)	3.9
C(26)	0.2008(8)	0.1723(5)	0.1179(6)	3.0
C(31)	0.1990(17)	0.0273(8)	0.4819(15)	8.6
C(32)	0.1685(17)	-0.0447(8)	0.4233(17)	8.5
C(33)	0.2260(14)	-0.0409(7)	0.3087(16)	7.3
C(34)	0.3334(12)	0.0325(7)	0.3271(12)	5.9
C(51)	0.7298(7)	0.3004(5)	0.7461(7)	2.8
C(52)	0.7888(9)	0.2609(6)	0.8483(9)	4.0
C(53)	0.8908(9)	0.2301(6)	0.8368(11)	4.6
C(54)	0.9369(10)	0.2367(7)	0.7316(11)	4.8
C(55)	0.8807(9)	0.2751(6)	0.6273(10)	4.5
C(56)	0.7778(9)	0.3055(6)	0.6358(8)	3.7
C(61)	0.3306(7)	0.3982(4)	0.5810(7)	2.6
C(62)	0.3575(8)	0.4233(5)	0.4651(8)	3.5
C(63)	0.2629(12)	0.4452(7)	0.3728(9)	5.1
C(64)	0.1428(9)	0.4438(7)	0.3939(10)	4.8
C(65)	0.1147(9)	0.4183(6)	0.5070(10)	4.6
C(66)	0.2074(8)	0.3945(5)	0.6012(8)	3.1
C(71)	0.5451(8)	0.2912(5)	0.1897(7)	2.9
C(72)	0.6619(9)	0.2804(6)	0.1708(8)	3.8
C(73)	0.7737(10)	0.3316(7)	0.2274(12)	5.1
C(74)	0.7719(10)	0.3946(6)	0.3001(9)	4.6
C(75)	0.6580(9)	0.4059(5)	0.3204(9)	3.9
C(76)	0.5452(9)	0.3547(5)	0.2645(8)	3.5
C(81)	0.0911(8)	0.1506(6)	0.1753(7)	3.4
C(82)	0.0577(9)	0.2022(7)	0.2538(8)	4.1
C(83)	-0.0507(11)	0.1815(9)	0.2990(11)	6.1
C(84)	-0.1319(11)	0.1127(10)	0.2662(13)	6.6
C(85)	-0.1018(11)	0.0578(9)	0.1877(14)	7.1
C(86)	0.0111(10)	0.0790(7)	0.1462(11)	5.1
C(91)	0.1775(17)	0.3815(11)	-0.0001(14)	8.3
C(92)	0.1013(13)	0.4366(8)	-0.0643(11)	6.2
C(93)	0.0368(12)	0.4727(7)	0.0304(10)	5.6

[a)]Positional parameters are in fraction of cell edges and B_{eq} is the equivalent isotropic temperature factors calculated from the corresponding anisotropic thermal parameters.

Table 3-15. Selected Bond Distances (Å) and Angles (°) for Nonhydrogen Atoms in $NbCl_3[O\text{-}2,6\text{-}(CH_3)_2C_6H_3]_2(THF)$ (**8**) with Estimated Standard Deviations in Parentheses

Bond distance

Nb	- Cl(1)	2.366(3)	Nb	- Cl(2)	2.391(3)
Nb	- Cl(3)	2.388(3)	Nb	- O(1)	1.829(6)
Nb	- O(2)	1.854(6)	Nb	- O(3)	2.194(6)
O(1)	- C(11)	1.360(11)	O(2)	- C(21)	1.360(10)
O(3)	- C(31)	1.483(13)	O(3)	- C(34)	1.458(19)
C(11)	- C(12)	1.392(14)	C(11)	- C(16)	1.383(14)
C(12)	- C(13)	1.392(16)	C(12)	- C(17)	1.509(16)
C(13)	- C(14)	1.418(19)	C(14)	- C(15)	1.380(19)
C(15)	- C(16)	1.397(16)	C(16)	- C(18)	1.498(16)
C(21)	- C(22)	1.404(13)	C(21)	- C(26)	1.380(13)
C(22)	- C(23)	1.412(16)	C(22)	- C(27)	1.507(16)
C(23)	- C(24)	1.361(18)	C(24)	- C(25)	1.420(18)
C(25)	- C(26)	1.373(15)	C(26)	- C(28)	1.530(14)
C(31)	- C(32)	1.542(19)	C(32)	- C(33)	1.442(23)
C(33)	- C(34)	1.521(25)			

Bond angle

Cl(1)	-Nb	-Cl(2)	168.8(1)	Cl(1)	-Nb	-Cl(3)	88.7(1)
Cl(1)	-Nb	-O(1)	95.0(2)	Cl(1)	-Nb	-O(2)	92.5(2)
Cl(1)	-Nb	-O(3)	84.5(2)	Cl(2)	-Nb	-Cl(3)	86.4(1)
Cl(2)	-Nb	-O(1)	95.2(2)	Cl(2)	-Nb	-O(2)	90.8(2)
Cl(2)	-Nb	-O(3)	85.0(2)	Cl(3)	-Nb	-O(1)	92.7(2)
Cl(3)	-Nb	-O(2)	170.8(2)	Cl(3)	-Nb	-O(3)	84.7(2)
O(1)	-Nb	-O(2)	96.3(3)	O(1)	-Nb	-O(3)	177.4(3)
O(2)	-Nb	-O(3)	86.3(2)	Nb	-O(1)	-C(11)	173.2(6)
Nb	-O(2)	-C(21)	170.2(5)	Nb	-O(3)	-C(31)	122.6(6)
Nb	-O(3)	-C(34)	126.7(8)	C(31)	-O(3)	-C(34)	110.3(9)
O(1)	-C(11)	-C(12)	116.9(8)	O(1)	-C(11)	-C(16)	119.0(8)
C(12)	-C(11)	-C(16)	124.1(9)	C(11)	-C(12)	-C(13)	117.1(9)
C(11)	-C(12)	-C(17)	122.6(9)	C(13)	-C(12)	-C(17)	120.3(10)
C(12)	-C(13)	-C(14)	120.4(11)	C(13)	-C(14)	-C(15)	119.9(12)
C(14)	-C(15)	-C(16)	120.8(11)	C(11)	-C(16)	-C(15)	117.6(10)
C(11)	-C(16)	-C(18)	121.5(9)	C(15)	-C(16)	-C(18)	121.0(10)
O(2)	-C(21)	-C(22)	118.0(8)	O(2)	-C(21)	-C(26)	120.1(8)
C(22)	-C(21)	-C(26)	121.9(8)	C(21)	-C(22)	-C(23)	117.7(9)
C(21)	-C(22)	-C(27)	122.6(9)	C(23)	-C(22)	-C(27)	119.7(10)
C(22)	-C(23)	-C(24)	120.8(11)	C(23)	-C(24)	-C(25)	120.1(12)
C(24)	-C(25)	-C(26)	120.1(11)	C(21)	-C(26)	-C(25)	119.3(9)
C(21)	-C(26)	-C(28)	120.9(8)	C(25)	-C(26)	-C(28)	119.7(9)
O(3)	-C(31)	-C(32)	104.0(9)	C(31)	-C(32)	-C(33)	104.7(12)
C(32)	-C(33)	-C(34)	108.2(14)	O(3)	-C(34)	-C(33)	104.8(13)

Table 3-16. Selected Bond Distances (Å) and Angles (°) for Nonhydrogen Atoms in $NbCl_3[O\text{-}2,6\text{-}(C_6H_5)_2C_6H_3]_2(THF)$ (**8b**) with Estimated Standard Deviations in Parentheses

Bond distance

Nb	- Cl(1)	2.360(2)	Nb	- Cl(2)	2.363(2)
Nb	- Cl(3)	2.384(3)	Nb	- O(1)	1.855(5)
Nb	- O(2)	1.883(5)	Nb	- O(3)	2.217(7)
O(1)	- C(11)	1.377(9)	O(2)	- C(21)	1.368(9)
O(3)	- C(31)	1.513(20)	O(3)	- C(34)	1.475(15)
C(11)	- C(12)	1.383(11)	C(11)	- C(16)	1.409(10)
C(12)	- C(13)	1.411(11)	C(12)	- C(51)	1.492(11)
C(13)	- C(14)	1.363(13)	C(14)	- C(15)	1.383(13)
C(15)	- C(16)	1.375(12)	C(16)	- C(61)	1.475(11)
C(21)	- C(22)	1.398(12)	C(21)	- C(26)	1.417(12)
C(22)	- C(23)	1.399(13)	C(22)	- C(71)	1.483(12)
C(23)	- C(24)	1.334(15)	C(24)	- C(25)	1.410(15)
C(25)	- C(26)	1.406(13)	C(26)	- C(81)	1.446(12)
C(31)	- C(32)	1.377(26)	C(32)	- C(33)	1.485(25)
C(33)	- C(34)	1.548(21)			

Bond angle

Cl(1)	-Nb	-Cl(2)	168.9(1)	Cl(1)	-Nb	-Cl(3)	88.1(1)
Cl(1)	-Nb	-O(1)	91.3(2)	Cl(1)	-Nb	-O(2)	95.5(2)
Cl(1)	-Nb	-O(3)	83.0(2)	Cl(2)	-Nb	-Cl(3)	86.1(1)
Cl(2)	-Nb	-O(1)	98.2(2)	Cl(2)	-Nb	-O(2)	88.6(2)
Cl(2)	-Nb	-O(3)	86.9(2)	Cl(3)	-Nb	-O(1)	91.0(2)
Cl(3)	-Nb	-O(2)	168.6(2)	Cl(3)	-Nb	-O(3)	83.2(2)
O(1)	-Nb	-O(2)	99.7(2)	O(1)	-Nb	-O(3)	172.0(2)
O(2)	-Nb	-O(3)	86.5(2)	Nb	-O(1)	-C(11)	146.0(5)
Nb	-O(2)	-C(21)	154.2(5)	Nb	-O(3)	-C(31)	128.2(8)
Nb	-O(3)	-C(34)	121.7(6)	C(31)	-O(3)	-C(34)	108.5(10)
O(1)	-C(11)	-C(12)	120.2(6)	O(1)	-C(11)	-C(16)	118.2(6)
C(12)	-C(11)	-C(16)	121.4(7)	C(11)	-C(12)	-C(13)	118.2(7)
C(11)	-C(12)	-C(51)	124.1(7)	C(13)	-C(12)	-C(51)	117.6(7)
C(12)	-C(13)	-C(14)	121.1(8)	C(13)	-C(14)	-C(15)	119.1(9)
C(14)	-C(15)	-C(16)	122.5(8)	C(11)	-C(16)	-C(15)	117.4(7)
C(11)	-C(16)	-C(61)	122.9(7)	C(15)	-C(16)	-C(61)	119.4(7)
O(2)	-C(21)	-C(22)	118.9(7)	O(2)	-C(21)	-C(26)	118.2(7)
C(22)	-C(21)	-C(26)	122.8(7)	C(21)	-C(22)	-C(23)	116.8(8)
C(21)	-C(22)	-C(71)	122.3(8)	C(23)	-C(22)	-C(71)	120.9(8)
C(22)	-C(23)	-C(24)	123.0(10)	C(23)	-C(24)	-C(25)	120.0(10)
C(24)	-C(25)	-C(26)	120.8(9)	C(21)	-C(26)	-C(25)	116.4(8)
C(21)	-C(26)	-C(81)	124.6(8)	C(25)	-C(26)	-C(81)	118.9(8)
O(3)	-C(31)	-C(32)	109.4(15)	C(31)	-C(32)	-C(33)	108.0(16)
C(32)	-C(33)	-C(34)	107.4(13)	O(3)	-C(34)	-C(33)	102.0(10)

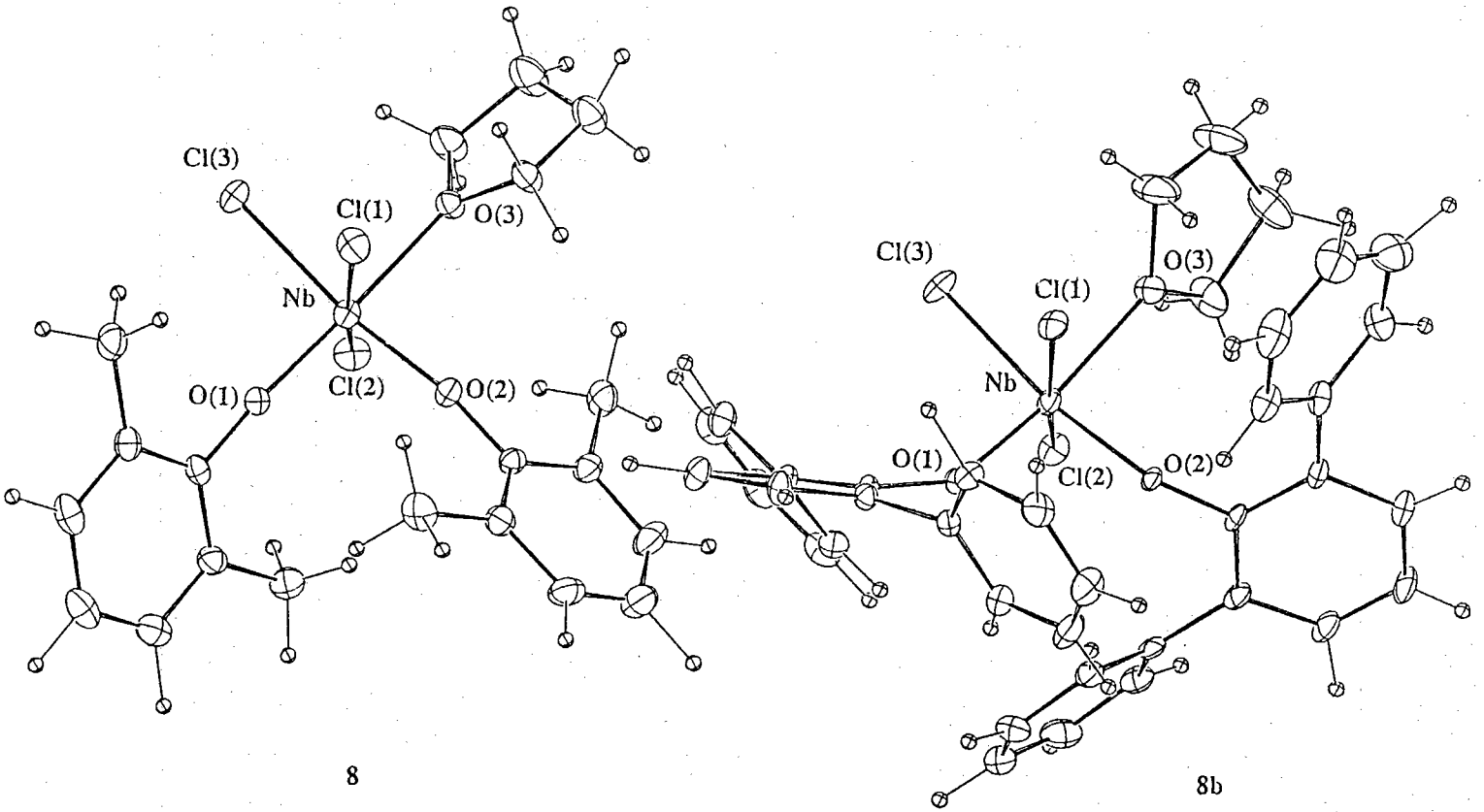

Fig. 3-3. Molecular structures of (a) $NbCl_3[O\text{-}2,6\text{-}(CH_3)_2C_6H_3]_2(THF)$ (**8**), and (b) $NbCl_3[O\text{-}2,6\text{-}(C_6H_5)_2C_6H_3](THF)$ (**8b**).

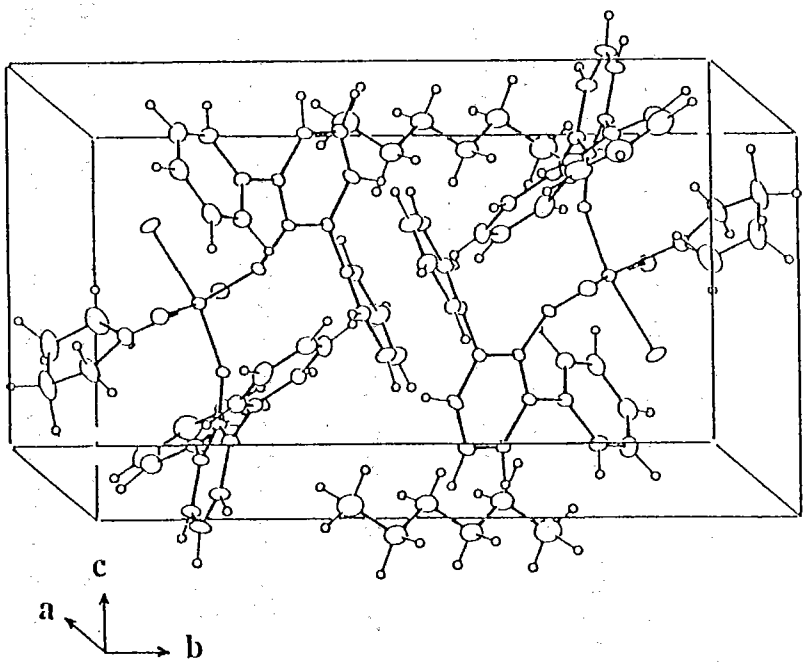

8b

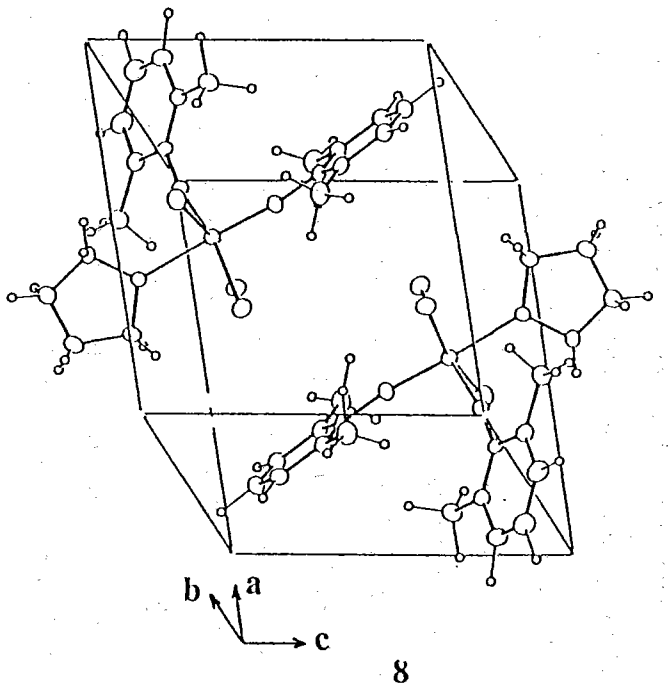

8

Fig. 3-4. Crystal structures of (a) $NbCl_3[O\text{-}2,6\text{-}(CH_3)_2C_6H_3]_2(THF)$ (**8**), and (b) $NbCl_3[O\text{-}2,6\text{-}(C_6H_5)_2C_6H_3](THF)$ (**8b**).

positions in both complexes. The Cl(1)-Nb-Cl(2) angles (168.8° in **8** and 168.9° in **8b**) shows the slight deformations for two chloride ligands from the exact *trans* position and two chlorine atoms tilt away from phenoxy ligands in both complexes. Central metal atoms lie on the basal plane defined by O(1), O(2), O(3) and Cl(3) atoms for both complexes, and the sum of bond angles around the metal atoms in basal planes is 360.0° in **8** and 360.4° in **8b**, respectively. O(phenoxy)-Nb-O(phenoxy) angles are much larger than the right angle in both complexes. These aspects are also found in complex **4** and **5**. While the O(THF)-Nb-Cl(3) angles (84.7° in **8** and 83.2 in **8b**) are smaller than 90°. These aspect are also found in complex **1**. In complex **8b** Nb-O-C(phenoxy) angles (146.0 and 154.2°) are much smaller than the corresponding angles in complex **8** (173.2 and 170.2°) for the steric repulsion of phenyl substituent on 2,6 position of phenoxy ligand. In both complexes the longer Nb-O(2) distances as compared with Nb-O(1) is the result of stronger *trans* influence of C atom than THF ligand.

Crystal structures of complex **8** and **8b** are shown in Fig. 3-4. In complex **8b**, during the crystallization, solvent *n*-hexane might penetrate as spacer. One half of *n*-hexane positioned around the (0, 1/2, 0) inversion center with clean *trans* zigzag shape. Another one-half *n*-hexane may occupied the position around the (1/2, 0, 0) inversion center but these can not be assigned.

3.3. Versatile Bonding Character of Tungsten Phenoxides

3-3-1. Molecular Structures of Tungsten phenoxides $WCl_5[O\text{-}2,6\text{-}(CH_3)_2C_6H_3]$ (9) and $WCl_4[O\text{-}2,6\text{-}(CH_3)_2C_6H_3]_2$ (10)

Crystals of **9** and **10** are dark purple and dark blue in color with regular prismatic shape. Crystal data, data collection, and parameters for structure refinement of **9** and **10** are summarized in Table 3-17. No significant intensity

decay of the standard reflection was observed for both crystals. The usual Lorentz and polarization effects were corrected for the intensity data together with the absorption correction for **9**. Fractional atomic coordinates and equivalent isotropic temperature factors for nonhydrogen atoms in **9** and **10** are listed in Table 3-18.

The molecular structures of **9** and **10** are shown in Fig. 3-5 by ORTEP drawings together with the atomic numberings. X-ray structure analyses of **9** and **10** revealed that the crystallographic molecular symmetry is C_{2v}(mm) for **9** and C_{2h}(2/m) for **10**, respectively. Therefore, two phenoxy ligands in **10** are *trans* to each other in contrast to the *cis* configuration in analogous complex $WCl_4[O\text{-}2,6\text{-}(C_6H_5)_2C_6H_3]_2$[11]. In complex **9**, one of two crystallographic mirror planes passes through all the non-hydrogen atoms except Cl(2), to which another mirror plane is perpendicular including Cl(1), W, C(1) and C(4) atoms. In complex **10**, two phenoxy ligands and W atom locate on the mirror plane, perpendicular to which a 2-fold axis passes through the tungsten atom. Therefore, the bond angle of W-O-C(phenoxy) in **9** is exactly 180°, while that in **10**(179°) is essentially but not exactly 180°. These are the first example of tungsten phenoxy complex with straight W-O-C bond. Interatomic bond distances and angles in **9** and **10** are summarized in Tables 3-19 and 3-20, respectively. In Complex **9**, W-Cl(1) bond *trans* to phenoxy ligand is 2.299(9) Å, which is equal to W-Cl(2) bond (2.307(3) Å) *cis* to phenoxy ligand. These W-Cl bonds are rather longer than that found in inorganic complex such as $WClF_5$ (2.251 Å). The W-O bond distances of 1.82(2) Å is the shortest in the tungsten-phenoxides hitherto reported, though the many comparable W-O distances were reported in $WCl_3[O\text{-}2,6\text{-}(i\text{-}Pr)_2C_6H_3]_3$[12]; 1.832(2), 1.836(2), and 1.848(2) Å, in $W[O\text{-}2,6\text{-}(i\text{-}Pr)_2C_6H_3]_4$[13]; 1.849(4), 1.851(6), 1.851(5), and 1.866(5) Å, and $W[O\text{-}2,6\text{-}(CH_3)_2C_6H_3]4$[13]; 1.843(4) Å, etc. The $W[O\text{-}2,6\text{-}(i\text{-}Pr)_2C_6H_3]_4$ and $W[O\text{-}2,6\text{-}(CH_3)_2C_6H_3]_4$ complexes include phenoxy ligand as the sole ligand, and are suitable complex to see the standard value of W-

Table 3-17. Crystal Data and Experimental Parameters for X-Ray Structure Determination of $WCl_5[O\text{-}2,6\text{-}(CH_3)_2C_6H_3]$ (**9**) and $WCl_4[O\text{-}2,6\text{-}(CH_3)_2C_6H_3]_2$ (**10**)

Complex	**9**	10
Formula	$WCl_5OC_8H_9$	$WCl_4O_2C_{16}H18$
Formula weight	482.3	568.0
Crystal system	orthorhombic	monoclinic
Space group	*Cmcm*	*C2/m*
Temp., °C	23	20
a,[a] Å	12.952(5)	17.615(4)
b, Å	12.386(3)	7.188(2)
c, Å	8.279(3)	8.396(2)
β, deg		119.93(2)
V, Å^3	1328.0(10)	921.3(4)
Z	4	4
D_{calcd}, g cm^{-3}	2.412	2.047
F(000), e	896	544
μ(MoKα), cm^{-1}	98.7	72.2
Crystal size, mm	0.20x0.25x0.40	0.20x0.70x0.13
2θ range,[b] deg	6<2θ<55	4<2θ<60
Scan width, deg in 2θ	1.0+0.30tanθ	1.0+0.35tanθ
Scan speed,deg min^{-1}	8.0-16.0	4.0
Background count, s	50% of peak scan	5
Reflections measured	895	912
Reflections observed[c]	576	908
Radiation damage	no	no
No. of variables	43	101
GOF[d]	1.85	1.759
R[e]	0.048	0.029
R_w[f]	0.036	0.055

[a)]Least-squares refinement of the θ values for 25 reflections with 2θ>25°. [b)]Intensity data were collected on a Rigaku four-circle diffractometer using graphite-monochromatized MoKα radiation by the θ-2θ scan method. [c)]non-zero reflections. [d)]$[\Sigma w(|F_o|-|F_c|)^2/(n-m)]^{1/2}$, where *n* and *m* are the No. of reflections used and variables refined, respectively. [e)]$R=\Sigma(|F_o|-|F_c|)/\Sigma|F_o|$. [f)]$R_w=[\Sigma w(|F_o|-|F_c|)^2/\Sigma W|F_o|^2]^{1/2}$, $w=4F_{o2}/\sigma^2(F_{o2})$ for (**9**), and $w=[\sigma^2(F_o)+g(F_o)^2]^{-1}$, and $g=0.003$ for (**10**) respectively.

Table 3-18. Final Atomic Coordinates and Equivalent Isotropic Temperature Factors for Nonhydrogen Atoms in $WCl_5[O\text{-}2,6\text{-}(CH_3)_2C_6H_3]$ (**9**) and $WCl_4[O\text{-}2,6\text{-}(CH_3)_2C_6H_3]_2$ (**10**) with Estimated Standard Deviations in Parentheses[a)]

$WCl_5[O\text{-}2,6\text{-}(CH_3)_2C_6H_3]$ (**9**)

atom	x	y	z	B_{eq}
W	0	0.1828(1)	1/4	2.82(5)
Cl(1)	0	-0.0028(7)	1/4	5.4(5)
Cl(2)	0.1264(2)	0.1777(4)	0.0538(4)	5.0(2)
O	0	0.329(2)	1/4	4(1)
C(1)	0	0.443(3)	1/4	7(2)
C(2)	-0.100(1)	0.495(2)	1/4	4(1)
C(3)	-0.096(1)	0.607(2)	1/4	4(1)
C(4)	0	0.659(2)	1/4	4(2)
C(5)	-0.199(1)	0.432(2)	1/4	7(1)

$WCl_4[O\text{-}2,6\text{-}(CH_3)_2C_6H_3]_2$ (**10**)

Atom	x	y	z	B_{eq}
W	0.0	0.0	0.0	2.77
Cl(1)	-0.04868(13)	0.2303(3)	0.1237(4)	3.63
O	0.1090(5)	0.0	0.2132(14)	2.9
C(1)	0.1878(7)	0.0	0.366(3)	3.2
C(2)	0.1915(7)	0.0	0.537(3)	3.1
C(3)	0.2746(8)	0.0	0.687(4)	3.9
C(4)	0.3509(8)	0.0	0.675(4)	4.6
C(5)	0.3441(7)	0.0	0.502(4)	3.5
C(6)	0.2638(7)	0.0	0.347(3)	3.5
C(7)	0.1122(9)	0.0	0.547(3)	3.7
C(8)	0.2600(9)	0.0	0.160(4)	5.0

[a)]Positional parameters are in fraction of cell edges and B_{eq} is the equivalent isotropic temperature factors calculated from the corresponding anisotropic thermal parameters.

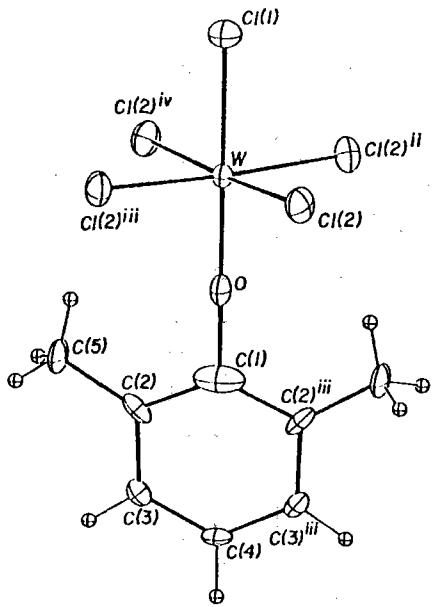

9

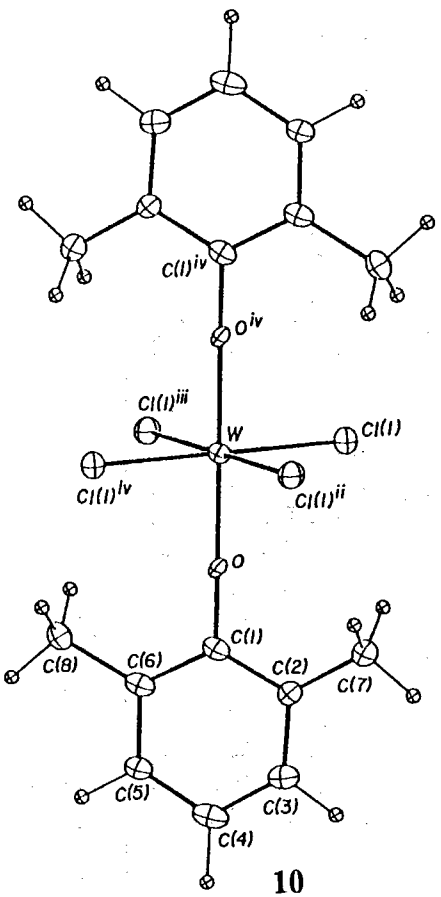

10

Fig. 3-5. Molecular structures of (a) $WCl_5[O\text{-}2,6\text{-}(CH_3)_2C_6H_3]$ (**9**), and (b) $WCl_4[O\text{-}2,6\text{-}(C_6H_5)_2C_6H_3]_2$ (**10**).

Table 3-19. Selected Bond Distances (Å) and Angles (°) for Nonhydrogen Atoms in $WCl_5[O\text{-}2,6\text{-}(C_6H_5)_2C_6H_3]$ (**9**) with Estimated Standard Deviations in Parentheses

(a) Bond Distances (Å)

W	- Cl(1)	2.299(9)	W	- Cl(2)	2.307(3)
W	- O	1.82(2)	O	- C(1)	1.41(4)
C(1)	- C(2)	1.45(2)	C(2)	- C(3)	1.38(2)
C(2)	- C(5)	1.49(2)	C(3)	- C(4)	1.41(2)

(b) Bond Angles (°)

Cl(1)	-W	-Cl(2)^{iii}	88.4(1)	Cl(2)	-W	-Cl(2)^{ii}	89.5(3)
Cl(2)	-W	-Cl(2)^{iii}	90.4(3)	Cl(2)	-W	-Cl(2)^{iv}	176.9(3)
Cl(1)	-W	-O	180.0	Cl(2)	-W	-O	91.6(1)
W	-O	-C(1)	180.0	O	-C(1)	-C(2)	116(2)
C(2)	-C(1)	-C(2)^{iii}	132(3)	C(1)	-C(2)	-C(3)	114(2)
C(1)	-C(2)	-C(5)	125(2)	C(3)	-C(2)	-C(5)	123(2)
C(2)	-C(3)	-C(4)	118(1)	C(3)	-C(4)	-C(3)^{iii}	125(2)

Code for superscript

i	x,	y,	z
ii	x,	y,	1/2-z
iii	-x,	y,	z
iv	-x,	y,	1/2-z

Table 3-20. Selected Bond Distances (Å) and Angles (°) for Nonhydrogen Atoms in $WCl_4[O\text{-}2,6\text{-}(C_6H_5)_2C_6H_3]_2$ (**10**) with Estimated Standard Deviations in Parentheses

(a) Bond Distances (Å)

W	- Cl(1)	2.333(3)	W	- O	1.860(7)
O	- C(1)	1.34(1)	C(1)	- C(2)	1.41(3)
C(1)	- C(6)	1.42(2)	C(2)	- C(3)	1.38(2)
C(2)	- C(7)	1.44(3)	C(3)	- C(4)	1.40(3)
C(4)	- C(5)	1.40(4)	C(5)	- C(6)	1.36(2)
C(6)	- C(8)	1.54(4)			

(b) Bond Angles (°)

Cl(1)	-W	-O	90.2(3)	W	-O	-C(1)	179(1)
O	-C(1)	-C(2)	118(1)	O	-C(1)	-C(6)	119(2)
C(2)	-C(1)	-C(6)	123(1)	C(1)	-C(2)	-C(3)	115(2)
C(1)	-C(2)	-C(7)	121(1)	C(3)	-C(2)	-C(7)	124(2)
C(2)	-C(3)	-C(4)	124(2)	C(3)	-C(4)	-C(5)	119(1)
C(4)	-C(5)	-C(6)	120(2)	C(1)	-C(6)	-C(5)	119(2)
C(1)	-C(6)	-C(8)	123(1)	C(5)	-C(6)	-C(8)	118(2)
Cl(1)^{iii}	-W	-O	89.8(1)	Cl(1)	-W	-Cl(1)^{ii}	90.4(1)
Cl(1)	-W	-Cl(1)^{iii}	89.6(1)	Cl(1)	-W	-Cl(1)^{iv}	180.0

Code for superscript

i	x,	y,	z
ii	x,	-y,	z
iii	-x,	y,	-z
iv	-x,	-y,	-z

O(phenoxy) distance. They distribute in a range from 1.843 to 1.866 Å. The W-O distance in **10** (1.860(7)Å) is comparable with these values, though a little longer than that in **9**. Very long W-O distances were also reported in WCl_3[O-2,6-$(C_6H_5)_2C_6H_3$]$_2$-[$P(CH_3)_2C_6H_5$] (1.877(5) and 1.853(4) Å] and WCl_2[O-2,6-$(C_6H_5)_2C_6H_3$]$_2$-[$P(CH_3)_2C_6H_5$] (1.966(4) Å][11], in which two phenoxy ligands are *trans* to each other.

3-3-2. Unique bonding character of phenoxy ligands in early transition metal complexes

Selected bond Angles in **1**, **4**, **5**, **7**, **8**, **8b**, **9**, and **10** are summarized in Table 3-21. Cl-M-Cl(*trans*) angles are all smaller than 180.0° except for **10** and two chlorine atoms tilt away from the phenoxy ligands. O(phenoxy)-M-O(phenoxy) angles are all lager than 90°. O(THF)-M-O(THF) angles all smaller than 90°. Selected bond distances in **1**, **4**, **5**, **7**, **8**, **8b**,**9**, and **10** are summarized in Table 3-22. First noteworthy characteristic is that M-Cl distances are nearly equal to the sum of covalent radius of metal and chlorine atoms. Second, all M-O(phenoxy) distances are shorter than the sum of the covalent radius of metal and oxygen atoms. Especially Ti-O distances(1.762 and 1.788 Å) are much shorter than the sum of the covalent radius (1.98 Å), this shortening may attained by the contribution of $d\pi$(metal)-$p\pi$(oxygen). Third, all the M-O(THF) distances are nearly equal to each other irrespective of the kind of metals. These observations suggest the unique character of M-O(phenoxy) bond.

Many works have been reported on the intramolecular C-H bond activation in the aliphatic or aromatic substituents of phenoxy ligands by the central atoms. In the case of O-2,6-di-*t*-butylphenoxide complexes, the intramolecular activation of C-H bond in methyl group results in the formation of 6-membered metallacycles for Ti[14] and Ta [1,15,16,17,18,]. On the other hand, an interesting variation of aromatic C-H bond activation gave η^6-arene

Table 3-21. Selected Bond Angles (°) in **1**, **4**, **5**, **7**, **8**, **8b**, **9**, and **10**.

		Cl-M-Cl	$\Sigma\phi$'s	ϕ_1	ϕ_3	θ_1,θ_2	
$TiCl_3R(THF)_2$	(1)	166.9	360.0		81.4	173.4	
$TiCl_2R_2(THF)_2$	(4)	165.0	360.0	99.2	80.6	165.7	170.0
$ZrCl_2R_2(THF)_2$	(5)	163.3	360.1	100.3	79.9	166.6	170.8
$NbCl_4R(THF)$	(7)	169.8	360.0			180.0	
$NbCl_3R_2(THF)$	(8)	168.8	360.0	96.3	84.7	170.2	173.2
$NbCl_3R'_2(THF)$	(8b)	168.9	360.4	99.7	83.2	146.0	154.4
WCl_5R	(9)	176.9	360.0			180.0	
WCl_4R_2	(10)	180.0	360.0	180.0		179.4	179.4

R = O-2,6-$(CH_3)_2C_6H_3$

R'= O-2,6-$(C_6H_5)_2C_6H_3$

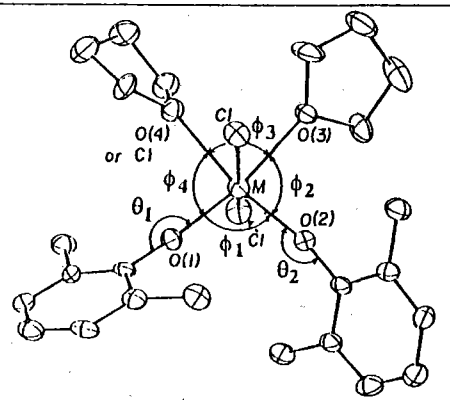

Table 3-22. Selected Bond Distances (Å) in **1**, **4**, **5**, **7**, **8**, **8b**, **9**, and **10**.

		M-Cl			M-O(phenoxy)		M-O(THF)	
		basal	apical					
$TiCl_3R(THF)_2$	(1)	2.273	2.327	2.330	1.762		2.168	2.171
$TiCl_2R_2(THF)_2$	(4)		2.374	2.347	1.788	1.788	2.202	2.197
$ZrCl_2R_2(THF)_2$	(5)		2.476	2.456	1.904	1.906	2.288	2.275
$NbCl_4R(THF)$	(7)	2.351	2.351	2.351	1.819		2.207	
$NbCl_3R_2(THF)$	(8)	2.388	2.366	2.391	1.829	1.854	2.194	
$NbCl_3R'_2(THF)$	(8b)	2.384	2.360	2.363	1.883	1.855	2.217	
WCl_5R	(9)	2.299	2.307	2.307	1.820			
WCl_4R_2	(10)	2.333	2.333	2.333	1.860			

covalent radii;

Ti : 1.32
Zr : 1.45
Nb : 1.34
W : 1.30
Cl : 0.99
O : 0.66

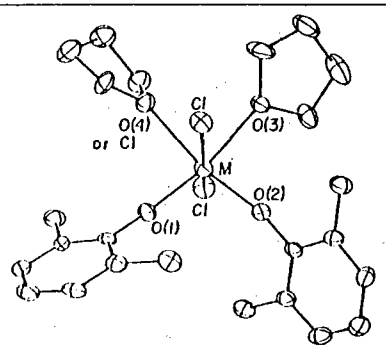

coordination or 6-membered metallacyclic structure for Mo[19,20] and W[21,22,23,24]. In our case of O-2,6-dimethyl(or diphenyl)phenoxide complexes, any intramolecular C-H bond activation or agostic interaction was not found because of the rather long interatomic bond distances between methyl(or phenyl) groups and metal centers.

In order to understand the bonding character of phenoxy ligand to the metals more clearly, it is interesting to see the correlation between early transition metal-O(phenoxy) distances and M-O-C(phenoxy) angles. All of the early-transition metal-phenoxides were extracted from the Cambridge Crystallographic Database. After excluding some structures with low accuracy, and phenoxides of Hf, V, and Cr which are found being few samples, the distribution of M-O distances and M-O-C angles are examined and summarized in Table 3-23. As for Hf, V, and Cr, only few samples were found and were omitted from the table. The retrieved metal-phenoxides are grouped into three types of bonding structure. Type-1 has phenoxy ligand without any direct interaction between the phenoxy substituent and metal atom. Type-2 includes η^6-phenyl substituent on 2-position of phenoxy ligand. Type-3 includes a metal-carbon σ-bond to the phenoxy substituent. From the comparison between the molecular structures of tungsten-phenoxides, the W-O(phenoxy) distances distribute in a wide range depending on many structural and/or electronic parameters. The correlation between W-O distances and W-O-C angles are plotted and is shown in Fig. 3-6. The constraint to the W-O-C bond angle for bending is largest in type-2, and next largest in type-3 by the easy understanding from the geometry illustrated in the figure. Complexes **16-20** in the figure include type-2 geometry, and have very long W-O bonds [2.033-2.163Å] and very small W-O-C angles [117.5-122.5°]. Complex **13** in the figure include type-3 geometry, and has a W-O bonds of 1.87 and 1.88Å and W-O-C angles of 140.7 and 143.5°, which are the middle values in the correlation plots. The W-O bond distances and W-O-C bond angles determined in the present work are

Table 3-23. Distribution of M-O Distances (Å) and M-O-C Angles (°) in Early Transition Metal-Phenoxides

		Distance			Angle			
4	Ti	1.726	~	1.88	143.6	~	179.1	type-3
	Zr	1.903	~	2.058	151.9	~	175.7	
	Hf	-----		-----	-----		-----	
5	V	-----		-----	-----		-----	
	Nb	1.819	~	2.181	147.8	~	180	η^4
	Ta	1.83	~	1.945	136.8	~	178.9	type-3
6	Cr	-----		-----	-----		-----	
	Mo	1.876	~	2.164	118.0	~	157.1	type-2, type-3
	W	1.82	~	2.163	117.5	~	180	type-2, type-3

Type-1

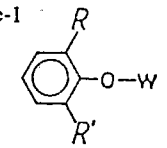

Type-2

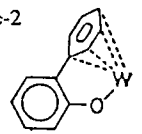

Type-3

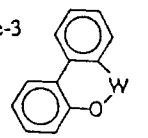

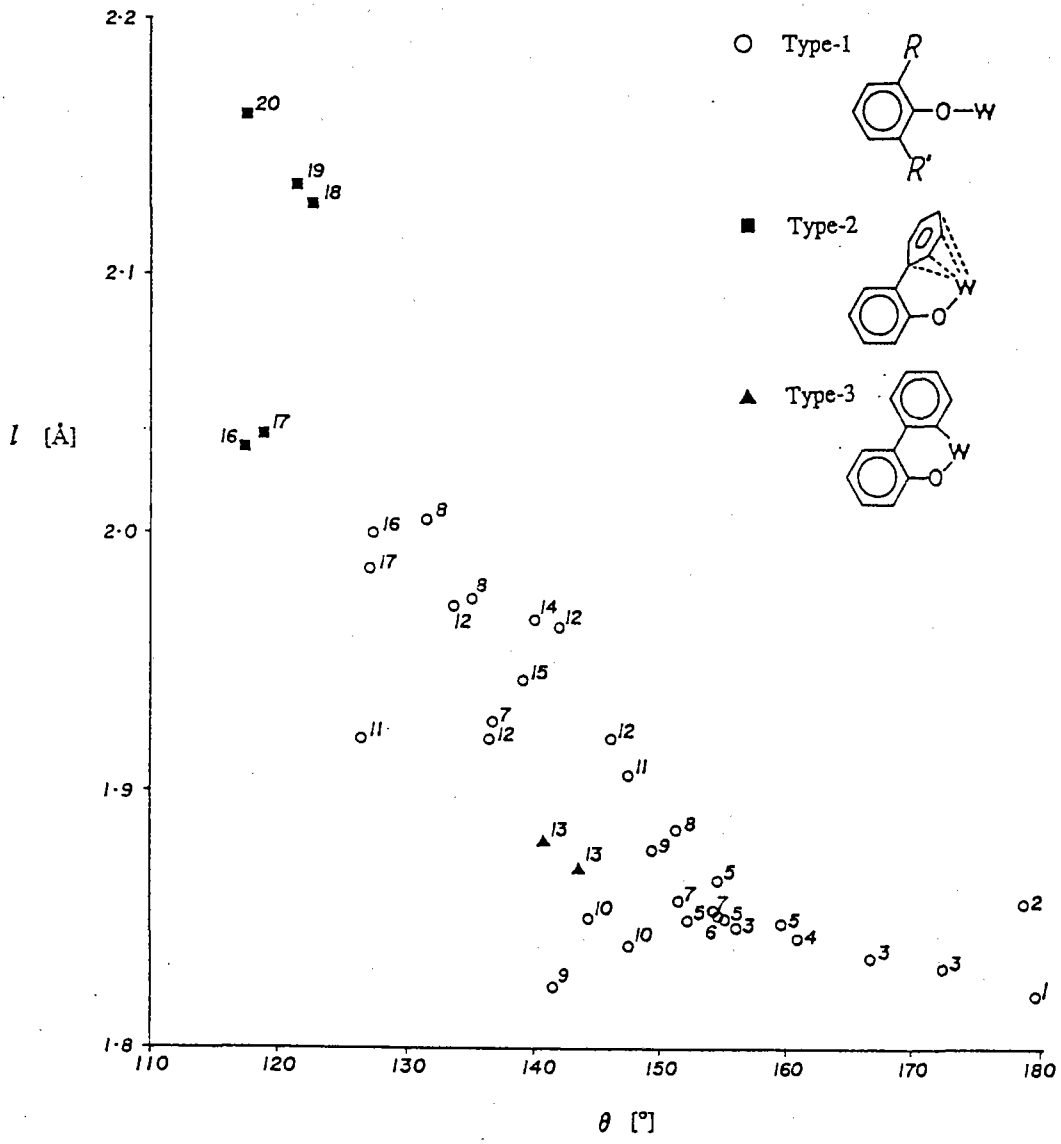

Fig. 3-6. Coordination geometry of phenoxy ligand in the molecular structures of tungsten-phenoxides by the W-O bond distance [*l*] vs. W-O-C bond angle [θ] plotting.[25)]

on another extreme in the correlation plots, the shortest W-O bond of 1.82(2)Å and largest W-O-C bond angle of 180° in **9**. The figure shows the correlation between the W-O bond distances and W-O-C bond angles make a hyperbolic curve as a good approximation. The correlation plot between these parameters shows the very flexible characteristics of W-phenoxy bond depending on the degree of geometrical constraint for the ligand. The versatile parameters of W-O bond may attained by the control of $p\pi$-$d\pi$ overlapping for the bond. The flexible W-O bond character may also make possible the several modes of C-H bond activation of phenoxy substituent by tungsten atom.

References

1) I. P. Rothwell, *Polyhedron*, **4**, 177(1985).

2) K. C. Walace, A. H. Liu, J. C. Dewan, and R. R. Schrock, *J. Am. Chem. Soc.*, **110**, 4964 (1988).

3) T. V. Lubben and P. T. Wolczanski, *J. Am. Chem. Soc* .,**109**, 424 (1987).

4) For a preliminary report, see H. Yasuda, K. Takei, and A. Nakamura, 56th Annual Meeting. Chem. Soc. Jpn., Abstract 2B01(1988).

5) For example, I. P. Rothwell, *Acc. Chem. Res.*, **21**, 153(1988).

6) For example, A. Flamini, D.J. Cole-hamioton, and G. Wilkinson, *J. Chem. Soc., Dalton*, 454 (1978).

7) MSC/AFC, Diffractometer Control Software, Molecular Structure Coorporation, 1990.

8) TEXSAN, Structure Analysis Software, Molecular Structure Coorporation, 1990.

9) XRAY-76, J. M. Stewart, Report TR-446, University of Maryland, MD, 1976.

10) ORTEP-II, C. K. Johnson, Report ORNL-5138, Oak Ridge National Laboratoly, Tennessee, 1976.

11) J. L. Kerschner, P. E. Fanwick, I. P. Rothwell, and J. C. Huffman, *Inorg. Chem.*, **28**, 780 (1989).

12) F. Quignard, M. Leconte, J-M. Bassel, L-Y. Hsu, J. J. Alexander, and S. G. Shore, *Inorg. Chem.*, **26**, 4272 (1987).

13) M. L. Listemann, R. R. Schrock, J. C. Dewan, and R. M. Kolodziej, *Inorg. Chem.*, **27**, 264 (1988).

14) S. L. Latesky, A. K. McMullen, I. P. Rothwell, and J. C. Huffman, *J. Am. Chem. Soc.* **107**, 5981 (1985)

15) l. R. Chamberlain, J. L. Kerschner, A. P. Rothwell, I. P. Rothwell, and J. C. Huffman, *J. Am. Chem. Soc.* **109**, 6471 (1987).

16) L. Chamberlain, J. Keddington, and I. P. Rothwell, and J. C. Huffman, *Organometallics* **1**, 1538 (1982).

17) B. D. Steffey, L. R. Chamberlain, R. W. Chesnut, D. E. Chebi, P. E. Fanwick, I. P. Rothwell, *Organometallics* **8**, 1419 (1989).

18) R. W. Chesnut, B. D. Steffey, I. P. Rothwell, and J. C. Huffman, *Polyhedron*, **7**, 753 (1988).

19) J. L. Kerschner, P. E. Fanwick, and I. P. Rothwell, *J. Am. Chem. Soc.*, **109**, 5840 (1987).

20) J. L. Kerschner, J. S. Yu, P. E. Fanwick, I. P. Rothwell, J. C. Huffman, *Organometallics*, **8**, 1414 (1989).
21) J. L. Kerschner, I. P. Rothwell, J. C. Huffman, and W. E. Streib, *Organometallics*, **7**, 1871 (1988).
22) J. L. Kerschner, P. E. Fanwick, and I. P. Rothwell, *J. Am. Chem. Soc*, **110**, 8235 (1988).
23) J. L. Kerschner, E. M. Torres, P. E. Fanwick, I. P. Rothwell, and J. C. Huffman, *Organometallics* , **8**. 1424 (1989).
24) J. L. Kerschner, P. E. Fanwick, I. P. Rothwell, and J. C. Huffman, *Organometallics*, **8**, 1431 (1989).
25) ***1***: complex **9** of my work; ***2***: complex **10** of my work; ***3,9***: ref. 12; ***4,5***: ref. 13; ***,6,17***: ref. 22; ***7,10,14***: ref. 11; ***8***: M.R. Churchill, J.W. Ziller, J.H. Freudenberger, and R.R. Schrock; Organometallics 3(1984) 1554; ***11,12***: ref.; ***13***: ref. 24; ***15***: J.I. Davies, J.F. Gibson, A.C. Skapski, G. Wilkinson, and W-K. Wong, Polyhedron 1(1982) 641; ***16***: ref. 21; ***18,19,20***: ref.23.

Concluding Remarks

A series of early transition metal complexes with active organic substrates have been studied by X-ray diffraction method. Molecular structures determined by this work revealed many important informations on the unique chemical behavior of this series of organometallic complexes.

Chapter 1 describes the unique coordination geometries of 1,3-diene ligand to the early transition metals. Especially important is the first determination of s-*trans*-diene coordination by X-ray diffraction method in zirconium(1,4-diphenylbutadiene) complex. The very distorted s-*trans*-conformation with the torsional angle of 126° around the central bond was found in diene ligand. The first crystal structure of magnesium-diene complex was also determined for penta-coordinated magnesium atom with s-*cis* diene ligand. From the structure analyses on mono- and bis(diene) complexes of niobium and tantalum, *supine* geometry was found as an stable coordination for mono(diene) complex, while unique *supine-prone* geometry was found stable for bis(diene) complexes. The mixed bis(diene) complexes revealed the diene with bulky substituent prefer *supine* geometry.

Chapter 2 concerns with the structural chemistry on the regio- and stereoselective reactions of early transition metal-diene complexes for heterocumulene, ketone, alkyne, and other active organic substrates. From the X-ray structure analyses of the insertion products of metal-diene complexes, the wide variety of coordination geometries were found for diene ligands to suggest the reaction intermediate and thus the reaction pathways. The important feature is that the structure of metallacycles obtained from the carbometallation determines the path for the insertion reactions. The conformation of the diene ligand converts from s-*trans* to allyl structure through the insertion of carbon dioxide or *t*-butylisocyanate, while s-*trans* geometry was found by the insertion of two molecules of phenylisocyanate. The zirconium-isoprene complex gave

a series of regio- and stereoselective insertion products. The insertion of diisopropylketone occurred on the sterically hindered zirconium-C1 bond and gave s-*cis* diene geometry, while that of 2-butyne occurred on less hindered zirconium-C4 bond and gave s-*trans* geometry. On the other hand, the insertion of diphenylketene occurred on zirconium-C3 bond through the unique hydrogen migration process. These variety of reaction pathways were interpreted by the versatile bonding geometry of diene ligand to the early transition metals.

Chapter 3 described on the structural chemistry of early transition metal-phenoxides with bulky substituent. From the crystal structure analyses, the wide varieties of structural parameters were found for titanium, zirconium, niobium, and tungsten-phenoxy bonds. Tungsten-phenoxides remarkably showed the versatile bonding character by the correlation analysis between W-O bond distances and W-O-C bond angles resulting the unique hyperbolic correlation curve. The observed bonding character explained various C-H bond activation hitherto reported.

List of Publications

Regular Papers

1. The X-Ray Structure of a Magnesium-1,3-diene Complex. The Unique Mode of Coordination of Diene Observed in Penta-coordinated $Mg(THF)_3$(*s-cis*-PhCH=CH-CH=CHPh)
   Y. Kai, N. Kanehisa, K. Miki, N. Kasai, K. Mashima, H. Yasuda, A. Nakamura
   Chem. Lett., **1982**, 1277-1280.

2. X-Ray Evidence for a Mononuclear *s-trans*-η4-1,3-Diene Complex; Molecular Structure of $Zr(\eta^5\text{-}C_5H_5)_2$(*s-trans*-PhCH=CH-CH=CHPh)
   Y. Kai, N. Kanehisa, K. Miki, N. Kasai, K. Mashima, K. Nagasuna, H. Yasuda, A. Nakamura
   J. Chem. Soc., Chem. Commun., **1982**, 191-192.

3. Molecular Structure of $[(\eta^5\text{-}C_5H_5)_2Zr(CH_2\text{-}C(CH_3)\text{-}CH\text{-}CH_2)\text{-}C(CH_3)=C(CH_3)]$ Prepared by Regioselective Insertion of 2-Butyne
   Y. Kai, N. Kanehisa, K. Miki, N. Kasai, K. Mashima, K. Nagasuna, H. Yasuda, A. Nakamura
   Chem. Lett., **1982**, 1979-1982.

4. The X-Ray and NMR Studies on the Regio- and Stereoselective Courses for Insertion of Ketones into the *s-cis*- and *s-trans*-Diene Complexes of Zirconium Leading to (Z)-1,2-oxa-zirconacyclohept-4-enes
   Y. Kai, N. Kanehisa, K. Miki, N. Kasai, M. Akita, H. Yasuda, A. Nakamura
   Bull. Chem. Soc. Jpn., **56**, 3735-3743 (1983).

5. Unique Bonding and Geometry in η-Cyclopentadienyltantalum-Diene Complexes. Preparation, X-ray Structural Analyses, and EHMO Calculations
   H. Yasuda, K. Tatsumi, T. Okamoto, K. Mashima, K. Lee, A. Nakamura, Y. Kai, N. Kanehisa, N. Kasai

J. Am. Chem. Soc., **107**, 2410-2422 (1985).

6. Synthesis and Catalysis of Novel Mono- and Bis-Diene Complexes of Niobium and X-Ray Structures of Binuclear[Nb(μ-Cl)(C_5H_5)(s-cis-butadiene)]$_2$ and Mononuclear Nb(C_5H_5)(*s-cis*-2,3-dimethylbutadiene)$_2$
T. Okamoto, H. Yasuda, A. Nakamura, Y. Kai, N. Kanehisa, N. Kasai
J. Am. Chem. Soc., **110**, 5008-5017 (1988).

7. Synthesis, X-Ray Crystal Structure and Nucleophilic Properties of Mixed Bis(diene)tantalum Complexes, Ta(η^5-C_5R_5)(η^4-C_4H_6)-(η^4-C_6H_{10})
T. Okamoto, H. Yasuda, A. Nakamura, Y. Kai, N. Kanehisa, N. Kasai
Organometallics, **7**, 2266-2273 (1988).

8. Diverse Reaction Courses in the Controlled Carbometalation of Carbonyl Compounds and Heterocumulenes with Zirconium-Diene Complexes and Molecular Structures of Carbon Dioxides, Isocyanate and Ketene 1:1 and 1:2 Inserted Compounds
H. Yasuda, T. Okamoto, Y. Matsuoka, K. Mashima, A. Nakamura, Y. Kai, N. Kanehisa, N. Kasai
Organometallics, **8**, 1139-1152 (1989).

9. Facile Synthesis of Group 4-6 Transition Metal Phenoxides and X-Ray Structures of $TiCl_2$[O-2,6-$(CH_3)_2C_6H_3$]$_2$(THF)$_2$ and $NbCl_3$[O-2,6-$(CH_3)_2C_6H_3$]$_2$(THF)
N. Kanehisa, Y. Kai, N. Kasai, H. Yasuda, Y. Nakayama, K. Takei, A. Nakamura
Chem. Lett., **1990**, 2167-2170.

10. Unique Molecular Structures of Tungsten Phenoxides
N. Kanehisa, Y. Kai, N. Kasai, H. Yasuda, Y. Nakayama, A. Nakamura
Bull. Chem. Soc. Jpn., in press.

11. Strucrure Studies on Early Transitioin Metal Mono-Phenoxides
N. Kanehisa, Y. Kai, N. Kasai, H. Yasuda, Y. Nakayama, A. Nakamura

Chem. Lett., in contribution.

12. Molecular Structures of Magnesium, Zirconium, and Hafnium 1,4-diphenylbutadiene
N. Kanehisa, Y. Kai, N. Kasai, H. Yasuda, Y. Nakayama, A. Nakamura
J. Organometallic Chem., in preparation.

Related Papers

1. The Molecular Structure of Methyltrichloro(acetylacetonato)-antimony(V), $CH_3SbCl_3(C_5H_7O_2)$
N. Kanehisa, Y. Kai, N. Kasai
Inorg. Nucl. Chem. Lett., **8**, 375-376 (1972).

2. The Crystal and Molecular Structures of Three (Acetylacetonato)-organoantimony(V) Compounds, $[(acac)RnSbX_{4-n}]$
N. Kanehisa, K. Onuma, S. Uda, K. Hirabayashi, Y. Kai, N. Yasuoka, N. Kasai
Bull. Chem. Soc. Jpn., **51**, 2222-2233 (1978).

3. X-Ray Crystal Structure Analysis of a 2H-Azurine. Unusually Long C-N Bond Fission in Thermal Reactions
N. Kanehisa, N. Yasuoka, N. Kasai, K. Isomura, H. Taniguchi
J. Chem. Soc., Chem. Commun., 98-99 (1980).

4. A Simple Isolable Monocyclic Thiepin. Synthesis, Structure, and Thermal Stability of 2,7-Di-*tert*-butylthiepin
K. Yamamoto, S. Yamazaki, Y. Kohashi, I. Murata, Y. Kai, N. Kanehisa, K. Miki, N. Kasai
Tetrahedron Lett., **23**, 3195-3198 (1982).

5. Azophenolic Acerands: Amine-Selective Coloration and Crystal Structure of a Piperidinium Saltex
T. Kaneda, S. Umeda, Y. Ishizaki, H-S. Kuo, S. Misumi, Y. Kai, N.

Kanehisa, N. Kasai
J. Am. Chem. Soc., **111**, 1881-1883 (1989).

6. Syntheses and Crystal Structure of Calix[4]quinone
Y. Morita, T. Agawa, Y. Kai, N. Kanehisa, N. Kasai, E. Nomura, H. Taniguchi
Chem. Lett., **1989**, 1349-1352.

7. Thermal and Nickel-catalysed Dimerization of Hexapentaene. Synthesis of Two [4]Radialenes with Planar, Stable Cyclobutadiene-like Geometry
M. Iyoda, M. Oda, Y. Kai, N. Kanehisa, N. Kasai
Chem. Lett., **1990**, 2149-2152.

8. Nickel-Catalyzed Cyclodimerization of Hexapentaenes: [4]Radialenes and [5]Radialenones with Cumulated Double Bonds
M. Iyoda, Y. Kuwatani, M. Oda, Y. Kai, N. Kanehisa, N. Kasai
Angew. Chem., **29**, 1062-1064 (1990).

9. Tercalicene and Quatercalicene
T. Sugimoto, M. Shibata, A. Sakai, H. Ando, Y. Arai, M. Sakaguchi, Z. Yoshida, Y. Kai, N. Kanehisa, N. Kasai
Angew. Chem., **103**, 454-456 (1991).

Acknowledgement

The author is greatly indebtd to Professor Nobutami Kasai and Associate Professosr Yasushi Kai for their constant direction and encouragement, and helpful discusstions throughout this research.

The author is deeply grateful to Professor Akira Nakamura, Department of Macromolecular Science, Faculty of Science, Osaka University, and Professor Hajime Yasuda, Department of Applied Chemisty, Faculty of Engineering, Hiroshima Universtiy, for their kindness to provide me a seiries of crystals used in the present X-ray studies and to give me much useful suggestions.

Thanks are extended to all the members of Kasai Laboratory for their helpful discussions and kind friendships.